THE UNIVERSITY OF MICHIGAN
COLLEGE OF ENGINEERING
Department of Meteorology and Oceanography

Technical Report No. 2

ON THE BAROCLINIC STABILITY OF ZONAL FLOW IN SIMPLE MODEL ATMOSPHERES

J. F. Derome
A. Wiin-Nielsen

ORA Project 06372

supported by:

NATIONAL SCIENCE FOUNDATION
GRANT NO. GP-2561
WASHINGTON, D.C.

administered through:

OFFICE OF RESEARCH ADMINISTRATION ANN ARBOR

October 1966

ensn
UMR0992

TABLE OF CONTENTS

LIST OF TABLES

LIST OF FIGURES

LIST OF FIGURES (Continued)

LIST OF FIGURES (Continued)

LIST OF FIGURES (Concluded)

ABSTRACT

Four special cases of a quasi-geostrophic model are investigated to bring out the way in which the baroclinic stability properties of wave disturbances are affected by (a) the vertical wind shear, (b) the variation of the Coriolis parameter with latitude (β effect), and (c) the static stability. It is found that the vertical wind shear tends to make the waves unstable whereas the β effect and the static stability tend to stabilize the very long and very short waves, respectively. In addition the vertical structure of the wave disturbances is discussed for each of the four cases.

A baroclinic stability analysis is also made for each of three special cases of a model based on the primitive equations. By comparing the results obtained with these three cases, it is found that the vertical wind shear and the β effect play essentially the same role as in the quasi-geostrophic models; the role of the static stability, on the other hand, is not investigated for the non-geostrophic model. It is also found that the non-geostrophic effects included in the model stabilize the very short waves. In addition to the solutions corresponding to Rossby waves, solutions are also obtained for gravity and inertia waves and the effects of the vertical wind shear and the β term on these waves are discussed.

The energy transformations taking place during the growth or decay of a disturbance in a quasi-geostrophic model are then considered in an attempt to throw some light on the nature of the physical processes responsible for baroclinic instability.

Treatments of model atmospheres similar to those discussed in this report already appear in the meteorological literature, but here for the first time, to the authors' knowledge, the various models are brought together and presented in a unified manner. In the non-geostrophic cases there is the additional difference that we consider compressible and vertically infinite atmospheres.

1. INTRODUCTION

The problem of determining the stability properties of a baroclinic atmosphere has been extensively investigated in the past two decades. Charney (1947) was the first investigator to show theoretically that a large horizontal temperature gradient (or, equivalently, a large vertical wind shear) in the atmosphere could be responsible for the growth of wave disturbances. The investigations which followed Charney's study are so numerous that no attempt will be made to summarize them here but the following short list of papers should prove useful as a source of further references: Eady (1949); Fjørtoft (1950), Kuo (1952, 1953), Holmboe (1959), Burger (1962), 'Arnason (1963), Barcilon (1964), Miles (1964a,b,c), Huppert and Miles (1965), Pedlosky (1965), and Bretherton (1966a,b).

Our main purpose in this report is to present in a unified manner a series of special cases of baroclinic instability which already appear in the literature. The cases that we have chosen are those which can be solved analytically in terms of elementary functions, using methods which are familiar to the student taking a first course in Dynamic Meteorology. We hope, therefore, that this report can be of some pedagogical value in helping the student bridge the gap between the brief treatments offered in the standard texts of meteorology and the detailed and often complex treatments given in the many papers on the subject.

The cases which we have selected fall in two main classes: (1) those based on a quasi-geostrophic model (Chapter 2), and (2) those based on a "primitive equations" model (Chapter 3). Using the quasi-geostrophic model we investigate separately the effects of the vertical wind shear, the Beta term and the static stability on the behavior of the perturbations. In resume, we find that the vertical wind shear tends to make the perturbations unstable while the Beta term and the static stability tend to stabilize the long and short waves, respectively. In Chapter 2 we also make a special effort to help the student visualize the perturbations by presenting a number of diagrams showing the amplitude and phase of the waves as functions of pressure along with vertical cross-sections of the waves.

Within the framework of the primitive-equations model we study the effect of the Beta term and find that it stabilizes the long waves, just as it does in the quasi-geostrophic model. In addition, we find that the ageostrophic component of the wind tends to stabilize the short waves.

For all cases we assume that the perturbations consist of troughs and ridges of infinite North-South extent. In the quasi-geostrophic model this assumption is introduced only as a matter of convenience since the mathematical analysis could also be carried out without it but, as will become apparent

in the following chapter, this assumption introduces no loss in generality. In the primitive-equations model, on the other hand, we make use of this assumption in order to be able to solve the system of partial differential equations by the method of separation of variables. As was pointed out by Phillips (1964), by neglecting the meridional variation of the perturbations we are probably neglecting some important non-geostrophic effects but, as we shall see in Chapter 3, our simplified model can still demonstrate some features of non-geostrophic flow.

Finally in Chapter 4 we discuss briefly the energetics of our quasi-geostrophic model. More precisely, we derive the equations describing the time rate of change of the perturbation kinetic and available potential energies and discuss the general nature of the atmospheric motions taking place during the growth or decay of a disturbance.

2. BAROCLINIC INSTABILITY IN A QUASI-GEOSTROPHIC MODEL

2.1 THE GENERAL EIGEN-VALUE PROBLEM

The model that we use in this chapter is based on the following simple, but consistent, form of the vorticity equation:

$$\frac{\partial \zeta}{\partial t} + \vec{V} \cdot \nabla (\zeta + f) = f_o \frac{\partial \omega}{\partial p} \qquad (2.1)$$

and the thermodynamic equation for adiabatic flow in the form

$$\frac{\partial}{\partial t} \left(\frac{\partial \psi}{\partial p}\right) + \vec{V} \cdot \nabla \left(\frac{\partial \psi}{\partial p}\right) + \frac{\sigma}{f_o} \omega = 0 \qquad (2.2)$$

where t is the time, p the pressure, ψ the stream function, f the Coriolis parameter (f_o a standard value), $\vec{V} = k \times \nabla\psi$ the horizontal wind vector, k the unit vertical vector, $\zeta = \nabla^2\psi \equiv \partial^2\psi/\partial x^2 + \partial^2\psi/\partial y^2$ the relative vorticity, $\omega = dp/dt$, $\sigma = -\alpha\, \partial \ln \theta/\partial p$ a measure of the static stability, α being the specific volume and θ the potential temperature. In our Cartesian coordinate system x increases to the east and y to the north.

In (2.1) we have neglected the vertical advection of vorticity and the terms expressing the turning of the vortex tubes (tilting-twisting terms), which is equivalent to neglecting the vertical advection of momentum ($\omega\, \partial u/\partial p$, $\omega\, \partial v/\partial p$) in the two equations of motion from which (2.1) is derived. On the right-hand side of (2.1) we have also assumed the relative vorticity to be negligibly small as compared to f and, for consistency (Wiin-Nielsen, 1959), we have adopted a constant value of f. In (2.2) we have introduced the further approximation that

$$\frac{\partial \phi}{\partial p} = f_o \frac{\partial \psi}{\partial p} \qquad (2.3)$$

where ϕ is the geopotential. The nature of this approximation was discussed by Phillips (1958). Finally, it should be noticed that we have omitted all reference to diabatic heating and friction.

In the following we assume that the flow consists of small perturbations superimposed on a basic zonal current. The perturbations are assumed to be periodic in both the east-west direction and time but independent of the y coordinate, while the speed of the basic zonal current U is assumed to be a function of pressure alone. We can therefore write the stream function for the

total flow as

$$\psi(x,y,p,t) = \psi^{\circ}(y,p) + \psi'(x,p,t) \tag{2.4}$$

$$= -U(p)\,y + \psi'(x,p,t) \tag{2.5}$$

where ψ° is the stream function for the basic flow and ψ' that for the perturbation.

Substituting (2.5) into (2.1) and (2.2) and neglecting products of perturbation quantities we obtain

$$\frac{\partial}{\partial t}\left(\frac{\partial^2\psi'}{\partial x^2}\right) + U\frac{\partial}{\partial x}\left(\frac{\partial^2\psi'}{\partial x^2}\right) + \beta\frac{\partial\psi'}{\partial x} = f_o\frac{\partial\omega'}{\partial p} \tag{2.6}$$

and

$$\frac{\partial}{\partial t}\left(\frac{\partial\psi'}{\partial p}\right) + U\frac{\partial}{\partial x}\left(\frac{\partial\psi'}{\partial p}\right) - \frac{dU}{dp}\frac{\partial\psi'}{\partial x} + \frac{\sigma}{f_o}\omega' = 0 \tag{2.7}$$

where $\beta = df/dy$ is taken to be a constant. We notice that (2.6) and (2.7) are linear partial differential equations containing only two unknowns, ψ' and ω'. Using the method os separation of variables we assume that the solutions have the form

$$\begin{aligned} \psi'(x,p,t) &= \Psi(p)e^{ik(x-ct)} \\ \omega'(x,p,t) &= \Omega(p)e^{ik(x-ct)} \end{aligned} \tag{2.8}$$

where c is the phase speed, $k = 2\pi/L$ is the zonal wave number and L is the wavelength.

Substituting (2.8) into (2.6)and (2.7) we obtain

$$ik[k^2(c-U) + \beta]\Psi - f_o\frac{d\Omega}{dp} = 0 \tag{2.9}$$

and

$$-ik(c-u)\frac{d\Psi}{dp} - ik\frac{dU}{dp}\Psi + \frac{\sigma}{f_o}\Omega = 0 \tag{2.10}$$

from which we can easily eliminate Ψ to arrive at the following differential equation for Ω:

$$(c-U)\left(c-U+\frac{\beta}{k^2}\right)\frac{d^2\Omega}{dp^2}+\left[2(c-U)+\frac{\beta}{k^2}\right]\frac{dU}{dp}\frac{d\Omega}{dp}$$

$$-\frac{k^2\sigma}{f_o^2}\left(c-U+\frac{\beta}{k^2}\right)^2\Omega=0. \qquad (2.11)$$

For convenience we nondimensionalize the independent variable by substituting

$$p = p_* p_o \qquad (0 \leq p_* \leq 1,\ p_o = 1000 \text{ mb}) \qquad (2.12)$$

into (2.11) which then takes the form

$$(c-U)\left(c-U+\frac{\beta}{k^2}\right)\frac{d^2\Omega}{dp_*^2}+\left[2(c-U)+\frac{\beta}{k^2}\right]\frac{dU}{dp_*}\frac{d\Omega}{dp_*}$$

$$-\frac{k^2\sigma p_o^2}{f_o^2}\left(c-U+\frac{\beta}{k^2}\right)^2\Omega=0. \qquad (2.13)$$

Equation (2.13) together with the boundary conditons

$$\Omega = 0 \text{ for } p_* = 0 \text{ and } p_* = 1 \qquad (2.13)$$

constitutes the general eigenvalue problem for Ω and c.

We should recall at this point that the perturbations have been assumed to be independent of the y coordinate. As mentioned in the introduction, this was done only as a matter of convenience since we could also have carried out the analysis by assuming the perturbations to be periodic in the north-south direction as well as in the east-west direction. In fact, it is easy to show that if we had assumed the perturbations to be of the form

$$\psi'(x,y,p,t) = \Psi(p)e^{i(kx + \ell y - kct)}$$

$$\omega'(x,y,p,t) = \Omega(p)e^{i(kx + \ell y - kct)}$$

where ℓ is the north-south wave number, then (2.13) would have taken the same form except that the factor k^2 would have been replaced by $(k^2 + \ell^2)$.

Neglecting the y dependence of the perturbations, our task will then consist in finding the expressions for Ω and c which satisfy both the differential equation (2.13) and the boundary conditions (2.14). Since the speed of the basic zonal wind, U, appears in the coefficients of (2.13), it follows that we must know the analytic expression relating U to p_*. In the following sections we shall assume two different vertical wind profiles. In section 2.2 we consider the case where the basic zonal wind speed does not vary with pressure (i.e., U = constant) which is tantamount, of course, to saying that the basic state is barotropic. We emphasize, however,that even though the basic flow is barotropic the perturbations can still be baroclinic.

After our investigation of the wave disturbances in a barotropic basic state we proceed to an investigation of the wave disturbances in a baroclinic basic flow, that is, one in which the basic zonal wind varies with pressure. In view of the complexity of (2.13) we restrict our study to an atmosphere where U varies linearly with pressure. Even with this simple linear relationship between U and p_*, however, (2.13) is so complex that no exact analytical solution has been found for it. Because of this we proceed by considering special (solvable) cases of (2.13) in an attempt to gain some insight into the behavior of the distrubances. In section 2.3 we assume that U varies linearly with pressure and that $\beta = \sigma = 0$. This case is not a realistic one from the atmospheric point of view but it serves a useful purpose as a basis of comparison for the subsequent, more realistic cases. In section 2.4 we ingestigate the effects of the β term on the characteristics of the disturbances. We do this by essentially repeating our analysis of the previous section except that in section 2.4 we <u>do</u> take the β effect into account. Similarly, in section 2.5 we investigate the effect of the static stability on the disturbances by doing an analysis similar to the one in section 2.3 except that in section 2.5 we include the σ terms in our equations.

2.2 THE CASE U = CONST. > 0, σ = CONST. > 0, β = CONST. > 0

Our treatment of the case where the basic zonal current has no vertical shear and the static stability parameter, σ, is constant follows the one given by Wiin-Nielsen (1962) and differs only slightly from the given by 'Arnason (1961) and Fleagle (1965).

The differential equation for Ω

$$\frac{d^2\Omega}{dp_*^2} + q\,\Omega = 0 \qquad (2.15)$$

where
$$q = -\frac{k^2\sigma p_o^2}{f_o^2} \cdot \frac{c-U+\frac{\beta}{k^2}}{c-U} \tag{2.16}$$

is obtained by simply setting dU/dp_* equal to zero in (2.13).

Considering first the case where

$$q > 0,$$

corresponding to the inequality

$$U - \beta/k^2 < c < U, \tag{2.17}$$

we can then write the solution of (2.15) in the form

$$\Omega = A \sin(\sqrt{q}\, p_*) + B \cos(\sqrt{q}\, p_*) \tag{2.18}$$

where A and B are constants.

Using the boundary conditions (2.14) we then find that B = 0 and

$$\sqrt{q} = m\pi, \qquad m = \pm 1, \pm 2, \ldots \tag{2.19}$$

so that (2.18) becomes

$$\Omega = A \sin(m\pi p_*) \qquad m = \pm 1, \pm 2, \ldots . \tag{2.20}$$

Turning now to the case where

$$q < 0$$

we write the solution to (2.15) in the form

$$\Omega = Ae^{-\sqrt{-q}\, p_*} + Be^{\sqrt{-q}\, p_*} \tag{2.21}$$

The upper boundary condition gives

$$A + B = 0 \tag{2.22}$$

while the lower boundary condition gives

$$Ae^{\sqrt{-q}} + Be^{-\sqrt{-q}} = 0 \tag{2.23}$$

To satisfy (2.22) and (2.23) simultaneously we must then have

$$\sinh \sqrt{-q} = 0$$

which cannot be satisfied for any $q < 0$, so that there is no solution to (2.15) satisfying the boundary conditions when q is negative.

Finally, considering the case

$$q = 0 \tag{2.24}$$

we can write the solution to (2.15) as

$$\Omega = Ap_* + B.$$

Using the boundary conditions we then find that $A = B = 0$ so that in this case the solution is

$$\Omega = 0. \tag{2.25}$$

The complete solution to (2.15), obtained by combining (2.25) for the case $q = 0$ and (2.20) for the case $q > 0$, can then be written in the form

$$\Omega = A \sin (m\pi p_*), \qquad m = 0, \pm 1, \pm 2, \ldots \tag{2.26}$$

which is merely (2.20) plus the case $m = 0$.

We see from (2.19) and (2.24) that the possible values of q are given by

$$\sqrt{q} = m\pi, \qquad m = 0, \pm 1, \pm 2, \ldots \tag{2.27}$$

Substituting (2.27) into (2.16) we then obtain the following expression for the phase speed:

$$c = U - \frac{\beta/k^2}{1 + \dfrac{m^2\pi^2 f_o^2}{p_o^2 k^2 \sigma}} \qquad m = 0, \pm 1, \pm 2 \ldots \tag{2.28}$$

In Figure 1 the phase speed is given as a function of the wavelength, $L = 2\pi/k$, for the vertical modes $m = 0$, 1 and 2. We emphasize that for the mode $m = 0$ we have $\omega = 0$ but that for the modes $m = 1$ and 2, ω has a sinusoidal variation with pressure (see 2.26). By the equation of continuity,

$$\frac{\partial u}{\partial x} + \frac{\partial v}{\partial y} = - \frac{\partial \omega}{\partial p} ,$$

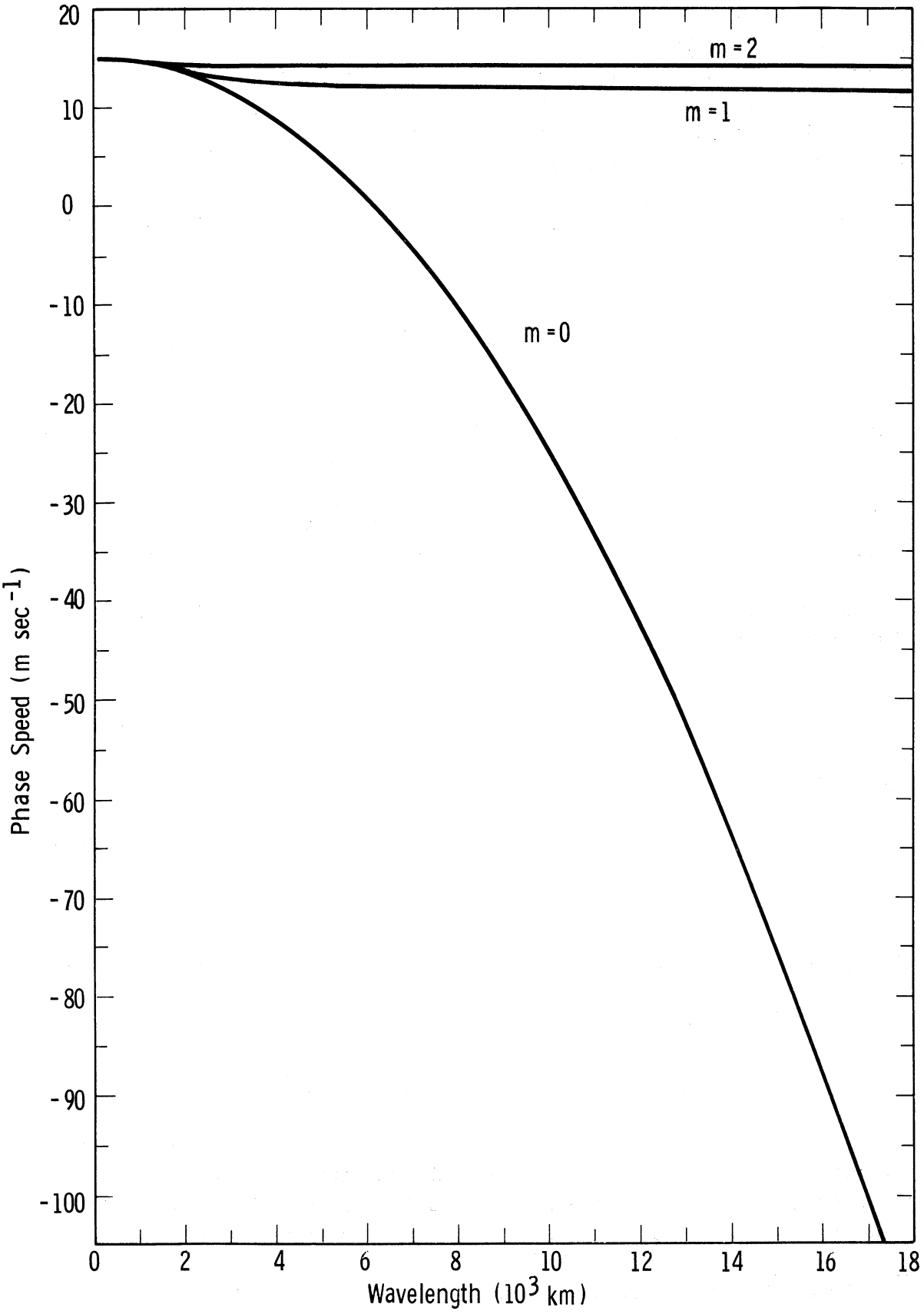

Figure 1. Phase speed as a function of the wavelength for the vertical modes m = 0, 1 and 2. Parameters: U = 15 m sec^{-1}, σ = 2MTS units, $\beta = 16 \times 10^{-12}$ m^{-1} sec^{-1}.

this means that the horizontal divergence $\partial u/\partial x + \partial v/\partial y$ is identically zero for $m = 0$ but not for $m = 1, 2$. As can be seen from Figure 1, the very short waves travel at about the same speed for all modes but the ultra-long waves, on the other hand, do not. For the nondivergent mode ($m = 0$) the ultra-long waves travel westward very rapidly whereas for the divergent modes they are found to travel eastward somewhat more slowly than the basic current.

Turning now to the structure of the waves, we note from (2.26) and (2.8) that[1]

$$\omega(x,p_*,t) = A \sin (m\pi p_*) e^{ik(x-ct)} \tag{2.29}$$

so that

$$\omega_r(x,p_*,t) = A \sin (m\pi p_*) \cos k(x-ct). \tag{2.30}$$

In (2.30) and the following equations we use the subscripts r and i to denote the real and imaginary parts, respectively, of a complex quantity.

By substituting ω from (2.29) and c from (2.28) into (2.9) we then find the following expression for $\Psi(p_*)$:

$$\Psi(p_*) = - i D \cos (m\pi p_*) \tag{2.31}$$

where

$$D = \frac{Af_o m\pi}{\beta p_o k} \left(1 + \frac{p_o^2 k^2 \sigma}{m^2\pi^2 f_o^2}\right) \tag{2.32}$$

Combining (2.31) and (2.8) we then find that the real part of the stream function is given by

$$\psi_r(x,p_*,t) = D \cos (m\pi p_*) \sin k (x-ct). \tag{2.33}$$

We see from (2.30) and (2.33) that both the vertical velocity and the stream function waves have amplitudes which vary with pressure but not with time so that the disturbances are neutral.[2] In addition we notice that the two waves

1. From now on we will omit the primes on $\omega(x,p_*,t)$ and $\psi(x,p_*,t)$.

2. As is commonly done in the meteorological literature, we use the terms "stable" and "neutral" synonymously to characterize waves whose amplitudes are independent of time.

have ridge (or trough) lines which are displaced horizontally from each other by half a wavelength. As an example, the case for which m = 1 is depicted in Figure 2 in the form of a vertical cross-section.

So far we have seen that when the speed of the basic zonal wind is constant all the waves are stable and propagate with a speed which depends on both the vertical mode and the wavelength. In the remaining sections of this chapter we shall investigate the stability and structure of wave disturbances in an atmosphere where U is no longer a constant but rather varies linearly with pressure.

2.3 THE CASE $dU/dp_* = \text{CONST.} < 0$, $\sigma = \beta = 0$

2.3.1 The Stability Analysis

As a first step in our study of wave disturbances in an atmosphere where the basic zonal wind varies linearly with pressure, we shall consider a very simple model in which the basic state has a dry adiabatic lapse rate (i.e. $\sigma = 0$) and in which the variation of the Coriolis parameter with latitude is neglected (i.e. $\beta = 0$). We know from earlier investigations of similar models by Fjørtoft (1950) and 'Arnason (1963) that the case we are about to present is unrealistic from the atmospheric point of view. We shall nevertheless investigate it in some detail, considering it as a control case to be used as a basis of comparison for the subsequent, more realistic cases.

For the present case the differential equation relating the amplitude of the ω wave to the pressure, obtained by setting σ and β equal to zero in (2.13), takes the form

$$(c-U)\frac{d^2\Omega}{dp_*^2} + 2\frac{dU}{dp_*}\frac{d\Omega}{dp_*} = 0. \qquad (2.34)$$

If we now assume that the variation of the basic zonal wind with pressure is given by

$$U(p_*) = U_0 + U_T(1 - p_*) \qquad (2.35)$$

where U_0 is the constant value of the zonal wind speed at the lower boundary and

$$U_T = -\frac{dU}{dp_*} = \text{constant}, \qquad (2.36)$$

we can then rewrite (2.34) as

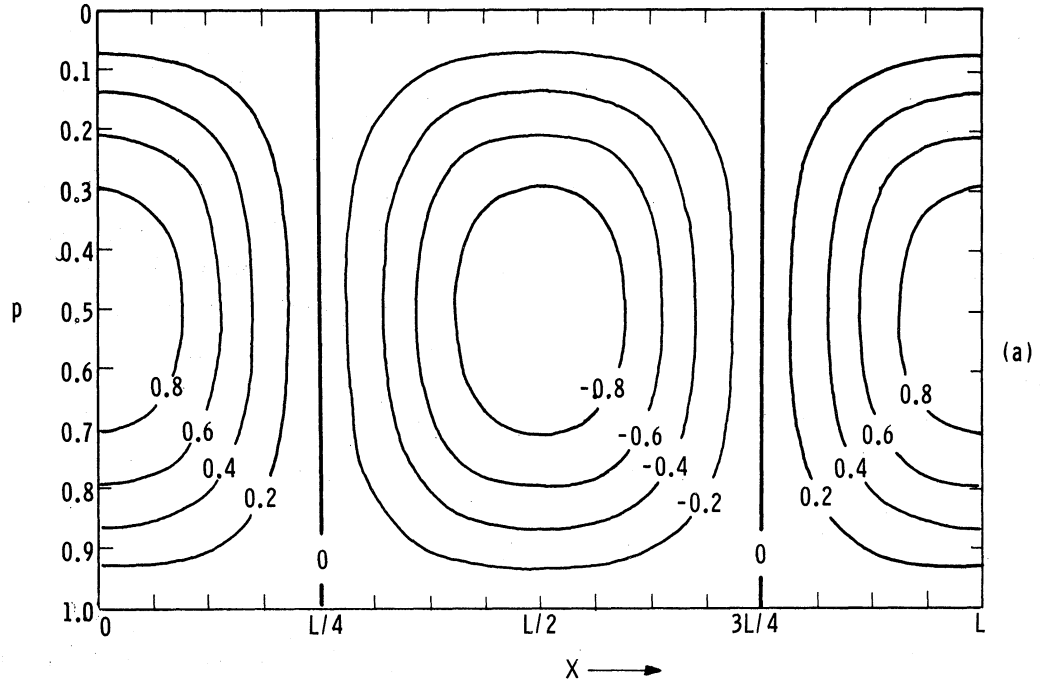

Figure 2(a). Cross-section showing ω as a function of p_* and x for the mode m = 1. The values have been normalized so that the maximum is 1. Parameters: σ = 2MTS units, $\beta = 16 \times 10^{-12}$ m^{-1} sec^{-1}.

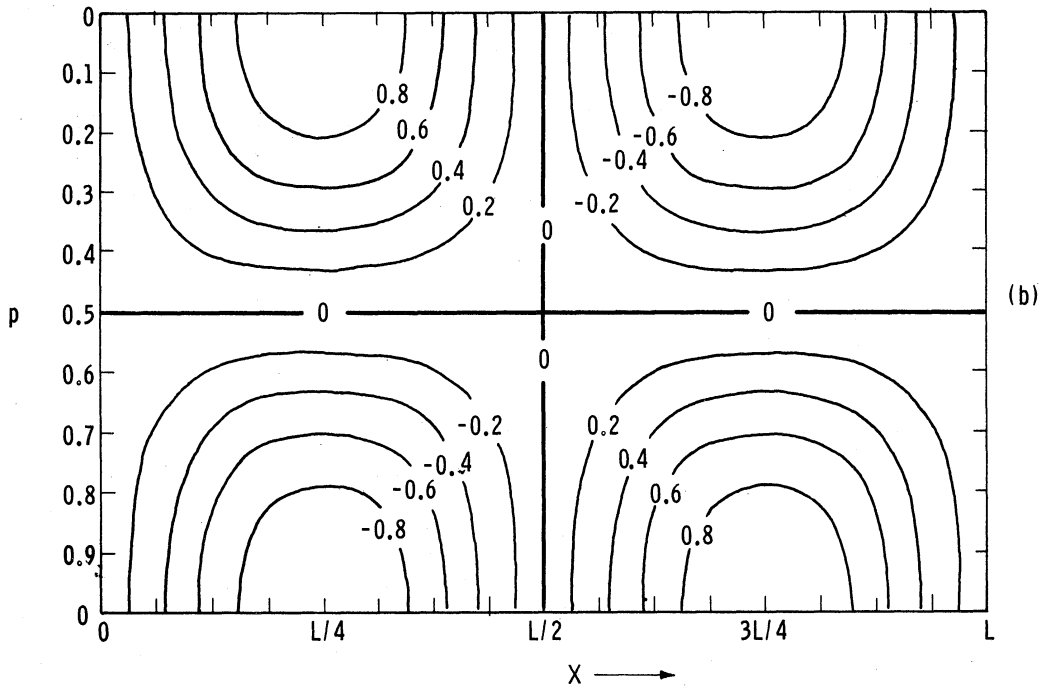

Figure 2(b). Cross-section showing ψ as a function of p_* and x for the mode m = 1. The values have been normalized so that the maximum is 1. Parameters: σ = 2MTS units, $\beta = 16 \times 10^{-12}$ m^{-1} sec^{-1}.

$$(p_* - 1 + c_*)\frac{d^2\Omega}{dp_*^2} - 2\frac{d\Omega}{dp_*} = 0 \tag{2.37}$$

where $c_* = \dfrac{c-U_o}{U_T}$. (2.38)

The solution of (2.37) is easily found to be

$$\Omega(p_*) = A(p_* - 1 + c_*)^3 + B \tag{2.39}$$

where A and B are constants. Using the boundary conditions (2.14) we then obtain the system

$$\begin{aligned} -A(1-c_*)^3 + B &= 0 \\ A\,c_*^3 + B &= 0 \end{aligned} \tag{2.40}$$

which has non-trivial solutions provided that the determinant of the coefficients is equal to zero, that is, provided that

$$3c_*^2 - \frac{1}{2} + 1 = 0$$

or

$$c_*^{\pm} = \frac{1}{2} \pm i\frac{\sqrt{3}}{6}. \tag{2.41}$$

If we then eliminate c_* between (2.38) and (2.41) we find that the phase speed is given by

$$c^{\pm} = U_o + \frac{1}{2}\,U_T \pm i\,\frac{\sqrt{3}}{6}\,U_T \quad . \tag{2.42}$$

Alternately we can rewrite (2.42) as

$$c^{\pm} = U(1/2) \pm i\,\frac{\sqrt{3}}{6}\,U_T \tag{2.43}$$

since by (2.35)

$$U_o + \frac{1}{2}\,U_T = U(1/2) \quad .$$

When c is complex, as in (2.43), we can write ω as

$$\omega(x,p_*,t) = \Omega(p_*)\, e^{ik(x-ct)} =$$

$$[\Omega(p_*)\, e^{kc_i t}] \cdot e^{ik(x-c_r t)} \qquad (2.44)$$

which shows that the disturbance travels in the x direction at a speed given by c_r and undergoes a change in amplitude at a rate determined by kc_i. We note from (2.43) that for the very simple case treated in this section <u>all</u> waves travel at a speed given by U(1/2), the speed of the basic zonal current at $p_* = 1/2$ (p = 500 mb).

In discussing unstable waves, we will use the "e-folding" time T, defined as the time required for the amplitude of the wave to change by a factor e, as a convenient measure of the instability. We see from the expression within the square brackets in (2.44) that

$$T = \frac{1}{kc_i^+} \qquad (2.45)$$

which, after substitution for c_i^+ from (2.43), takes the form

$$T = \frac{2\sqrt{3}}{kU_T} \quad . \qquad (2.46)$$

Using the hydrostatic equation we can express U_T as

$$U_T \equiv -\frac{dU}{dp_*} = \frac{p_o}{g\rho}\frac{dU}{dZ} \qquad (2.47)$$

where g is the acceleration of gravity (9.8 m sec^{-2}), ρ is the density and Z is the height above ground. If we use a constant representative value of 0.5 x 10^{-3} t m^{-3} for ρ and take p_o = 1000 mb, (2.47) can then be written in the simple form

$$U_T = 20\,\frac{dU}{dZ} \qquad (2.48)$$

where U_T is in m sec^{-1} and dU/dZ is in m sec^{-1} km^{-1}. Finally, substituting (2.48) into (2.46) we obtain

$$\frac{dU}{dZ} = 0.32 \frac{\ell}{T_d} \qquad (2.49)$$

where T_d is the e-folding time in days and ℓ is the wavelength in thousands of km.

Figure 3 is the usual stability diagram showing the graph of (2.49) for various values of the e-folding time T. We note that all waves are unstable but for a given wind shear the short waves are the most unstable. In addition we see that the greater the wind shear the greater the instability. This model is obviously not realistic from the atmospheric point of view since it shows that the e-folding time approaches zero as the wavelength approaches zero, indicating that even with a very small wind shear the short waves would amplify with an extreme rapidity (the so-called "ultraviolet catastrophe"). As we shall see in sections 2.5 and 3.4, this "ultraviolet catastrophe" can be removed by considering an atmosphere which is either statically stable ($\sigma > 0$) or not quasi-geostrophic.

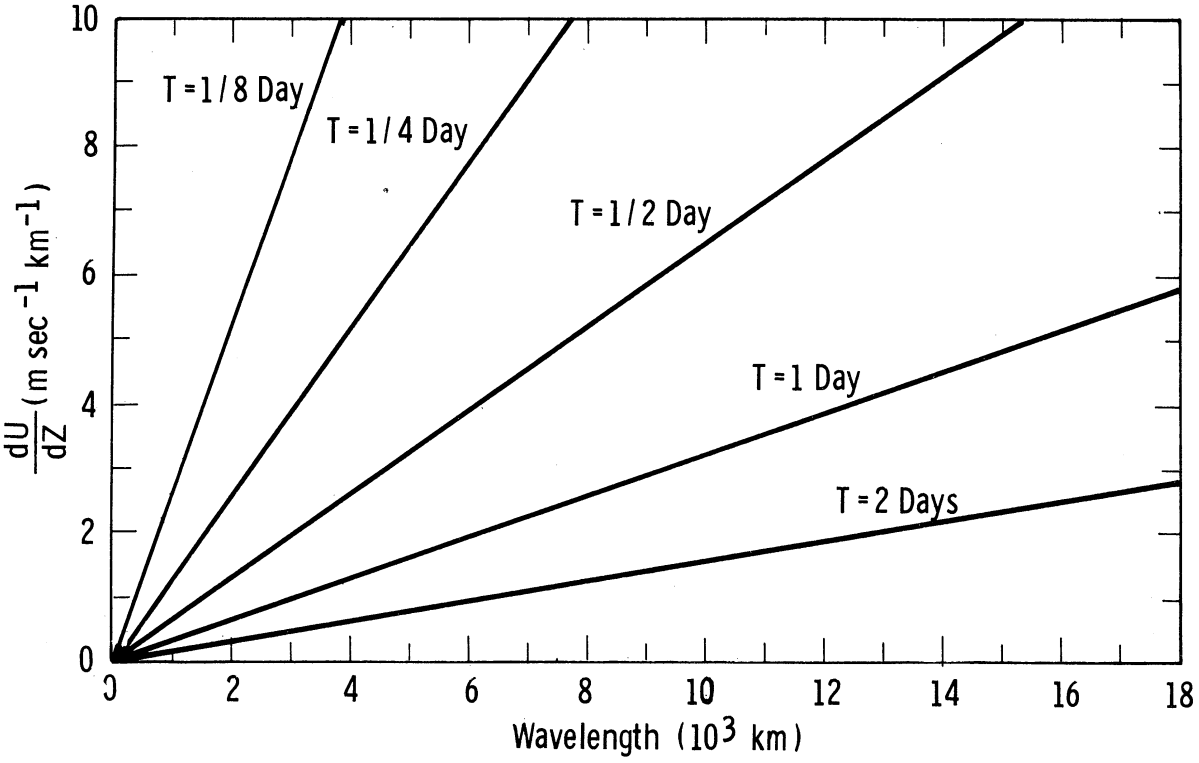

Figure 3. Stability diagram showing the variation of the e-folding time T as a function of the vertical wind shear and the wavelength. Parameters: $\beta = \sigma = 0$.

2.3.2 THE WAVE STRUCTURE

If we substitute the expression for c_* from (2.41) and that for B from the second part of (2.40) into (2.39) we obtain, after some manipulation,

$$\Omega^{\pm}(p_*) = Ap_*(p_* - 1)\left(p_* - \frac{1}{2} \pm \frac{i\sqrt{3}}{2}\right) \tag{2.50}$$

so that ω_r, the real part of $\Omega(p_*)e^{ik(x-ct)}$, can be written in the form

$$\omega_r^{\pm} = Ae^{kc_i^{\pm}t}\, p_*(1-p_*)\left[\left(\frac{1}{2} - p_*\right)\cos k\,(x-c_r t) \pm \frac{\sqrt{3}}{2}\,\sin k\,(x - c_r t)\right]$$

or

$$\omega_r^{\pm} = D^{\pm}\cos\left[k(x-c_r t) - \alpha^{\pm}\right] \tag{2.51}$$

where
$$D^{\pm} = Ae^{kc_i^{\pm}t}p_*(1-p_*)(p_*^2 - p_* + 1)^{1/2} \tag{2.52}$$

and
$$\alpha^{\pm} = \tan^{-1}\left[\frac{\pm\sqrt{3}}{1 - 2p_*}\right]. \tag{2.53}$$

In (2.51) the upper and lower signs correspond to the amplifying ($c_i > 0$) and damped waves ($c_i < 0$), respectively. The same notation will be used in all our discussions of unstable waves.

To find an expression for the stream function $\psi(x,p_*,t)$ we first eliminate $\Omega(p_*)$ between (2.50) and (2.9), neglecting the Beta term, and obtain

$$\Psi^{\pm}(p_*) = \frac{Af_o}{2ik^3 p_o(c^{\pm}-U)}\left[6p_*^2 - 6p_* + 1 \pm i\sqrt{3}\,(2p_* - 1)\right].$$

We then multiply both sides of this equation by $e^{ik(x-c^{\pm}t)}$, substitute for $c^{\pm}$ from (2.43) and for U_T from (2.48) and finally equate the real parts to obtain

$$\psi^{\pm}(x,p_*,t) = E^{\pm}\cos\left[k(x-c_r t) - \theta^{\pm}\right] \tag{2.54}$$

where

$$E^{\pm} = \frac{20\,A\,f_o\,dU/dZ}{\sqrt{3}\,p_o k^3}\,e^{kc_i^{\pm}t}\,(3p_*^2 - 3p_* + 1) \tag{2.55}$$

and
$$\theta^{\pm} = \tan^{-1}\frac{\left[\sqrt{3}(2p_*-1)\right]}{\pm\sqrt{3}}. \tag{2.56}$$

The variation of the amplitude of ω_r and ψ_r with pressure, as given by (2.52) and (2.55), respectively, can be found in Figure 4(a) where both amplitudes have been normalized to have a maximum value of 1. Since $D^+/|D^+|_{max} = D^-/|D^-|_{max}$ and $E^+/|E^+|_{max} = E^-/|E^-|_{max}$, the normalized amplitudes shown in Figure 4(a) apply to both the amplifying and the damped waves alike. Both curves are symmetric about the point $p_* = 1/2$. We note that it is precisely at this level that the amplitude of the stream function reaches its minimum value, just as in case 1 (see Figure 2).

Figure 4(b) shows the variation with pressure of the phase angles α^+ and θ^+ for the amplifying waves as given by (2.53) and (2.56), respectively. Just as the normalized amplitudes of Figure 4(a), these phase angles are independent of the wavelength. We note that a range of 360 degrees in these phase angles corresponds to a distance L (the wavelength) along the x axis. Thus we see that the amplifying stream function waves, ψ^+, slope westward by 120 degrees or one third of a wavelength from $p_* = 1.0$ to $p_* = 0$. The ω^+ waves, on the other hand, slope westward by only 60 degrees or one sixth of a wavelength in the same pressure interval.

In Figure 5(a) we present a vertical cross-section along the x-axis for the ω^+ wave as obtained from (2.51). Again all the values have been normalized so that the maximum is 1. Figure 5(b) is a similar diagram for the stream function wave ψ^+ as given by (2.54).

2.4 THE CASE $dU/dp_* = \text{CONST.} < 0$, $\beta = \text{CONST.}$, $\sigma = 0$

2.4.1 The Stability Analysis

In this section we investigate the effect of the β term on the stability and structure of baroclinic disturbances. As in section 2.3 we assume that $\sigma = 0$ (dry adiabatic lapse rate) and that the basic zonal wind varies linearly with pressure as given by (2.35). Although our model differs slightly from the one used by Fjørtoft (1950) for a similar study, it yields essentially the same results concerning the effect of the β term on the stability of the waves.

When (2.35) is substituted into (2.13) and σ set equal to zero we find that the differential equation for this case is

$$(p_* + c_* - 1)(p_* + c_* - 1 + C_{R*})\frac{d^2\Omega}{dp_*^2} - [2(p_* + C_* - 1) + C_{R*}]\frac{d\Omega}{dp_*} = 0 \qquad (2.57)$$

where $C_{R*} = \dfrac{\beta}{k^2 U_T}$ (2.58)

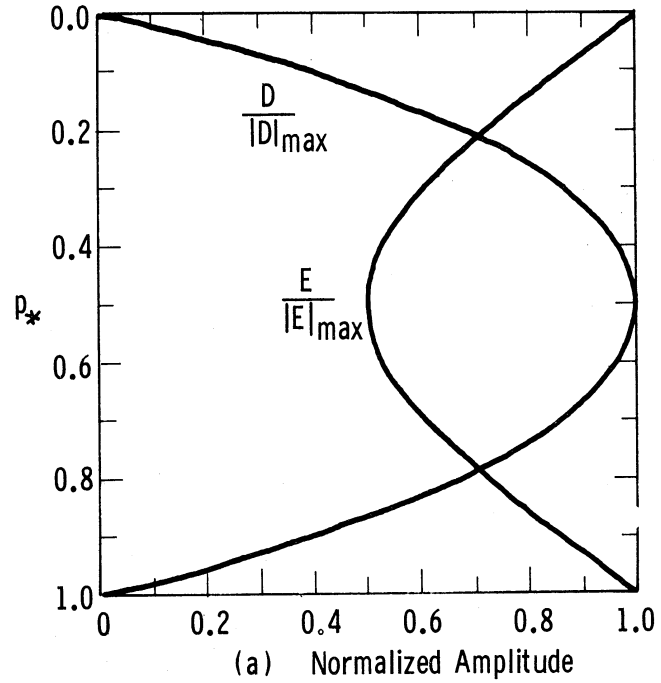

Figure 4(a). Normalized amplitudes of the $\omega\pm$ waves ($D/|D|_{max}$) and of the $\psi\pm$ waves ($E/|E|_{max}$) as functions of pressure. These normalized amplitudes are independent of the wavelength. Parameters: $\sigma = \beta = 0$.

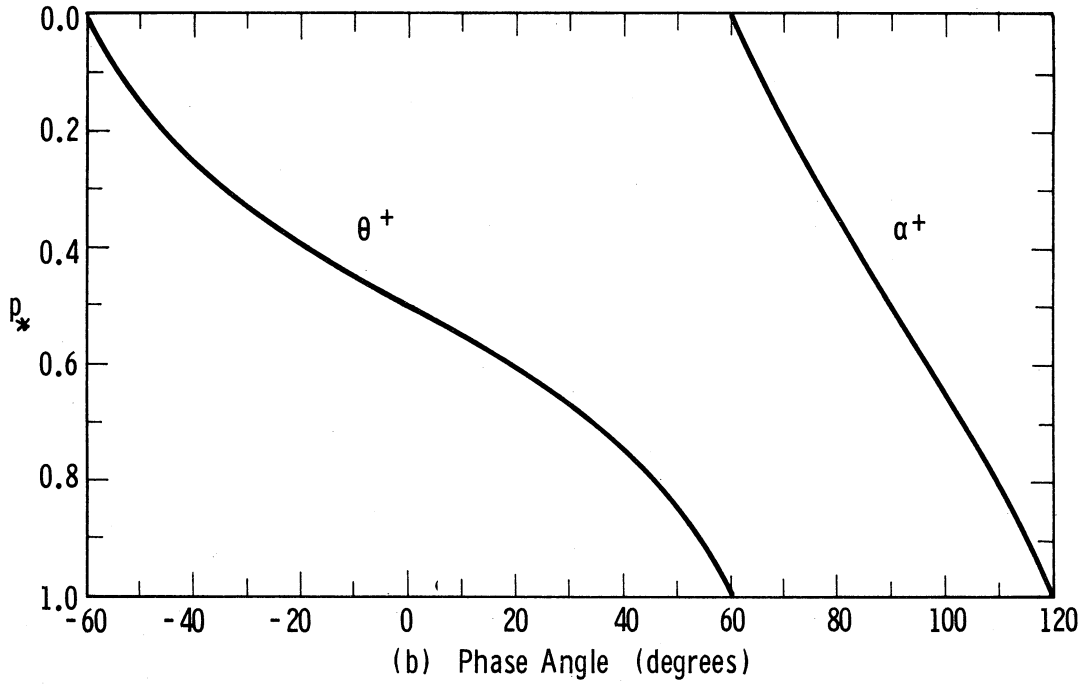

Figure 4(b). Phase angle of the amplifying ω waves ($\alpha+$) and of the amplifying ψ waves ($\theta+$) as function of pressure. These phase angles are independent of the wavelength. An increment of 360 degrees in the abscissa corresponds to a distance of one wavelength along the x axis. Parameters: $\sigma = \beta = 0$.

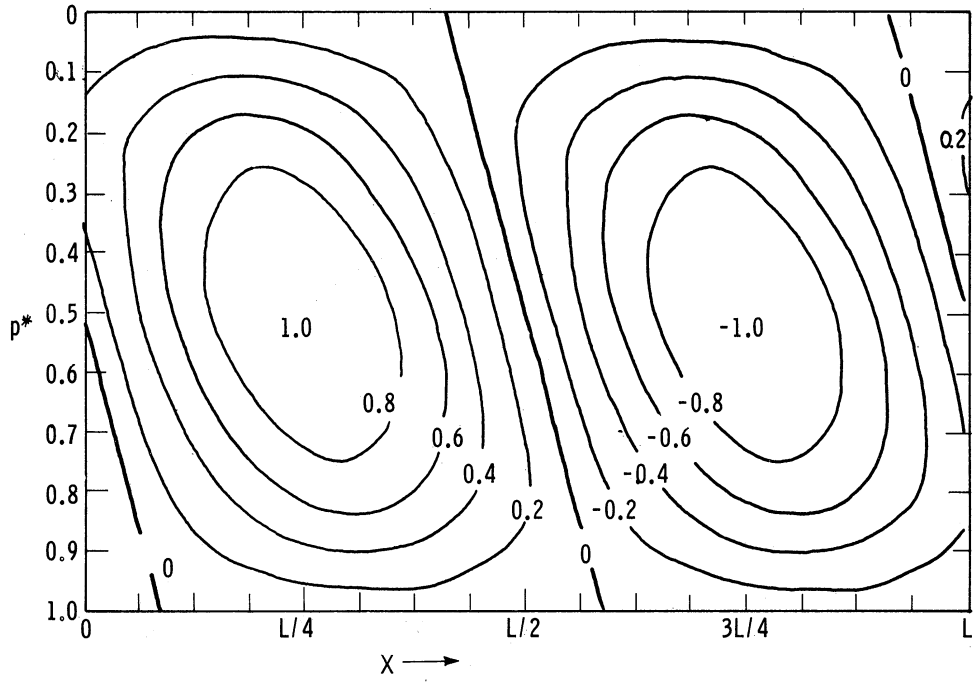

Figure 5(a). Cross-section showing ω^+ as a function of p_* and x. The values have been normalized so that the maximum is 1. Parameters: $\sigma = \beta = 0$.

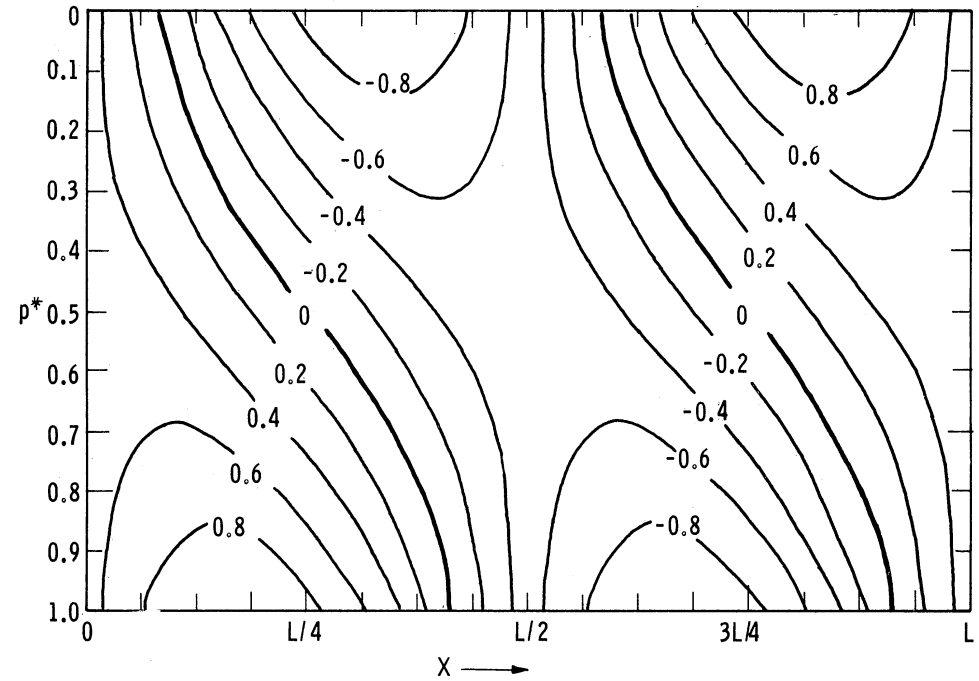

Figure 5(b). Cross-section showing ψ^+ as a function of p_* and x. The values have been normalized so that the maximum is 1. Parameters: $\sigma = \beta = 0$.

and again $c_* = \dfrac{c - U_o}{U_T}$. (2.59)

If we now let

$$\xi = (p_* - 1 + c_*)/C_{R*} \tag{2.60}$$

we can write (2.57) as

$$\xi(\xi + 1) \frac{d^2\Omega}{d\xi^2} - (2\xi + 1) \frac{d\Omega}{d\xi} = 0 \tag{2.61}$$

the solution of which can be found by standard methods to be

$$\Omega = A(\frac{1}{3} \xi^3 + \frac{1}{2} \xi^2) + B \tag{2.62}$$

where A and B are constants. With the new independent variable ξ, the boundary conditons (2.14) become

$$\Omega = 0 \text{ at } \xi = \frac{c_* - 1}{C_{R*}}$$

and (2.63)

$$\Omega = 0 \text{ at } \xi = \frac{c_*}{C_{R*}} .$$

Applying the solution (2.62) at the two boundaries we obtain

$$A[\frac{(c_*-1)^3}{3C_{R*}^3} + \frac{(c_*-1)^2}{2C_{R*}^2}] + B = 0$$

and (2.64)

$$A[\frac{c_*^3}{3C_{R*}^3} + \frac{c_*^2}{2C_{R*}^2}] + B = 0 .$$

This system of equations has non-trivial solutions provided that the determinant of the coefficients is equal to zero, that is, provided that

$$3c_*^2 - 3(1 - C_{R*})\, c_* + (1 - \tfrac{3}{2} C_{R*}) = 0$$

or

$$c_*^{\pm} = \tfrac{1}{2}(1 - C_{R*}) \pm \tfrac{1}{6}\sqrt{3(3C_{R*}^2 - 1)} \quad . \tag{2.65}$$

If we eliminate c_* between (2.65) and (2.59) and note that $C_{R*} = \beta/k^2 U_T$, we obtain the following expression for the phase speed:

$$c^{\pm} = U_o + \tfrac{1}{2} U_T - \frac{\beta}{2k^2} \pm \tfrac{1}{6} [3(3\beta^2/k^4 - U_T^2)]^{1/2}$$

or

$$c^{\pm} = U(\tfrac{1}{2}) - \frac{\beta}{2k^2} \pm \tfrac{1}{6}[3\beta^2/k^4 - U_T^2)]^{1/2} \tag{2.66}$$

since by (2.35) $U_o + \frac{1}{2} U_T = U(1/2)$.

From (2.66) it is easy to see that the perturbations are stable (c real) if $3\beta^2/k^4 - U_T^2 \geq 0$ and unstable (c complex) if $3\beta^2/k^4 - U_T^2 < 0$. The stable and unstable regimes are therefore separated by the condition

$$3\beta^2/k^4 - U_T^2 = 0,$$

which can be written, using (2.48) and $\beta = 16 \times 10^{-12}$ m^{-1} sec^{-1}, as

$$\frac{dU}{dZ} = 0.046\, \ell^2 \tag{2.67}$$

where ℓ is the wavelength in thousands of km and dU/dZ is given in m sec^{-1} km^{-1}. The plot of (2.67) appears as the heavy line labelled "neutral curve" in Figure 6. To the right of this curve we have $3\beta^2/k^4 - U_T^2 > 0$ so that the waves in that region are stable; to the left of the neutral curve, on the other hand, we have $3\beta^2/k^4 - U_T^2 < 0$ and hence the waves in that region are unstable.

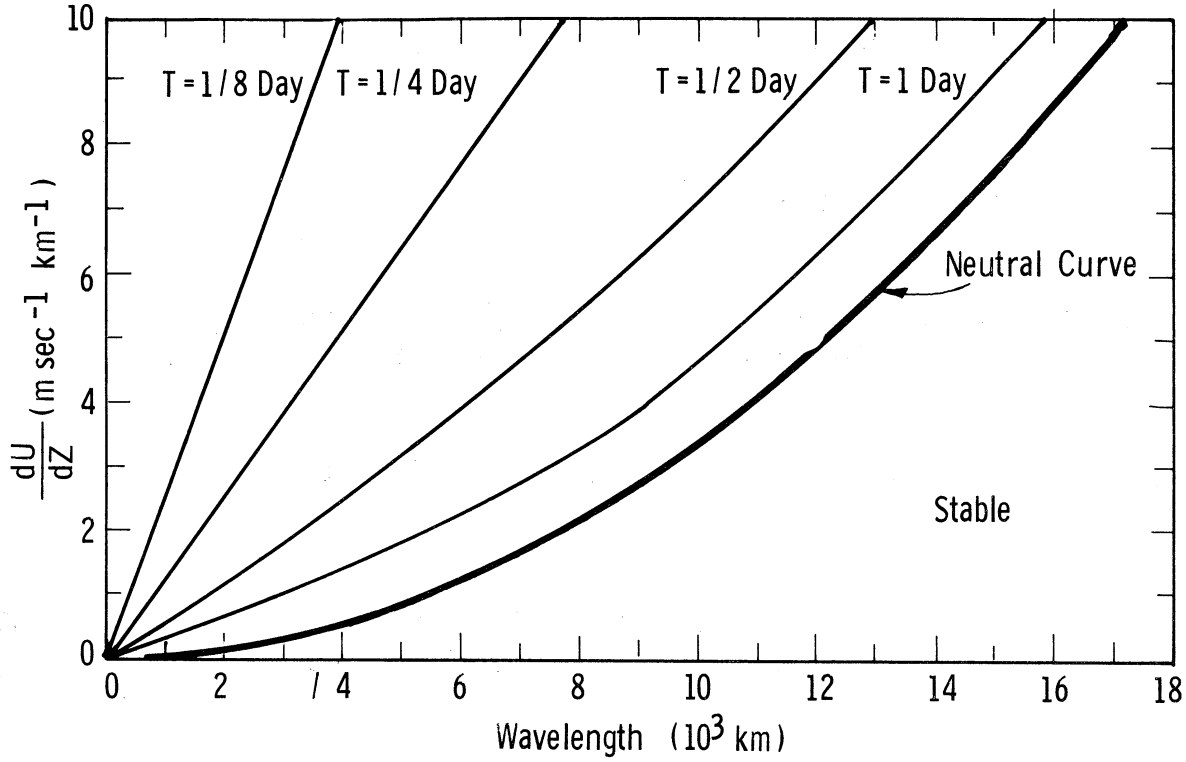

Figure 6. Stability diagram showing the variation of the e-folding time T as a function of the vertical wind shear and the wavelength. Parameters: $\sigma = 0$, $\beta = 16 \times 10^{-12}$ m^{-1} sec^{-1}.

As a measure of the instability we use again the e-folding time given by

$$T = 1/kc_i^+ . \tag{2.68}$$

From (2.66) we see that the positive imaginary part of the phase speed is given by

$$c_i^+ = \frac{1}{6}\left[3(U_T^2 - 3\beta^2/k^4)\right]^{1/2}$$

which can be rewritten, after using (2.48), as

$$c_i^+ = \frac{\sqrt{3}}{6}\left[(20\,\frac{dU}{dZ})^2 - 3\beta^2/k^4\right]^{1/2} \tag{2.69}$$

If we now eliminate c_i^+ between (2.68) and (2.69), noticing that

$$k = \frac{2\pi}{L} = \frac{2\pi}{\ell \times 10^6}$$

$$\beta = 16 \times 10^{-12} \text{ m}^{-1} \text{ sec}^{-1},$$

we obtain

$$\frac{dU}{dZ} = \frac{\sqrt{3}}{10} (0.04\, \ell^2 + 3.35\, T_d^{-2})^{1/2}\, \ell \qquad (2.70)$$

where T_d is the e-folding time in days and ℓ is the wavelength in thousands of km.

Figure 6 illustrates the graph of (2.70) for selected e-folding times ranging from one-eight of a day to one day. We see that to the left of the neutral stability curve, the smaller the wavelength and/or the larger the vertical wind shear, the more pronounced the instability. We recall that a similar result has been obtained in section 2.3.1 where the β term had been neglected. In fact, if we compare the stability diagram for section 2.3.1 (see Figure 3) with the one given in Figure 6, we see that they are nearly identical in the short wave domain; in other words, the β term has practically no effect on the e-folding time of the short waves. The β term does have, on the other hand, the important effect of stabilizing the long waves. We note also from Figure 6 that the range of wavelengths which are stabilized by the β term increases as the vertical wind shear decreases.

We recall from section 2.3.1 that when both the β term and the σ term are neglected all waves are unstable and propagate eastward with a speed $U(1/2)$, the speed of the basic current at $p_* = 1/2$ or $p = 500$ mb. Figure 7 shows the speed of propagation c_r, obtained from 2.66, that is, for the case where the β term is retained. The solid curve was computed using $dU/dZ = 2$ m sec^{-1} km^{-1} and $U(1/2) = 10$ m sec^{-1} to simulate summer conditions while the dashed curve was computed using $dU/dZ = 4$ m sec^{-1} km^{-1} and $U(1/2) = 15$ m sec^{-1} to simulate winter conditons.

We see from (2.66) and Figure 7 that in the unstable domain (i.e. for $3\beta^2/k^4 - U_T^2 < 0$) c_r, the real part of the phase speed, is a single valued function which tends to $U(1/2)$ as the wavelength tends to zero. In other words, as the wavelength tends to zero we revert to the phase speed obtained in the model without the β term. Thus, as was also found to be the case for the e-folding time, the speed of propagation of the very short (unstable) waves is practically unaffected by the β term.

We also see from (2.66) and Figure 7 that in the stable domain (i.e., for $3\beta^2/k^4 - U_T^2 > 0$) c_r is a double valued function of the wavelength. In our notation, c_r^+ and c_r^- refer to the real part of the phase speed obtained by choosing the upper and lower signs, respectively, in (2.66). It is interesting to note that

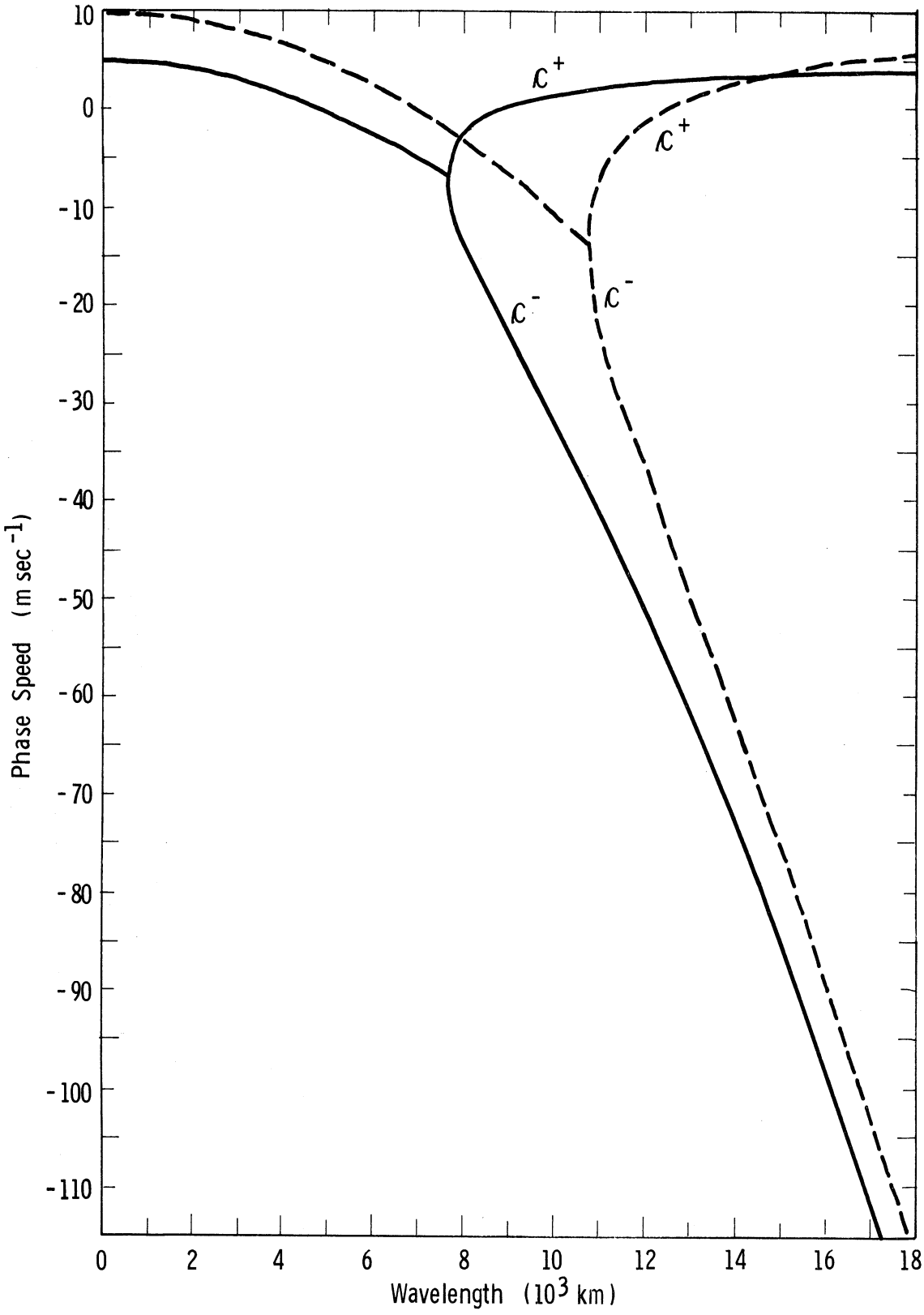

Figure 7. Phase speed as a function of wavelength for the case $\sigma = 0$, $\beta = 16 \times 10^{-12}$ m^{-1} sec^{-1}. For the solid curve $dU/dZ = 2$ m sec^{-1} km^{-1}, $U(1/2) = 10$ m sec^{-1} and $U(1/2) = 15$ m sec^{-1}.

$$c_r^+ \to U(1/2) \text{ and } c_r^- \to -\infty \text{ as } L \to \infty$$

The very long waves, in other words, tend either to propagate eastward at the speed of the basic current at $p_* = 1/2$ ($p = 500$ mb) or to retrogress rapidly just as the non-divergent waves (mode $m = 0$) in section 2.2 (see (2.28) and Figure 1).

2.4.2 The Wave Structure

We can obtain a convenient expression for Ω as a function of p_* by first eliminating ξ and B from (2.62) using (2.60) and the second part of (2.64), respectively, and then eliminating c_* from the resulting equation by means of (2.65). The result is

$$\Omega^{\pm}(p_*) = \frac{A}{6C_{R*}^3} p_*(p_*-1)\,(2p_*-1 \pm \sqrt{3(3C_{R*}^2-1)}) \tag{2.71}$$

where again (see (2.58) and (2.48))

$$C_{R*} = \beta/(k^2 U_T) = \beta/(20k^2 \frac{dU}{dZ}) . \tag{2.72}$$

To obtain $\omega_r(x,p_*,t)$ we multiply both sides of (2.71) by $e^{ik(x-ct)}$ and equate real parts.

For the <u>unstable</u> domain (i.e. for $3C_{R*}^2 - 1 < 0$) the result is

$$\omega_r^{\pm}(x,p_*,t) = D^{\pm} \cos\,[k(x-c_r t) - \alpha^{\pm}] \tag{2.73}$$

where

$$D^{\pm} = \frac{Ae^{kc_i^{\pm}t}}{6C_{R*}^3}\, p_*(1-p_*)\sqrt{4[1-p_*\,(1-p_*)] - 9C_{R*}^2} \tag{2.74}$$

and

$$\alpha^{\pm} = \tan^{-1}\left[\frac{\pm\sqrt{3(1-3C_{R*}^2)}}{1-2p_*}\right] . \tag{2.75}$$

For the <u>stable</u> domain (i.e. for $3C_{R*}^2 - 1 > 0$), on the other hand, we obtain

$$\omega_r^{\pm}(x,p_*,t) = B^{\pm}\cos k(x-c^{\pm}t) \qquad (2.76)$$

where

$$B^{\pm} = \frac{A}{6C_{R*}^3}\, p_*(p_*-1)[2p_*-1\pm 3(3C_{R*}^2-1)]\,. \qquad (2.77)$$

If we refer to Figure 6 we find that for a vertical wind shear dU/dZ of 4 m sec^{-1} km^{-1} any wave with a wavelength of about 10,700 km or less is unstable. The normalized amplitude $D/|D|_{max}$ for each of two unstable waves (L = 6000 km and L = 10,600 km) appears as a function of pressure in Figure 8(a). Since $D^+/|D^+|_{max} = D^-/|D^-|_{max}$, the curves shown in this figure apply to both the amplifying and the damped waves alike. In Figure 8(b) the phase angle α^+ (corresponding to the amplifying wave), as given by (2.75), appears as a function of pressure again for L = 6000 km and L = 10,600 km.

We note that for L = 6000 km the variation with pressure of the amplitude of the $\omega^{\pm}$ waves is very similar to the one given in Figure 4(a) for the case where the β term had been neglected. In addition, Figure 8(b) shows that the ω^+ wave slopes westward with decreasing pressure in very nearly the same manner as the ω^+ wave in Figure 4(b) (curve labelled α^+). We can then conclude that for a wavelength of 6000 km the β term has nearly no effect on the structure of the ω^+ wave.

If we consider a wave with L = 10,600 km, however, we see from Figure 8(a) that the amplitude of the ω^+ waves has two maxima, one at about p_* = 0.25 (p = 250 mb) and the other at about p_* = 0.75 (p = 750 mb). From Figure 8(b) we notice that as the wavelength of the unstable ω^+ disturbances increases their slope with pressure also increases. We should keep in mind, here, that a range of 360 degrees in the abscissa of Figure 8(b) corresponds to one wavelength.

A cross-section showing ω^+, for L = 10,600 km, as a function of p_* and x can be found in Figure 9. This cross-section should be compared with the one appearing in Figure 5(a) for the case when the β term is neglected. Again we see the two-fold effect of the β term on the structure of the ω^+ wave, namely, the increase in slope with pressure and the change from a single maximum in the amplitude at p_* = 1/2 (p = 500 mb) to two maxima, one at p_* = 0.25 (p = 250 mb) and the other at p_* = 0.75 (p = 750 mb).

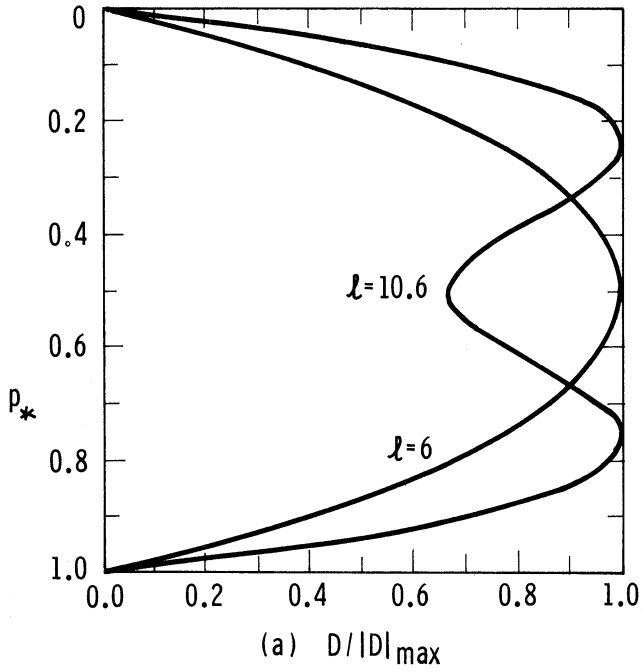

Figure 8(a). Normalized amplitude of the unstable $\omega \pm$ waves as a function of pressure for wavelengths of 6000 km and 10,600 km. Parameters: $\sigma = 0$, $\beta = 16 \times 10^{-12}$ m^{-1} sec^{-1}, $dU/dZ = 4$ m sec^{-1} km^{-1}.

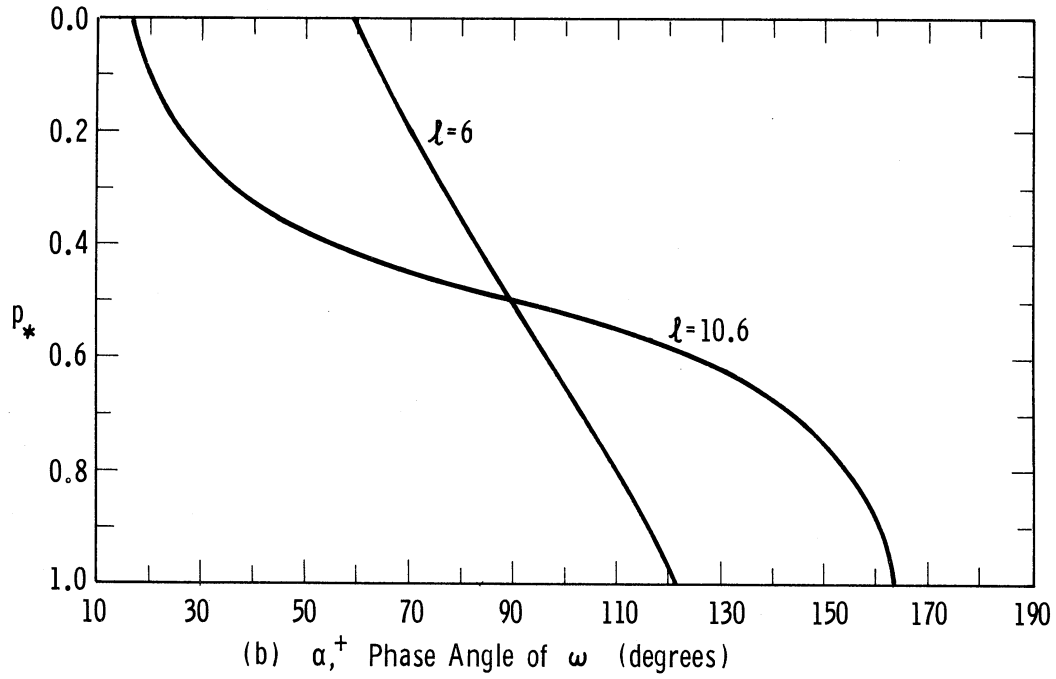

Figure 8(b). Phase angle of the amplifying ω wave as a function of pressure for wavelengths of 6000 km and 10,600 km. Parameters: $\sigma = 0$, $\beta = 16 \times 10^{-12}$ m^{-1} sec^{-1}, $dU/dZ = 4$ m sec^{-1} km^{-1}.

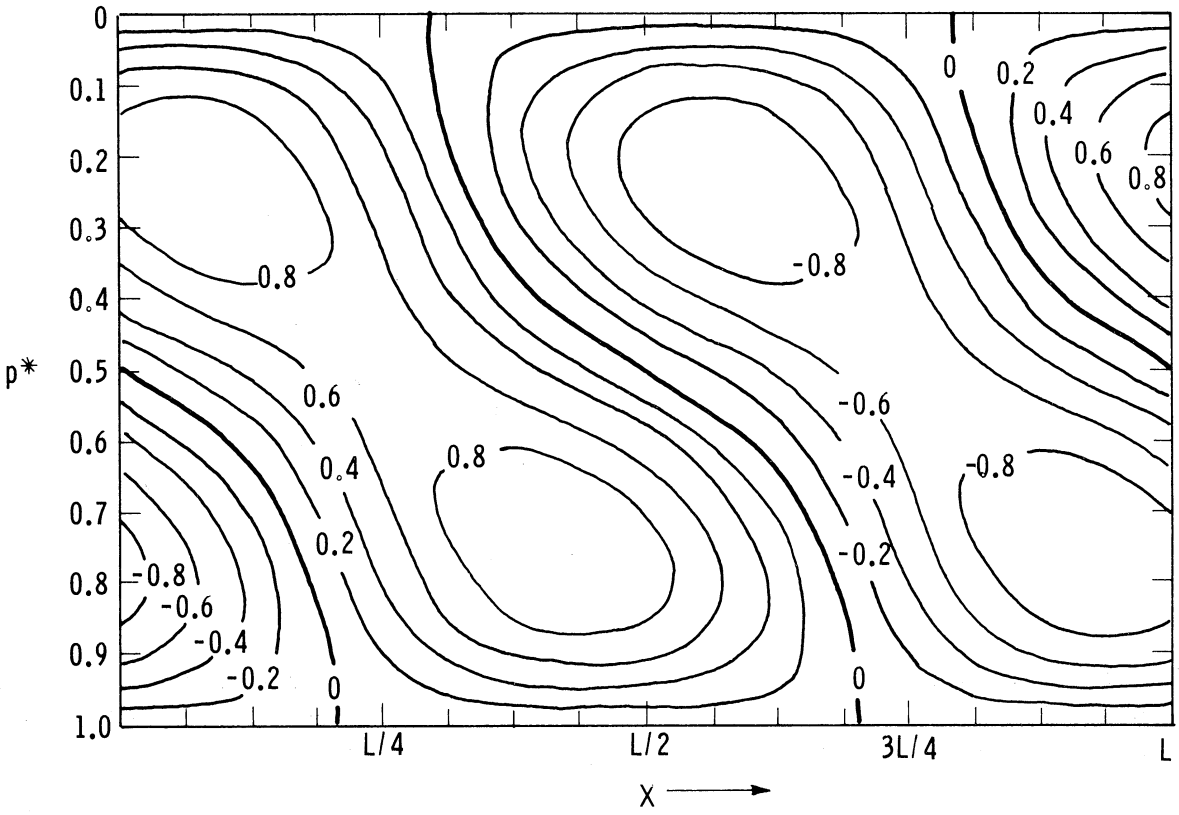

Figure 9. Cross-section showing ω^+ as a function of p_* and x for a wavelength of 10,600 km. The values have been normalized so that the maximum as 1. Parameters: $\sigma = 0$, $\beta = 16 \times 10^{-12}$ m^{-1} sec^{-1}, $dU/dZ = 4$ m sec^{-1} km^{-1}.

Having examined the structure of some unstable ω waves, we now turn our attention to the longer, stable $\omega^{\pm}$ waves whose structure is given by (2.76) and (2.77). First we notice from (2.76) that these stable waves do not slope with pressure, just as the stable waves of section 2.2. Moreover, we note that for a given wavelength we have two wave solutions to our equations, one given by $B^+ \cos k(x-c^+t)$ and the other by $B^- \cos k(x-c^-t)$. We recall that both phase speeds, c^+ and c^-, are functions of the wavelength and that $c^+ \geq c^-$ (see Figure 7). The normalized amplitudes for ω, $B^+/|B^+|_{max}$ and $B^-/|B^-|_{max}$, appear as functions of pressure in Figure 10(a) and (b), respectively, for three different wavelengths. The curve labelled ℓ_N in each diagram gives the normalized amplitude of a wave on the neutral stability curve, where $3\beta^2/k^4U_T^2 - 1 = 0$ or $3C_{R*}^2 - 1 = 0$ (see the equations preceding (2.67)). We see from (2.77) that for the wavelength ℓ_N we have $B^+/|B^+|_{max} = B^-/|B^-|_{max}$, as is also evident in Figure 10(a) and (b). For this wavelength B^+ and B^- are large and positive at $p_* = 0.2$ (p = 200 mb), zero at $p_* = 1/2$ (p = 500 mb) and large and negative at $p_* = 0.8$ (p = 800 mb). For a wavelength of 18,000 km, however, we note that B^+ has a single minimum at about $p_* = 0.55$ (p = 550 mb) while B^- has a single maximum at about $p_* = 0.45$ (p = 450 mb).

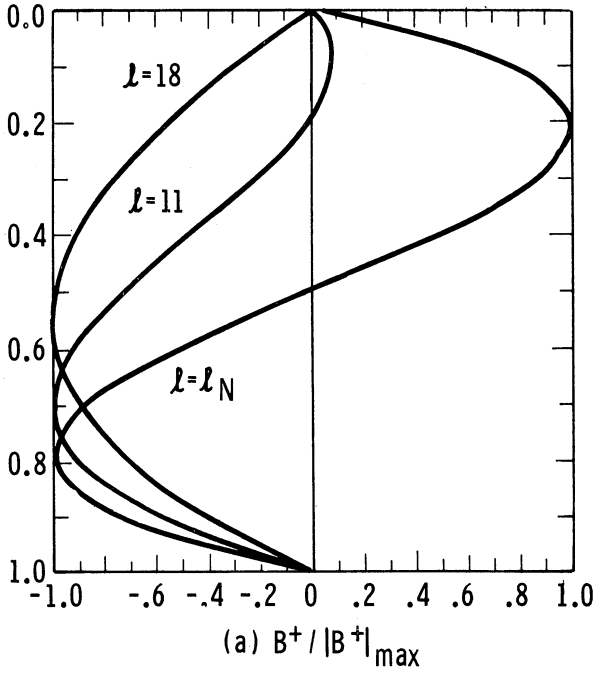

Figure 10(a). Normalized amplitudes of the stable ω^+ wave as a function of pressure. The curve labeled l_N refers to a wave on the neutral stability curve. Parameters: $\sigma = 0$, $\beta = 16 \times 10^{-12}$ m^{-1} sec^{-1}, $dU/dZ = 4$ m sec^{-1} km^{-1}.

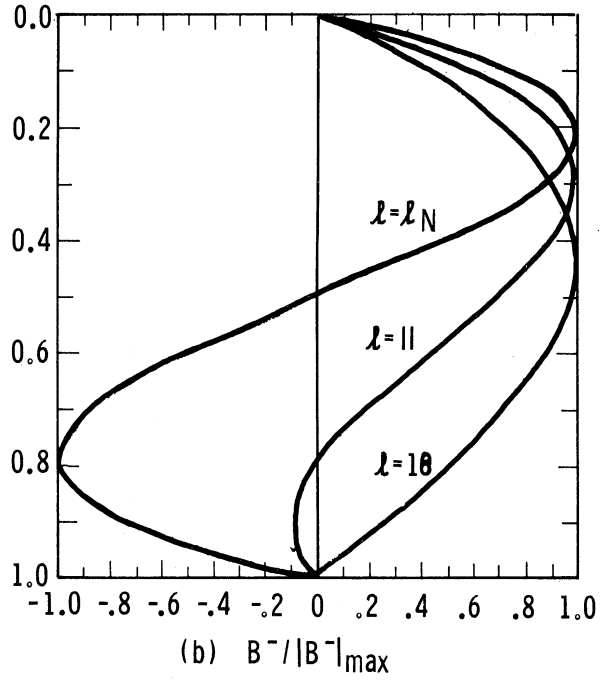

Figure 10(b). Same as Figure 10(a) but for the stable ω^- wave.

Our next step is to study the structure of the ψ waves. A convenient expression for $\psi(x,p_*,t)$ can be obtained by first eliminating $\Omega(p_*)$ between (2.9) and (2.71) and then substituting for c from (2.66). Finally we multiply the resulting equation for $\Psi(p_*)$ by $e^{ik(x-ct)}$ and equate the real parts.

For the unstable domain (i.e. when $3C_{R*}^2 - 1 < 0$) the result is

$$\psi_r^{\pm}(x,p_*,t) = F^{\pm} \cos [k(x-c_r t) - \theta^{\pm}] \tag{2.78}$$

where

$$F^{\pm} = \frac{Af_o e^{kc_i^{\pm} t}}{6C_{R*}^3 p_o [c_i^2 + (c_r - U + \beta/k^2)^2]} \cdot \sqrt{a_1^2 + a_2^2} \tag{2.79}$$

$$\theta^{\pm} = \tan^{-1} \left[\frac{a_2}{a_1^{\pm}}\right] \tag{2.80}$$

$$a_1^{\pm} = -c_i^{\pm}(6p_*^2 - 6p_* + 1) \pm (c_r - U + \beta/k^2) \sqrt{3(1-3C_{R*}^2)}(2p_* - 1) \tag{2.81}$$

$$a_2 = (c_r - U + \beta/k^2)(6p_*^2 - 6p_* + 1) \mp c_i^{\pm} \sqrt{3(1-3C_{R*}^2)}(2p_* - 1) \tag{2.82}$$

and c_r and $c_i^{\pm}$ can be obtained from (2.66).

For the stable domain (i.e. when $3c_{R*}^2 - 1 > 0$), obtain

$$\psi_r^{\pm}(x,p_*,t) = G^{\pm} \sin k(x-c^{\pm}t) \tag{2.83}$$

where

$$G^{\pm} = \frac{Af_o}{C_{R*}^3 p_o k^3 U_T} \cdot \frac{6p_*^2 \pm \sqrt{3(3C_{R*}^2 - 1)}(2p_* - 1) - 6p_* + 1}{6p_* \pm \sqrt{3(3C_{R*}^2 - 1)} + 3(C_{R*} - 1)} \tag{2.84}$$

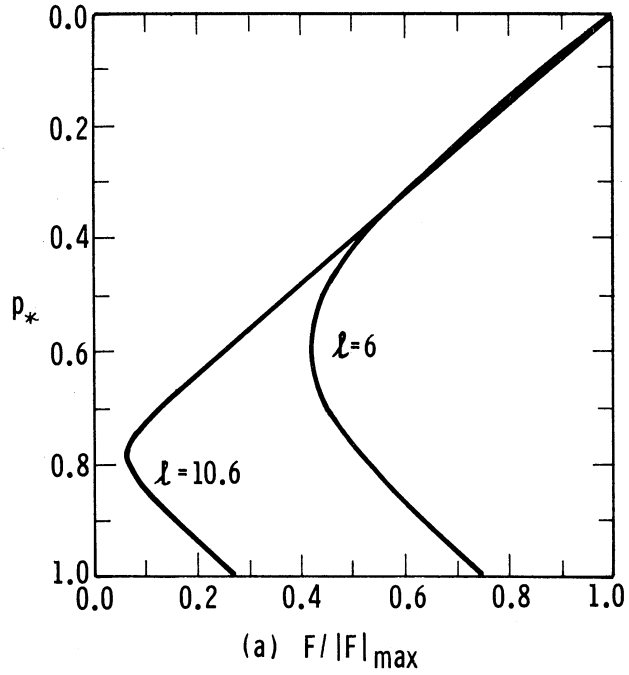

Figure 11(a). Normalized amplitude of the unstable $\psi^{\pm}$ waves as a function of pressure for wavelengths of 6000 km and 10,600 km. Parameters: $\sigma = 0$, $\beta = 16 \times 10^{-12} m^{-1} sec^{-1}$, $dU/dZ = 4$ m sec^{-1} km^{-1}.

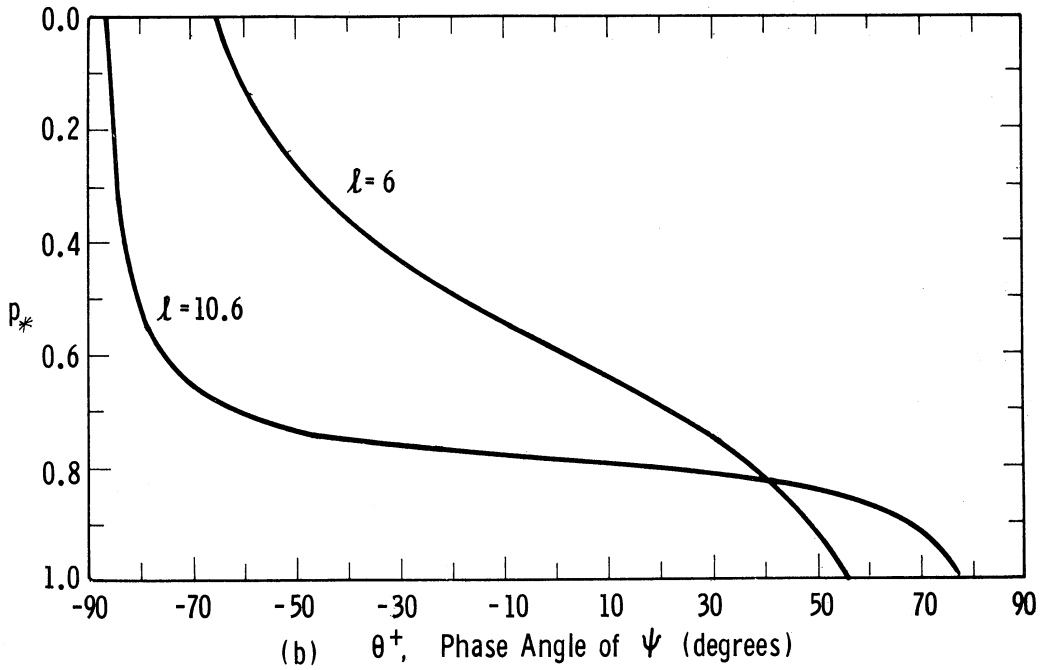

Figure 11(b). Phase angle of the amplifying ψ wave as a function of pressure for wavelengths of 6000 km and 10,600 km. Parameters: $\sigma = 0$, $\beta = 16 \times 10^{-12}$ m^{-1} sec^{-1} $dU/dZ = 4$ m sec^{-1} km^{-1}.

We see from (2.79) that for a given wavelength the normalized amplitude of the amplifying wave, $F^+/|F^+|_{max}$, is identical to the normalized amplitude of the damped wave, $F^-/|F^-|_{max}$. This normalized amplitude, denoted by $F/|F|_{max}$ for convenience, appears as a function of pressure in Figure 11(a) for wavelenths of 6000 km and 10,600 km. For both wavelengths the maximum in the amplitude appears at $p_* = 0$, while the minimum progresses to higher pressures as the wavelength increases. The slope of these waves with pressure is given by (2.80). Figure 11(b) shows the plot of θ^+, the phase angle of the amplifying wave, as a function of pressure for the same wavelengths as above.

To find the effect of the β term on the structure of the amplifying ψ waves, we compare the curves of Figure 11 to those referring to the stream function in Figure 4. For a wavelength of 6000 km we note that the main effect of the β terms is to modify the variation of the amplitude with pressure whereas only a small effect can be found on the slope of the wave. The other curves in Figure 11 reveal that the β term becomes more important as the wavelength increases. The wave with L = 10,600 km is seen to be quite different from the one shown in Figure 4 in the variation of both the amplitude and the phase angle with pressure. A cross-section of this wave can be found in Figure 12. The effects of the β term can again be visualized by comparing this cross-section to the one found in Figure 5(b). We note in particular the difference in the amplitudes near $p_* = 1.0$ (p = 1000 mb) and in the slopes near $p_* = 0.8$ (p = 800 mb).

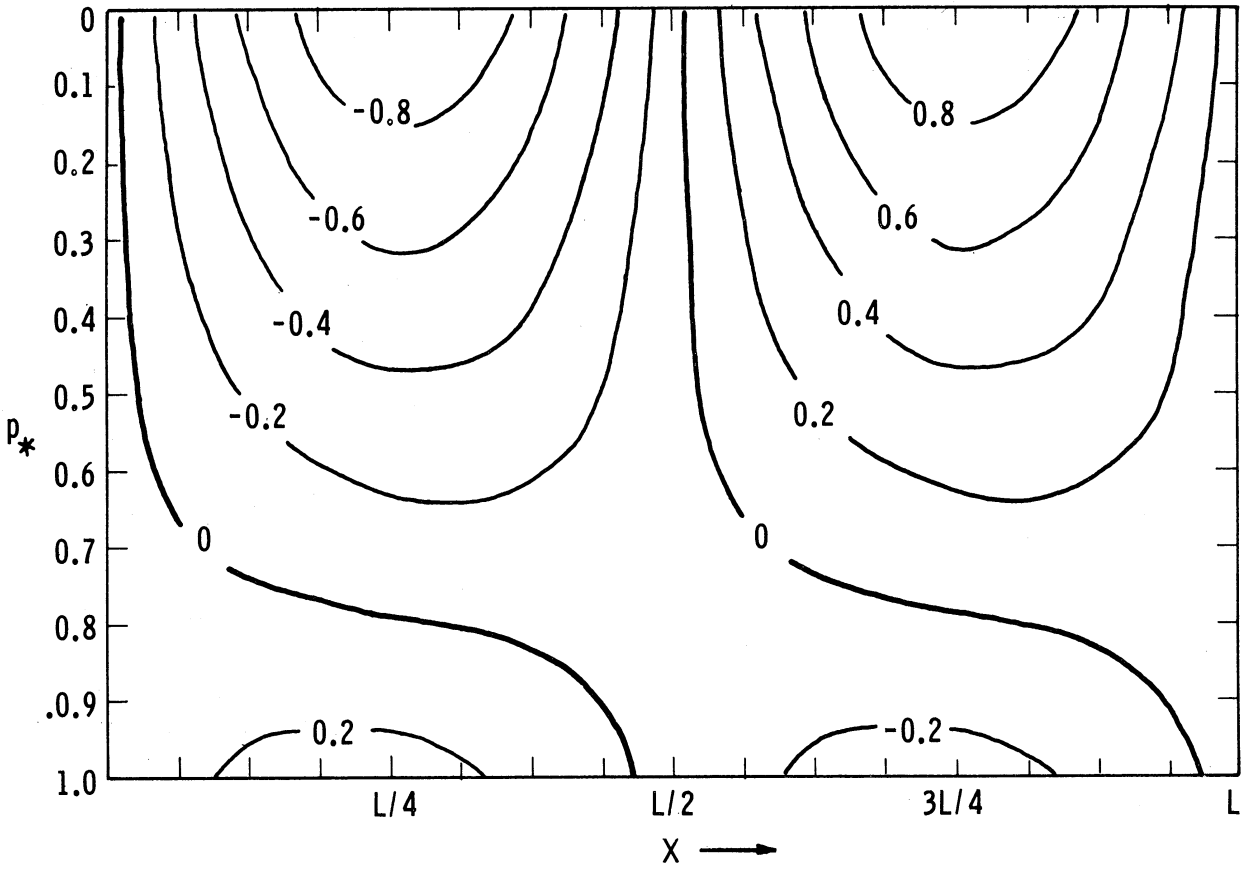

Figure 12. Cross-section showing ψ^+ as a function of p_* and x for a wavelength of 10,600 km. Parameters: $\sigma = 0$, $\beta = 16 \times 10^{-12}$ m sec^{-1} km^{-1}, $dU/dZ = 4$ m sec^{-1} km^{-1}.

The longer, stable ψ waves can have either of the two amplitudes given by (2.84). The normalized amplitudes $G^+/|G^+|_{max}$ and $G^-/|G^-|_{max}$ are shown in Figure 13(a) and (b), respectively. Just as in Figure 10, ℓ_N refers to a wavelength falling on the neutral stability curve where, we recall, $3C^2_{R*} - 1 = 0$. We note in Figure 13(a) that for all wavelengths G^+ is large and negative in the upper levels while its value at $p_* = 1$ ($p = 1000$ mb) is positive and increases with the wavelength. From (2.83) we see, therefore, that these waves consist of a series of alternating vertical troughs and ridges in the upper levels, lying above a series of alternating vertical ridges and troughs in the lower levels, in about the same manner as the ψ wave shown in Figure 2(b). The ψ waves with amplitude G^- differ from those with amplitude G^+ in that for very large wavelengths G^- remains negative for the entire pressure interval $0 \leq p_* \leq 1$ (Figure 13(b)). These very long waves, therefore, consist of alternating vertical troughs and ridges which extend throughout the atmosphere.

2.5 THE CASE $dU/dp_* = \text{CONST.} < 0$, $\beta = 0$, $\sigma = \text{CONST.}$

2.5.1 The Stability Analysis

Our objective in this section is to investigate the effect of the static stability parameter σ on the stability and structure of baroclinic disturbances. As in section (2.3) we neglect the variation of the Coriolis parameter with latitude (i.e. $\beta = 0$) and assume that the basic zonal wind varies linearly with pressure as given by (2.35). A similar study, we note, was made by Eady (1949) using a slightly different model.

When the assumptions mentioned above are introduced in (2.13) we find that the differential equation for Ω becomes

$$(p_*-1+c_*)\frac{d^2\Omega}{dp_*^2} - 2\frac{d\Omega}{dp_*} - \frac{k^2\sigma p_o^2}{f_o^2}(p_*-1+c_*)\Omega = 0 \qquad (2.85)$$

where again

$$c_* = \frac{c-U_o}{U_T} .$$

If we now use

$$\xi^* = p_* - 1 + c_* \qquad (2.86)$$

and

$$q^2 = \frac{k^2\sigma p_o^2}{f_o^2} \qquad (2.87)$$

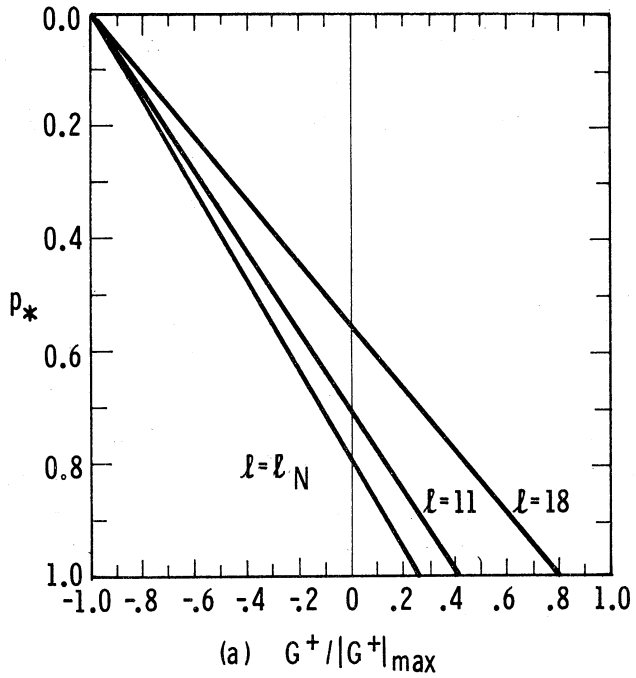

Figure 13(a). Normalized amplitude of the stable ψ^+ wave as a function of pressure. The curve labeled l_N refers to a wave on the neutral stability curve. Parameters: $\sigma = 0$, $\beta = 16 \times 10^{-12}$ m^{-1}, sec^{-1}, dU dZ = 4 m sec^{-1} km^{-1}.

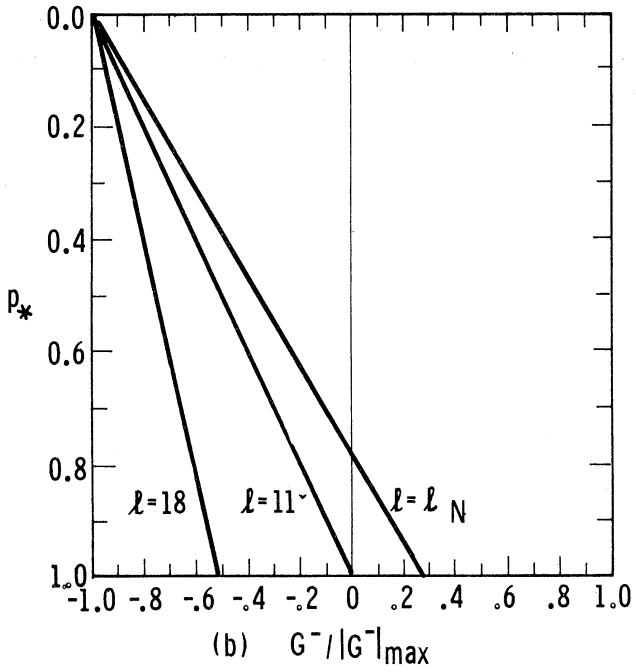

Figure 13(b). Same as Figure 13(a) but for the stable ψ^- wave.

we can rewrite (2.85) in the form

$$\xi^* \frac{d^2\Omega}{d\xi^{*2}} - 2 \frac{d\Omega}{d\xi^*} - q^2 \xi^* \Omega = 0 . \qquad (2.88)$$

With the new independent variable ξ^*, the boundary conditons (2.14) become

$$\Omega = 0 \quad \text{for } \xi^* = c_* - 1$$

and

$$\Omega = 0 \quad \text{for } \xi^* = c_* . \qquad (2.89)$$

The solution to (2.88), which can be found in Kamke (1943, p. 539, case 5.6), is

$$\Omega = \xi^{*2} \frac{d}{d\xi^*} \left(\frac{u}{\xi^*}\right) \qquad (2.90)$$

where u is the solution to the equation

$$\frac{d^2u}{d\xi^{*2}} - q^2 u = 0,$$

that is,

$$u = Ae^{q\xi^*} + Be^{-q\xi^*}$$

where A and B are constants. If we substitute this expression for u into (2.90), we arrive at the general solution to (2.88):

$$\Omega = Ae^{q\xi^*}(q\xi^* - 1) - Be^{-q\xi^*}(q\xi^* + 1). \qquad (2.91)$$

Introducing the boundary conditons given by (2.89) we obtain

$$Ae^{q(c_*-1)} [q(c_*-1)-1] - Be^{-q(c_*-1)} [q(c_*-1)+1] = 0$$

and (2.92)

$$Ae^{qc_*} (qc_*-1) - Be^{-qc_*} (qc_*+1) = 0.$$

This system of equations has non-trivial solutions provided that the determinant of the coefficients is equal to zero, that is, provided that

$$-e^{q(c_*-1)}(qc_*-q-1)e^{-qc_*}(qc_*+1)+e^{qc_*}(qc_*-1)e^{-q(c_*-1)} .$$

$$(qc_*-q+1) = 0,$$

or

$$q^2c_*^2 - q^2c_* - (1 - q \coth q) = 0,$$

which has the solutions

$$c_*^{\pm} = \frac{1}{2} \pm \frac{1}{2}\sqrt{\delta} \tag{2.93}$$

where

$$\delta = 1 + \frac{4}{q^2} (1 - q \coth q) \tag{2.94}$$

We recall that

$$c_* = \frac{c-U_o}{U_T}$$

so that eliminating c_* between (2.93) and this last equation we obtain

$$c^{\pm} = U_o + \frac{1}{2} U_T \pm \frac{U_T}{2}\sqrt{\delta}$$

or

$$c^{\pm} = U(\tfrac{1}{2}) \pm \frac{U_T}{2}\sqrt{\delta} . \tag{2.95}$$

From (2.95) we see that the perturbations are stable (c real) if $\delta \geq 0$ and unstable (c complex) if $\delta < 0$. The stable and unstable domains are therefore separated by the conditon $\delta = 0$, which can be rewritten, using (2.94), as

$$\tanh q = \frac{4q}{q^2+4} .$$

The solution to this transcendental equation can be found by trial and error to be approximately

$$q = 2.40.$$

Since by definition $q = \sigma^{\frac{1}{2}} kp_o/f_o = 2\pi\sigma^{\frac{1}{2}} p_o/Lf_o$

we have $L = \dfrac{2\pi p_o \sigma^{1/2}}{2.40\, f_o}$

or $L = 3.70 \times 10^3$ km

if we take $\sigma = 2$ MTS units. The wave length $L_N = 3.70 \times 10^3$ km, therefore, represents the "neutral curve" separating the stable and unstable domains. This result, we note, depends on the static stability σ but <u>not</u> on the vertical wind shear. The curve $L_N = 3.70 \times 10^3$ km appears as the heavy line in Figure 14. For $L < L_N$ we have $\delta > 0$ so that the waves are stable whereas for $L > L_N$ the reverse applies.

The e-folding time $T = 1/kc_i^+$ of the unstable waves can be computed by noting from (2.95) that the positive imaginary part of the phase speed c is given by

$$c_i^+ = \frac{U_T}{2}\sqrt{-\delta}$$

so that

$$T = \frac{2}{kU_T} \cdot \frac{1}{\sqrt{-\delta}} \qquad (2.96)$$

where δ is given by (2.94). Alternately, if we recall that $U_T = 20\, dU/dZ$ we can write (2.96) in the following more convenient form:

$$\frac{dU}{dZ} = \frac{1}{10kT\sqrt{-\delta}} \quad . \qquad (2.97)$$

Figure 14 shows the plot of (2.97) for selected values of T. The curves show that for a given vertical wind shear there is a certain wavelength for which the e-folding time is smallest. This wavelength would therefore grow faster than the others and hence may be called the most unstable wave. By inspection of Figure 14 we find that for our model this wavelength is approximately 5.53×10^3 km, independently of the vertical wind shear.

To gain an insight into the effect of the static stability on the behavior of the perturbations we should compare the stability diagram in Figure

14 to the one shown in Figure 3 which applies for the case where σ is set equal to zero.

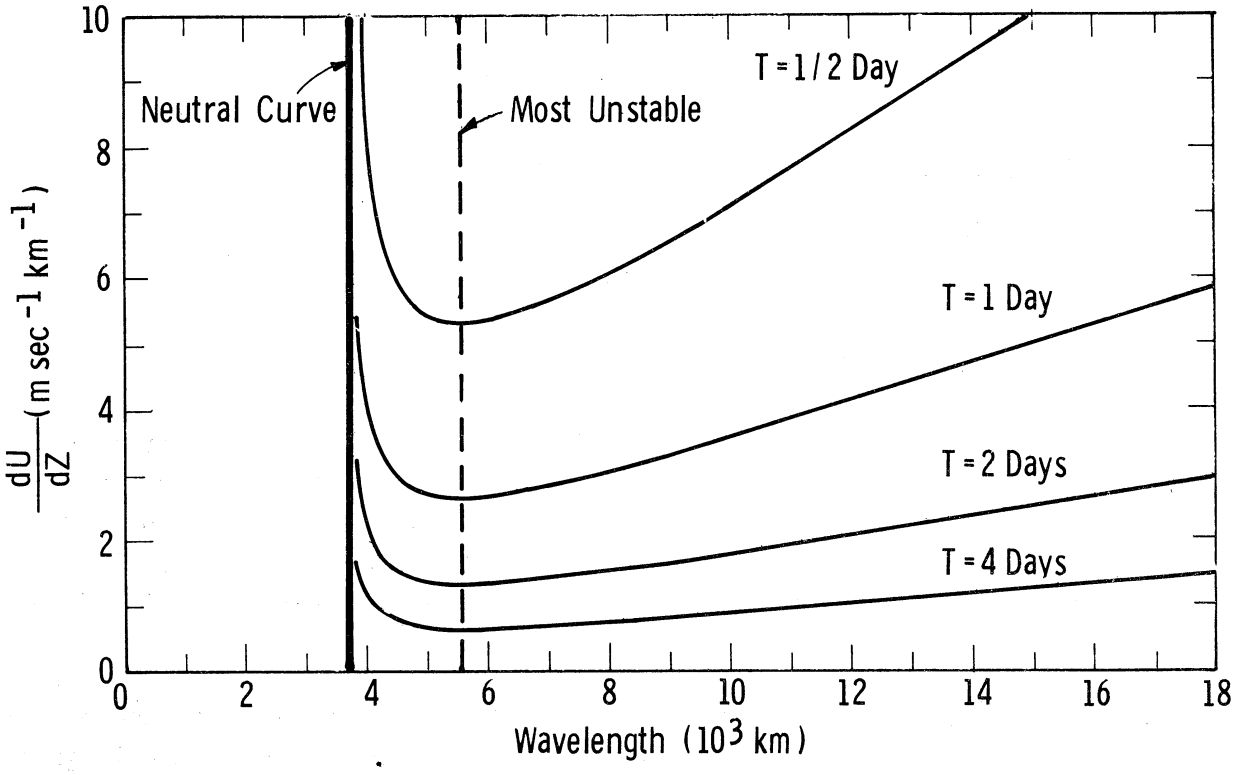

Figure 14. Stability diagram showing the variation of the e-folding time T as a function of the vertical wind shear and the wavelength. Parameters: σ = 2MTS units, $f_o = 10^{-4}$ sec^{-1}, β = 0.

We see that the most important effect of the static stability is to stabilize the very short waves. The longer waves are still unstable but the rate at which they amplify is now lower, especially for wavelengths not much larger than 3.70×10^3 km. For example, let us consider a wave with L = 4500 km and a wind shear of 3 m sec^{-1} km^{-1}. When σ = 0 we see (Figure 3) that the e-folding time is about 1/2 day whereas when σ = 2 (Figure 14) it is one day. For the longest wave shown, however, the two diagrams are very similar, indicating that the σ term has a negligible effect on the growth rates of these long waves.

The speed of propagation of these stable and unstable waves, as given by (2.95), appears as a function of wavelength in Figure 15. The dashed curve was computed using U(1/2) = 15 m sec^{-1} and dU/dZ = 4 m sec^{-1} km^{-1} while the solid curve was obtained using U(1/2) = 10 m sec^{-1} and dU/dZ = 2 m sec^{-1} km^{-1}. In the stable domain (δ > 0) we have two possible values for c since we can choose either sign in front of the last term in (2.95). In the unstable domain (δ < 0), however, c_r is single valued and equal to U(1/2), the speed of the basic current at $p_* = 1/2$ (p = 500 mb). We recall from section 2.3 that when both the β term and the σ term are neglected all the waves are unstable and propagate with a speed U(1/2). Thus the inclusion of the σ term does not

change the speed of propagation of those waves which are too long to be stabilized by it. It does, however, as we have seen above, change the rate at which they amplify.

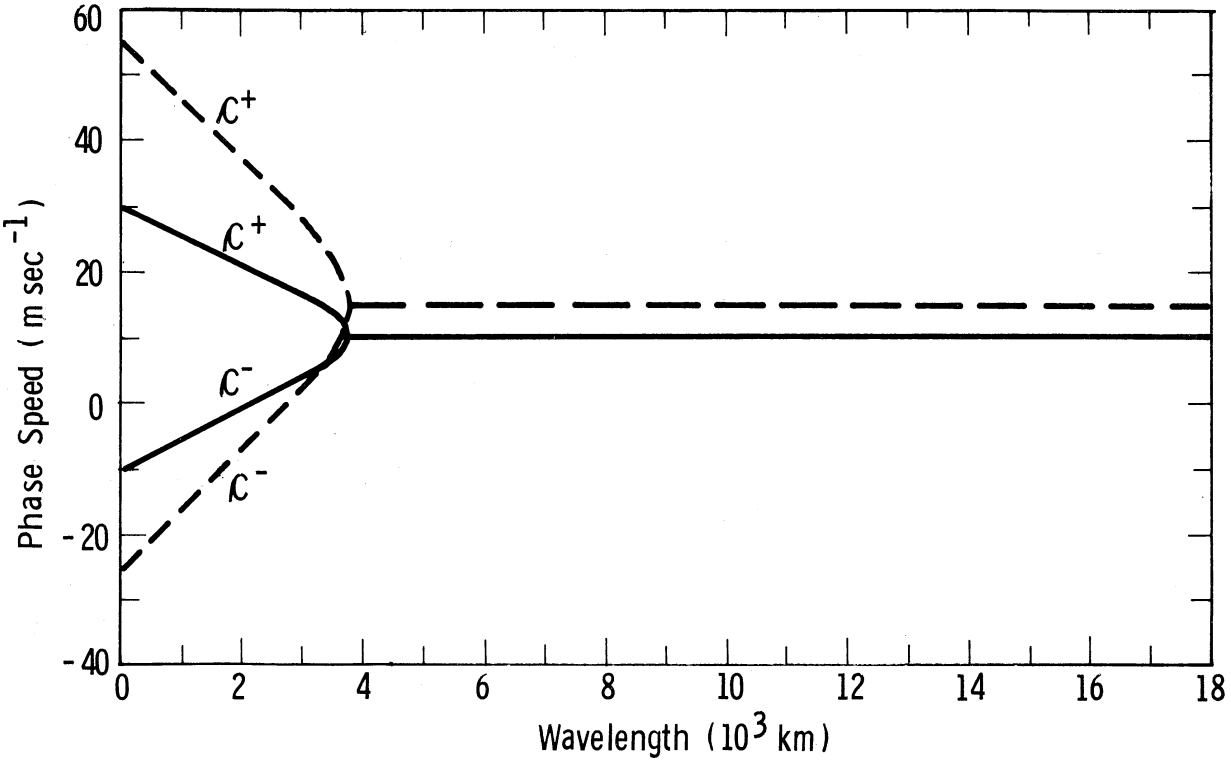

Figure 15. Phase speed as a function of wavelength for the case σ = 2MTS units, β = 0. For the solid curve dU/dZ = 2 m sec^{-1} km^{-1} and U(1/2) = 10 m sec^{-1}, while for the dashed curve dU/dZ = 4 m sec^{-1} km^{-1} and U(1/2) = 15 m sec^{-1}.

2.5.2 The Wave Structure

To study the structure of the ω wave we start with (2.91) from which we eliminate ξ^* by means of (2.86) and B by using the second equation in (2.92). The result can be expressed in the form

$$\Omega^{\pm}(p_*) = J^{\pm} \{[1-q^2 c_*^{\pm}(p_* + c_*^{\pm} - 1)] \sinh q(1-p_*) - q(1-p_*) \cosh q(1-p_*)\} \qquad (2.98)$$

where

$$J^{\pm} = \frac{2Ae^{qc_*^{\pm}}}{1 + qc_*^{\pm}}$$

and $c_*^{\pm}$ are given by (2.93). We then multiply (2.98) throughout by $e^{ik(x-ct)}$ and equate the real parts.

In the stable domain ($\delta > 0$) the resulting equation is

$$\omega_r^{\pm}(x,p_*,t) = K^{\pm} \cos k\,(x-c^{\pm}t) \tag{2.99}$$

where

$$K^{\pm} = \frac{2\,Ae^{qc_*^{\pm}}}{1+qc_*^{\pm}} \{[1 - q^2c_*^{\pm}(p_* + c_* - 1] \sinh q(1-p_*)$$

$$-q(1-p_*) \cosh q(1-p_*)\} \,. \tag{2.100}$$

In the unstable domain, where δ is negative and $c_*^{\pm}$ and $c^{\pm}$ are complex, the expression for ω_r takes the form

$$\omega_r^{\pm}(x,p_*,t) = Q^{\pm} \cos[k(x-c_rt)-\alpha^{\pm}] \tag{2.101}$$

where

$$Q^{\pm} = \frac{2\,Ae^{qc_{*r}}\, e^{kc_i^{\pm}t}}{(1+qc_{*r})^2 + q^2c_{*i}^2} \left[(aM - b^{\pm}N^{\pm})^2 + (b^{\pm}M + aN^{\pm})\right]^{1/2}$$

$$a = (1 + qc_{*r}) \cos q\,c_{*i}^{\pm} + qc_{*i}^{\pm} \sin qc_{*i}^{\pm}$$

$$b^{\pm} = -qc_{*i}^{\pm} \cos qc_{*i}^{\pm} + (1+qc_{*r}) \sin qc_{*i}^{\pm}$$

$$M = \{q^2[c_{*r}(p_* + c_{*r} - 1) - c_{*i}^2\,]-1\} \sinh q(1-p_*)$$

$$+ q(1-p_*) \cosh q(1-p_*)$$

$$N^{\pm} = q^2c_{*i}^{\pm}(p_* + 2c_{*r}-1) \sinh q(1-p_*)$$

and

$$\alpha^{\pm} = \tan^{-1}\left[\frac{b^{\pm}m + aN^{\pm}}{b^{\pm}N^{\pm} - aM}\right] \,. \tag{2.102}$$

We see from (2.99), which applies for the stable domain, that for a given wavelength we can have two distinct ω waves, one with an amplitude K^+ and a phase velocity c^+ and the other with an amplitude K^- and a phase velocity c^-. We note also that these waves do not slope with pressure. The normalized amplitudes $K^+/|K^+|_{max}$ and $K^-/|K^-|_{max}$ appear in Figures 16(a) and (b), respectively, as functions of pressure. We see that for short wavelengths the K^+ and K^- amplitudes attain their maximum absolute values in the upper and lower levels, respectively, the value of one amplitude at p_* being equal to the value of the other one at $1 - p_*$. As the wavelength increases to 3700 km we notice that the maximum absolute value in both K^+ and K^- is reached at $p_* = 1/2$ ($p = 500$ mb).

For the longer unstable waves, $\omega_r^{\pm}(x,p_*,t)$ are given by (2.101), where ω^+ and ω^- refer to the amplifying and damped waves, respectively. It should be pointed out that the normalized amplitudes $Q^+/|Q^+|_{max}$ and $Q^-/|Q^-|_{max}$ are identical so that Figure 17(a), which shows the normalized amplitude as a function of pressure, applies for both the amplifying wave and the damped one. The remarkable feature about these normalized amplitudes is that they vary very slowly with wavelength. Moreover, both curves shown in Figure 17(a) are quite similar to the ones given in Figure 16 for a neutral wave with $L = 3700$ km.

We should also note that the amplitudes of these unstable waves vary with pressure in very nearly the same manner as the amplitude of the unstable waves discussed in section 2.32, where the σ term had been neglected (see Figure 4(a)). We can therefore conclude that within the framework of our quasi-geostrophic model the static stability of the basic flow does not affect appreciably the way in which the amplitudes of the unstable ω waves vary with pressure. Now it remains to be seen whether or not the static stability can significantly change the slope of these waves with pressure.

We mentioned above that for a given wavelength both the amplifying and the damped waves have the same normalized amplitude $|Q|/|Q|_{max}$. The same, however, is not true for their phase angles. Since the damped wave is of little interest, only the phase angle of the amplifying wave, that is, α^+ as obtained from (2.102), is presented in Figure 17(b). To find the effect of the σ term on the slope of the waves, the curves of Figure 17(b) should be compared to the curve labelled α^+ in Figure 4(b). We recall that the latter was obtained with σ set equal to zero. We see that the effect of the σ term is to decrease the slope of the waves but that this effect is felt to a smaller and smaller degree as the wavelength increases. Thus we can conclude that the static stability of the basic current does not affect appreciably the slope of the very long waves. Since we have reached the same conclusion above concerning the effect of the σ term on the normalized amplitudes of the waves, we can then say that the static stability of the basic flow, important as it may be in determining the structure of the short ω waves, does not play an important role in determining the structure of the very long amplifying ω waves.

As in the previous sections, we follow our investigation of the ω waves

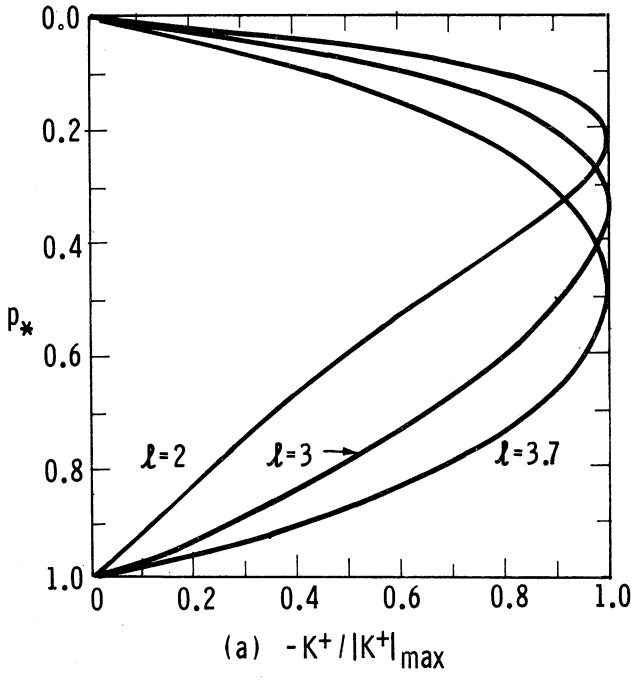

Figure 16(a). Normalized amplitude of the stable ω^+ wave as a function of pressure for wavelengths of 2000 km, 3000 km and 3700 km. Parameters: σ = 2MTS units, β = 0.

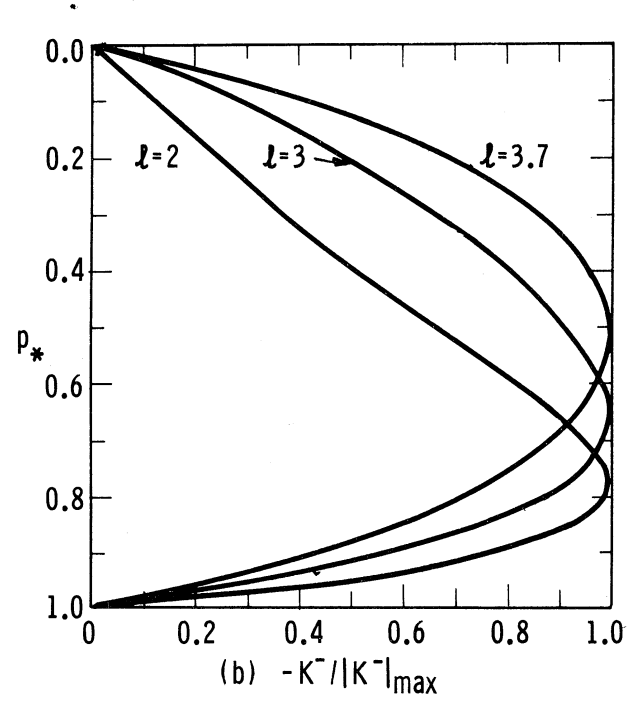

Figure 16(b). Same as Figure 16(a) but for the stable ω^- wave.

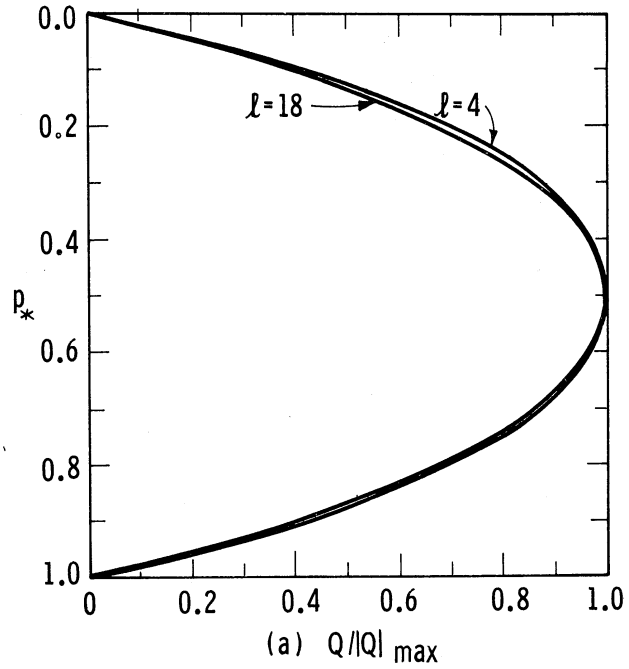

Figure 17(a). Normalized amplitude of the unstable $\omega^{\pm}$ waves as a function of pressure for wavelengths of 4000 km and 18,000 km. Parameters: σ = 2MTS units, β = 0.

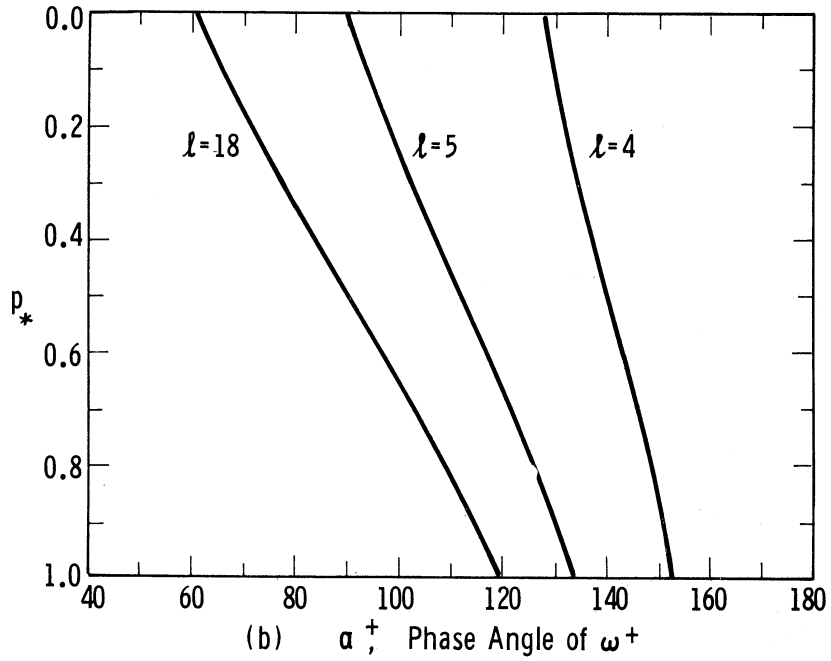

Figure 17(b). Phase angle of the amplifying ω wave as a function of pressure for wavelengths of 4000 km and 18,000 km. Parameters: σ = 2MTS units, β = 0.

with a similar investigation of the Ψ waves. To obtain an analytic expression for the stream function, we first substitute (2.98) into (2.9) with β set equal to zero. After making use of (2.35) and (2.38) to rewrite c-U as $U_T\ (p_* + c_* - 1)$, we obtain the following expression for $\Psi(p_*)$:

$$\Psi(p_*) = \frac{i\ 2\ Af_o q^2 e^{qc_*}}{k^3 p_o U(1 + qc_*)} \left[\sinh q(1-p_*) - qc_* \cosh q(1-p_*)\right].$$

The real part of the stream function, $\psi_r(x,p_*,t)$, is then obtained by multiplying both sides of the last equation by $e^{ik(x-ct)}$ and equating the real parts.

In the stable domain, where δ is positive and both c and c_* are pure real, the result is

$$\psi_r^{\pm}(x,p_*,t) = R^{\pm} \sin k(x - c^{\pm}t) \tag{2.103}$$

where

$$R^{\pm} = \frac{2\ Af_o q^2 e^{qc_*^{\pm}}}{k^3 p_o U_T (1 + qc_*^{\pm})} \left[qc_*^{\pm} \cosh q(1-p_*) - \sinh q(1-p_*)\right]. \tag{2.104}$$

In the unstable domain, however, where δ is negative and both c and c_* are complex, we obtain

$$\psi_r^{\pm}(x,p_*,t) = S^{\pm} \cos\left[k(x-c_r t) - \theta^{\pm}\right] \tag{2.105}$$

where

$$S^{\pm} = \frac{2Af_o q^2 e^{qc_{*r}}}{k^3 p_o U_T\left[(1+qc_{*r})^2 + q^2 c_{*i}^2\right]} \left[(ah - b^{\pm}d^{\pm})^2 + (b^{\pm}h + ad^{\pm})^2\right]^{1/2}$$

$$d^{\pm} = -qc_{*i}^{\pm} \cosh q(1 - p_*)$$

$$h = \sinh q(1 - p_*) - qc_{*r} \cosh q(1 - p_*)$$

$$\theta^{\pm} = \tan^{-1}\left(\frac{b^{\pm}d^{\pm} - ah}{-ad^{\pm} - b^{\pm}h}\right) \tag{2.106}$$

and a and $b^{\pm}$ have been defined after (2.101).

Again the two solutions for the stable domain, given by (2.103), are vertical waves, one having an amplitude R^+ and a phase speed c^+ and the other an amplitude R^- and a phase speed c^-. The normalized amplitudes $R^+/|R^+|_{max}$ and $R^-/|R^-|_{max}$ appear as functions of pressure in Figures 18(a) and (b), respectively. If we consider the wavelength L = 2000 km, we see that the ψ^+ wave has a much greater amplitude (R^+) at $p_* = 0$ than at $p_* = 1$ (p = 1000 mb) while the reverse is true for the ψ^- wave. We note, however, that as the wavelength increases the normalized amplitude of the ψ^+ wave at $p_* = 1$ tends to 1 while the same is true for the amplitude of the ψ^- wave at $p_* = 0$.

The structure of the unstable waves is given by (2.105) where ψ_r^+ and ψ_r^- refer to the amplifying and damped waves, respectively. Since the normalized amplitudes $S^{\mp}/|S^+|_{max}$ and $S^-/|S^-|_{max}$ are identical, Figure 19(a), which shows the normalized amplitude as a function of pressure, for both the amplifying and the damped waves alike. We observe from this figure that the normalized amplitude of the unstable $\psi^{\pm}$ waves changes very little with wavelength. To find the effect that the σ term has on the amplitude of these waves we should compare the curves of Figure 19(a) to the one giving the amplitude of the stream function in Figure 4, for which σ had been set equal to zero. We see that the effect of the σ term is small but especially so as the wavelength increases.

The phase angle of the amplifying ψ waves, θ^+, appears as a function of pressure in Figure 19(b) for three different wavelengths. We see that the slope of these waves increases with the wavelength. Moreover, we note that for a wavelength of 18,000 km the phase angle is very nearly the same as that shown in Figure 4(b) (curve labelled θ^+) for which σ had been set equal to zero. This indicates that as the wavelength increases the effect of the static stability factor σ on the slope of the ψ waves tends to become negligible. Since we have obtained the same result concerning the amplitude of the waves, we can then conclude that the effect of the σ term on the structure of the ψ waves is neglibible for sufficiently long waves.

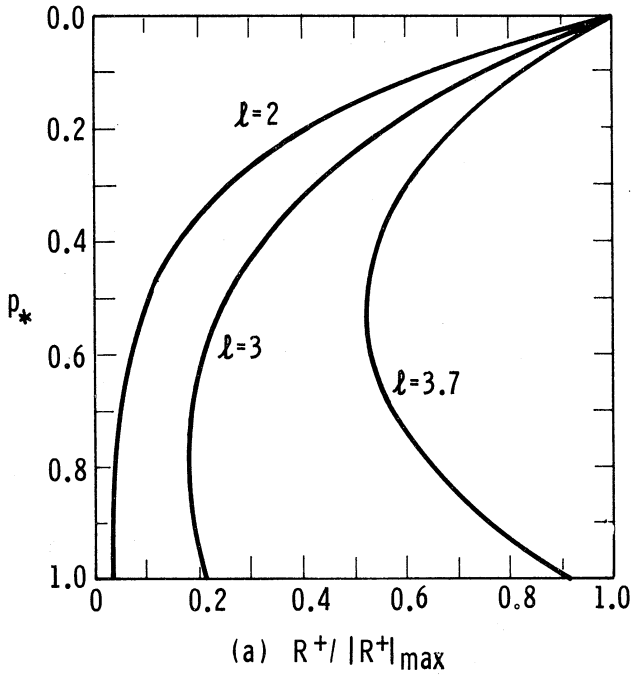

Figure 18(a). Normalized amplitude of the stable ψ^+ wave as a function of pressure for wavelengths of 2000 km, 3000 km and 3700 km. Parameters: σ = 2MTS units, β = 0.

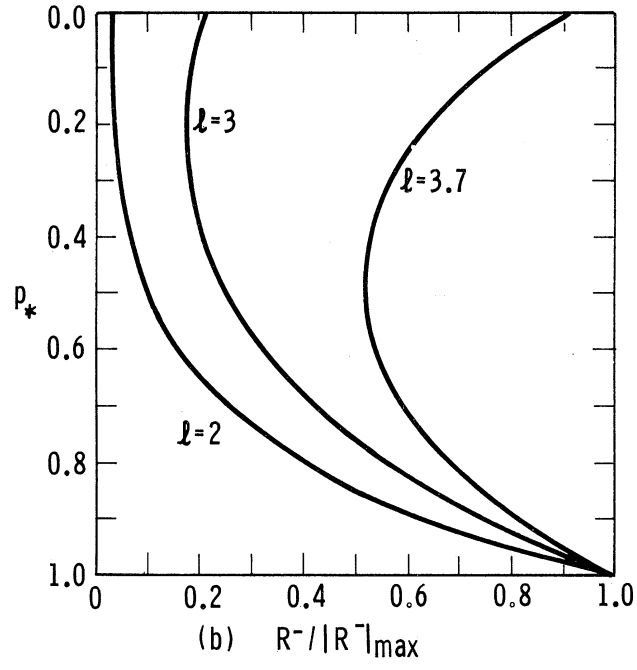

Figure 18(b). Same as Figure 18(a) but for the stable ψ^- wave.

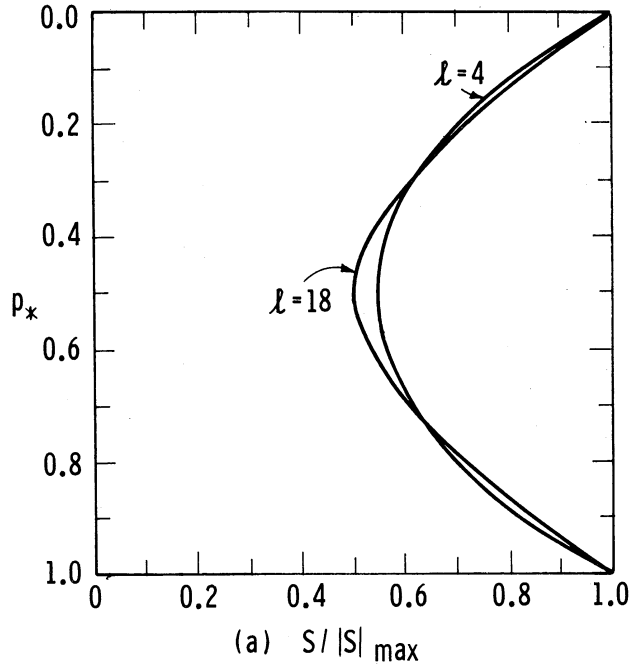

Figure 19(a). Normalized amplitude of the unstable $\psi^{\pm}$ waves as a function of pressure for wavelengths of 4000 km and 18,000 km. Parameters: σ = 2MTS units, β = 0.

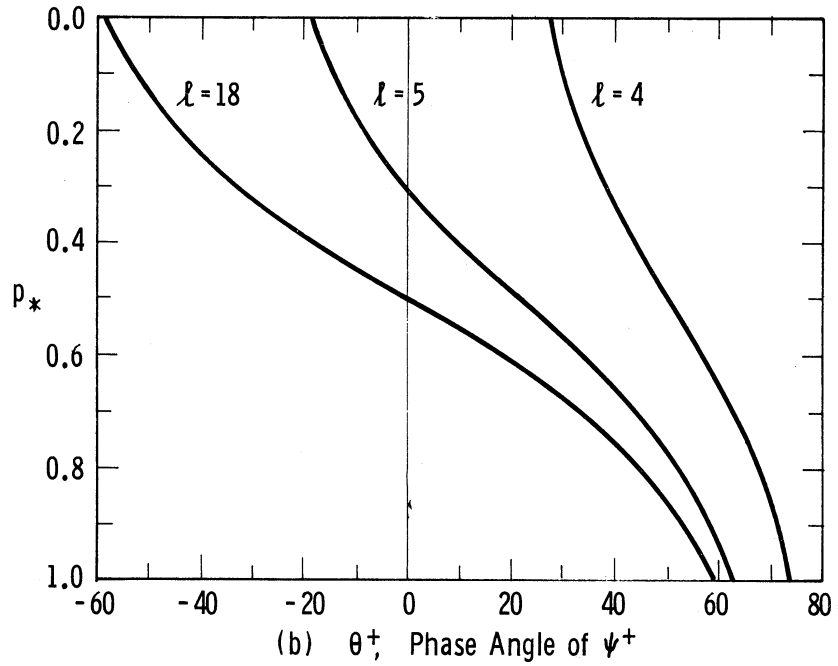

Figure 19(b). Phase angle of the amplifying ψ wave as a function of pressure for wavelengths of 4000 km, 5000 km and 18,000 km. Parameters: σ = 2MTS units, β = 0.

3. BAROCLINIC INSTABILITY IN A PRIMITIVE EQUATIONS MODEL

3.1 INTRODUCTION

In the previous chapter we investigated the problem of baroclinic instability in a quasi-geostrophic model based on simplified forms of the vorticity and thermodynamic equations. In these two equations we assumed that the absolute vorticity and the temperature (or density) were advected along isobaric surfaces by the non-divergent part of the wind alone. To close the system of equations, we then assumed that the simple geostrophic relation $\psi = \phi/f_o$ could be used to relate the geopotential to the stream function.

The first approximation, that is, using only the non-divergent part of the wind for advection purposes, has been used for several years in short range numerical forecasting models and in some studies of the general circulation of the atmosphere. Because the performance of these models often leaves something to be desired, there is now a growing interest in the so-called "primitive equations" models, in which this approximation is not made. It is the purpose of this chapter to investigate the stability of baroclinic waves in such a model and then to compare the results with those obtained with the quasi-geostrophic model.

Our approach here follows the one used in the previous chapter. In section 3.2 we present the equations which define our model and derive from them the differential equation relating the amplitude of the ω wave to the pressure. This equation is "general" in the sense that in deriving it we retain the vertical wind shear as well as both the β and the σ terms.

We recall that for the quasi-geostrophic model we have investigated the following four special cases:

(a) $dU/dp = 0$, β = constant, σ = constant

(b) dU/dp = constant < 0, $\beta = 0$, $\sigma = 0$

(c) dU/dp = constant < 0, β = constant, $\sigma = 0$

(d) dU/dp = constant < 0, $\beta = 0$, σ = constant.

In this chapter we investigate cases (a), (b) and (c) for the "primitive equations" model. For this model, unfortunately, case (d) is omitted since no exact analytical solution has been found for it. Just as in the previous chapter, the general case (i.e. dU/dp = constant < 0, β = constant > 0, σ = constant > 0) is also omitted due to its mathematical complexity.

Case (b) has been investigated by Fjørtoft (1950) and Thrane (1963) and case (c) by Holmboe (1959). The model atmospheres considered by these authors, however,are incompressible and vertically finite whereas ours are compressible and vertically infinite.

3.2 THE GENERAL EIGEN-VALUE PROBLEM

Just as in the previous chapter, we propose to investigate the properties of a model in which the perturbations have small amplitudes so that products of perturbation quantities can be neglected. Furthermore, we again restrict our investigation to perturbations which are independent of the y coordinate. As we pointed out in Chapter 1, by neglecting the y dependence in the perturbations we may be deleting some important non-geostrophic effects (Phillips, 1964), but we shall see in the following sections that even our simplified perturbations can serve a useful purpose by demonstrating some properties of non-geostrophic flow.

The linearized equations for our model are the following:

$$\frac{\partial u}{\partial t} + U\frac{\partial u}{\partial x} + \omega\frac{dU}{dp} = -\frac{\partial \phi}{\partial x} + f v \tag{3.1}$$

$$\frac{\partial v}{\partial t} + U\frac{\partial v}{\partial x} = -f u \tag{3.2}$$

$$\alpha = -\frac{\partial \phi}{\partial p} \tag{3.3}$$

$$\frac{\partial \alpha}{\partial t} + U\frac{\partial \alpha}{\partial x} + f_o \frac{dU}{dp} v - \sigma\omega = 0 \tag{3.4}$$

and

$$\frac{\partial u}{\partial x} + \frac{\partial \omega}{\partial p} = 0, \tag{3.5}$$

where α is the specific volume and the other symbols are as defined in the previous chapter. (3.1) and (3.2) are the first two equations of motion, (3.3) is the hydrostatic equation, (3.4) is the adiabatic thermodynamic equation and (3.5) is the continuity equation.

The first step in our procedure is to eliminate the geopotential ϕ from the above equations, thus reducing the system to one of four equations in four unknowns, namely, u, v, ω and α. We do this by first combining (3.1)

and (3.2) to give the vorticity equation

$$\frac{\partial}{\partial t}\left(\frac{\partial v}{\partial x}\right) + U\frac{\partial}{\partial x}\left(\frac{\partial v}{\partial x}\right) + \beta v = - f_o \frac{\partial u}{\partial x} \qquad (3.6)$$

and then eliminating ϕ between (3.1) and (3.3) to obtain, with the help of (3.5),

$$\frac{\partial}{\partial t}\left(\frac{\partial u}{\partial p}\right) + U\frac{\partial}{\partial x}\left(\frac{\partial u}{\partial p}\right) = \frac{\partial \alpha}{\partial x} + f_o \frac{\partial v}{\partial p} . \qquad (3.7)$$

Our system of equations then consists of (3.4), (3.5), (3.6) and (3.7). We note here that the β term, the effect of which we propose to investigate, appears only in the vorticity equation. We now solve this system of equations subject to the conditions that u, v, β and α are periodic in both x and t and that $\omega = 0$ at $p = 0$ and at $p = p_o$ (pressure at the ground). Using the method of separation of variables, we write the solutions in the form

$$(u,v,\omega,\alpha) = [\hat{u}(p),\hat{v}(p),\hat{\omega}(p),\hat{\alpha}(p)]e^{ik(x-ct)} \qquad (3.8)$$

where $\hat{u}$, $\hat{v}$, $\hat{\omega}$, $\hat{\alpha}$ are the amplitudes (possibly complex) of u, v, ω and α, respectively. We then substitute (3.8) into (3.4) to (3.7) and obtain

$$-ik(c-U)\hat{\alpha} + f_o \frac{dU}{dp}\hat{v} - \sigma\hat{\omega} = 0 \qquad (3.9)$$

$$ik\hat{u} + \frac{d\hat{\omega}}{dp} = 0 \qquad (3.10)$$

$$k^2(c - U + \frac{\beta}{k^2})\hat{v} + f_o\, ik\hat{u} = 0 \qquad (3.11)$$

$$-ik(c - U)\frac{d\hat{u}}{dp} - ik\hat{\alpha} - f_o \frac{d\hat{v}}{dp} = 0 . \qquad (3.12)$$

The procedure now consists in eliminating $\hat{\alpha}$ between (3.9) and (3.12) and then $\hat{v}$ from the resulting equation by means of (3.11). This gives us an equation which contains the two unknown variables $\hat{\omega}$ and $\hat{u}$, the latter of which we can then eliminate with the help of (3.10). The resulting equation for $\hat{\omega}$ can then be written in the form

$$(c - U)\,(c - U + C_R)\left[1 - \frac{(c-U)\,(c-U+C_R)}{C_I^2}\frac{d^2\hat{\omega}}{dp_*^2} + \right.$$

$$\left. + \left[2(c-U)+C_R\right]\frac{dU}{dp_*}\frac{d\hat{\omega}}{dp_*} - \frac{\sigma p_o^2}{C_I^2}(c-U+C_R)^2\hat{\omega}\right] = 0 \qquad (3.13)$$

where $C_R = \beta/k^2$, $C_I = f_o/k$ and p_* is defined as in the previous chapter.

(3.13) is the "general" differential equation relating the amplitude of the ω wave to pressure for our "primitive equations" model. We note here that whenever both $|c-U| \ll C_I$ and $|c-U+C_R| \ll C_I$ hold true (3.13) reduces to the quasi-geostrophic equation (2.13). The basic differences, therefore, between our quasi-geostrophic model and our "primitive equations" model is that in the former we have implicitly assumed that the two inequalities were satisfied whereas in the latter we do not.

Since we are unable to solve the "general" equation (3.13) exactly, we proceed by investigating three special cases of it in an attempt to gain some insight into the behavior of baroclinic "non-geostrophic" perturbations.

3.3 THE CASE U = CONST. ≥ 0, β = CONST. > 0, σ = CONST. > 0

In this section we investigate the behavior of perturbations (possibly baroclinic) embedded in a barotropic basic flow. We recall that we have also investigated this case in section 2.2 for our quasi-geostrophic model. A comparison of the results from the present section with those from section 2.2 will then reveal something about the influence of non-geostrophic effects on perturbations in a barotropic current. This interesting comparison, we note, has also been made by 'Arnason (1961).

For the present case, the differential equation relating the amplitude of the ω wave to the pressure, namely,

$$(c-U)\,(c-U+C_R)\left[1 - \frac{(c-U)\,(c-U+C_R)}{C_I^2}\right]\frac{d^2\hat{\omega}}{dp_*^2} - \frac{\sigma p_o^2}{C_I^2}(c-U+C_R)^2\hat{\omega} = 0 \qquad (3.14)$$

where U is a positive constant, is obtained by setting dU/dp_* equal to zero in (3.13). If we now write (3.14) in the form

$$\frac{d^2\hat{\omega}}{dp_*^2} + q\hat{\omega} = 0 \qquad (3.15)$$

where

$$q = -\frac{\sigma p_o^2}{C_I^2} \cdot \frac{(c-U+C_R)}{(c-U)} \cdot \frac{1}{\left[1-\frac{(c-U)\,(c-U+C_R)}{C_I^2}\right]} \qquad (3.16)$$

we see that (3.15) is identical in form to (2.15) but that the expression for q is now different. Moreover, the boundary conditons for (3.15) and (2.15) are the same, that is, $\omega = 0$ for $p_* = 0$ and for $p_* = 1$. By analogy to (2.15), therefore, we can write the solution of (3.15) as

$$\omega = A \sin(\sqrt{q}\, p_*) \qquad (3.17)$$

where, again,

$$\sqrt{q} = m\pi, \qquad m = 0, \pm 1, \pm 2, \ldots \qquad (3.18)$$

If we now substitute (3.18) into (3.16) to eliminate q we obtain

$$\frac{m^2\pi^2}{\sigma p_o^2}(c-U)\left[C_I^2 - (c-U)\,(c-U+C_R)\right] + (c-U+C_R) = 0. \qquad (3.19)$$

The object now is to find the various values of c which satisfy this equation and then to determine the type of atmospheric wave motion to which they pertain. First we note that for the vertical mode $m = 0$ (3.19) reduces to

$$c = U - C_R = U - \beta/k^2 \qquad (3.20)$$

so that, for this particular mode, only one type of wave motion can exist. By (3.18) and (3.17), $m = 0$ implies that $\omega(x, p_*, t)$ is identically zero which, by the continuity equation, implies in turn that the horizontal divergence is zero everywhere. The mode $m = 0$, therefore, corresponds to a non-divergent mode of motion with the famous Rossby phase speed given by (3.20). We recall that we have obtained an identical result for the mode $m = 0$ in our quasi-geostrophic model (see (2.28) and Figure 1). We conclude, therefore, that the non-geostrophic effects introduced in the present chapter do not affect the phase velocity of the non-divergent waves.

For the other vertical modes, that is, for each integral value of $m \neq 0$, (3.19) is a cubic equation in c and hence it has three possible solutions, say, c_1, c_2, and c_3. To solve this equation it is convenient to introduce the notation $X = c-U$ and rearrange terms in (3.19) so that it takes the form

$$X^3 + C_R X^2 - \left(\frac{\sigma p_o^2}{m^2\pi^2} + C_I^2\right) X - C_R \frac{\sigma p_o^2}{m^2\pi^2} = 0. \qquad (3.21)$$

The solutions to (3.21) can be obtained by using the standard formulae for a cubic equation. They are

$$X_1 = c_1 - U = A+B \qquad (3.22)$$

$$X_2 = c_2 - U = -\frac{1}{2}(A+B) + \frac{\sqrt{-3}}{2}(A-B) \qquad (3.23)$$

and

$$X_3 = c_3 - U = -\frac{1}{2}(A+B) - \frac{\sqrt{-3}}{2}(A-B) \qquad (3.24)$$

where

$$A = \left[-\frac{b}{2} + \left(\frac{b^2}{4} + \frac{a^3}{27}\right)^{1/2}\right]^{1/3}$$

$$B = \left[-\frac{b}{2} - \left(\frac{b^2}{4} + \frac{a^3}{27}\right)^{1/2}\right]^{1/3}$$

$$a = -\frac{\sigma p_o^2}{m^2\pi^2} - C_I^2 - \frac{1}{3} C_R^2$$

and

$$b = \frac{C_R}{27}\left(2C_R^2 - 18\frac{\sigma p_o^2}{m^2\pi^2} + 9C_I^2\right).$$

Since C_R and C_I are functions of the wavelength, the three phase speeds c_1, c_2 and c_3 are also functions of the wavelength. When these phase speeds are computed by the above formulae, (with p_o = 1000 mb, σ = 2MTS units, f_o = 10^{-4} sec^{-1}, β = 16 X $10^{-12} m^{-1} sec^{-1}$), we find that they have real values for all wavelengths ($0 < L \leq 18000$ km) so that the wave motions to which they pertain are stable for all wavelengths.

When the values of c_1 are computed for wavelengths ranging from 0 to 18,000 km and for the vertical modes m = 1, 2, and 3, we find that the results do not differ appreciably from those obtained with the quasi-geostrophic model (see Figure 1, curves m = 1 and 2). More precisely, we find that the phase velocities computed with the current "primitive equations" model and the quasi-geostrophic one differ by less than 0.2% of the quasi-geostrophic values for the above range of wavelengths. Since we have also found that the curve m = 0 in Figure 1 applies for both models, we can therefore conclude that all the curves shown in Figure 1 apply, with a reasonable accuracy, to both our quasi-

geostrophic and "primitive equations" model. This is tantamount, of course, to saying that the phase speeds of the "Rossby" waves have not been significantly affected by the non-geostrophic effects introduced in the present chapter.

The non-geostrophic effects, on the other hand, do play the important role of introducing two more possible phase speeds, namely, c_2 and c_3 as given by (3.23) and (3.24). These two phase speeds appear as functions of the wavelength in Figure 20 for the vertical modes m = 1, 2, and 3. The uppermost three curves in the figure refer to c_2 while the lowermost ones refer to c_3. The waves which travel at the speeds c_2 and c_3 are gravity-inertia waves. We note that the lower boundary condition that we use, namely, $\omega = 0$ for $p = p_0$ precludes the existence of external gravity waves (Hollmann, 1956). The waves under discussion, therefore, are internal gravity waves modified by the inertial forces due to the rotation of the earth. We note that for large wavelengths these waves can travel at very high speeds and that for any wavelength they can propagate both eastward and westward relative to the zonal current (U = 15 m sec^{-1} in Figure 20).

If, as we remarked above, c_2 and c_3 are the phase speeds of internal gravity waves modified by the inertial forces due to the rotation of the earth, we should then be able to obtain the phase speeds of the pure internal gravity waves by neglecting all references to the rotation of the earth in (3.21). We do this by setting $f = \beta = 0$ (which implies that $C_I = f/k = 0$ and $C_R = \beta/k^2 = 0$), in which case (3.21) becomes

$$X(X^2 - \frac{\sigma p_o^2}{m^2\pi^2}) = 0.$$

The three solutions to this equation are then

$$X_1 = c_1 - U = 0 \tag{3.25}$$

$$X_2 = c_2 - U = (\frac{\sigma p_o^2}{m^2\pi^2})^{1/2}, \quad m = \pm 1, \pm 2, \ldots \tag{3.26}$$

and

$$X_3 = c_3 - U = -(\frac{\sigma p_o^2}{m^2\pi^2})^{1/2}, \quad m = \pm 1, \pm 2, \ldots \tag{3.27}$$

where c_2 and c_3 are the phase speeds of pure internal gravity waves. We see that for $\sigma < 0$ c_2 and c_3 are complex so that the waves are unstable. This is not a surprising result, of course, since $\sigma < 0$ implies that the basic state has a superadiabatic lapse rate, in which case all vertical displacements are unstable. For $\sigma > 0$, on the other hand, c_2 and c_3 are both real which implies that the waves are stable. It is interesting to note, here, that in contrast to the gravity-inertia waves these pure gravity waves have phase speeds which are independent of the wavelength. Finally we note the important result

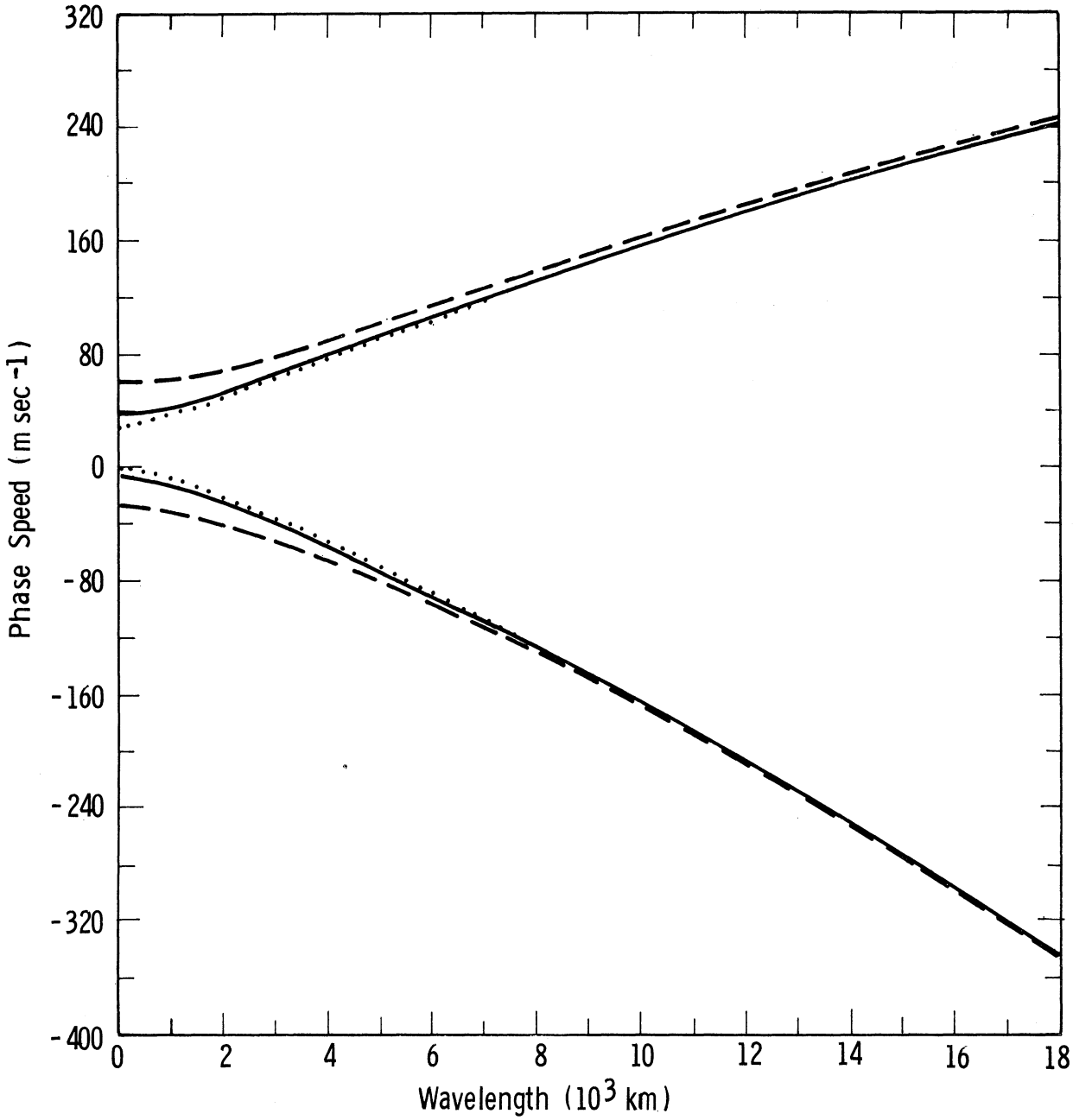

Figure 20. Phase speed of the gravity-inertia waves as a function of the wavelength. The dashed, solid and dotted curves refer to the vertical modes m = 1, 2 and 3, respectively. Parameters: U = 15 m sec^{-1}, σ = 2 MTS units, $\beta = 16 \times 10^{-12} m^{-1}$ sec^{-1}.

that when $\sigma = 0$ we have $c_2 = c_3 = U$; in other words, when the basic state has a dry adiabatic lapse rate the waves do not propagate relative to the basic zonal current. This is due to the fact that when the basic state has a dry adiabatic lapse rate there is no vertical restoring force to counteract any vertical displacement given to a parcel of air (assumed dry). The basic mechanism for the propagation of internal gravity waves is therefore absent and hence $\sigma = 0$ effectively filters out internal gravity waves.

If we now make use of this filter to preclude internal gravity wave solutions, we should be able to obtain the phase velocity of pure inertia waves from (3.21). With $\sigma = 0$, (3.21) takes the form

$$X(X^2+C_RX-C_I^2) = 0.$$

The three solutions to this equation are then

$$X_1 = c_1-U = 0 \tag{3.28}$$

$$X_2 = c_2-U = \frac{1}{2}[-C_R+(C_R^2+4C_I^2)^{1/2}] \tag{3.29}$$

and

$$X_3 = c_3-U = \frac{1}{2}[-C_R-(C_R^2+4C_I^2)^{1/2}] \tag{3.30}$$

where c_2 and c_3 are the phase speeds of the inertia waves. For very short wavelengths β/k^2 is much smaller than f/k (i.e. C_R is negligibly small compared to C_I) in which case, to a fair approximation, (3.29) and (3.30) can be written as

$$c_2-U = C_I = f/k \tag{3.31}$$

and

$$c_3-U = -C_I = -f/k \tag{3.32}$$

respectively.

We observe from (3.29) that since $(C_R^2+4C_I^2)^{1/2}$ is always greater than C_R it follows that X_2 is always positive. On the other hand, we see from (3.30) that X_3 is always negative. This indicates that the wave components with phase velocities c_2 and c_3 travel to the east and to the west, respectively, with respect to the basic current.

Before going on to the next section, where we investigate the behavior of wave disturbances in a "primitive equations" model with vertical wind shear

in the basic flow, it seems profitable to summarize the main results that we have obtained with our "primitive equations" model with a constant basic current. We have seen that the latter model has wave solutions of the Rossby and gravity-inertia types, all of which are stable for $\sigma \geq 0$. We found that the Rossby waves propagate to the west with respect to the basic current and at very nearly the same speed as the Rossby waves of section 2.2 (the quasi-geostrophic model). The gravity-inertia waves, on the other hand, propagate both to the east and to the west with respect to the basic flow and exist only in our "primitive equations" model.

In the next section we shall investigate the effects of vertical wind shear on the stability and speed of propagation of the wave disturbances. We shall assume that dU/dp is a negative constant and that both β and σ are zero. The model will therefore be analogous to the one investigated in section 2.3, differing only in that the flow will not be assumed to be quasi-geostrophic.

We emphasize that our assumption $\sigma = 0$ will filter out the internal gravity waves from our system while our lower boundary condition, $\omega = 0$ at $p = 1000$ mb, will filter out the external gravity waves. We can therefore expect that our model will yield wave solutions of the Rossby and inertia types as modified by the vertical wind shear.

3.4 THE CASE $dU/dp_* = \text{CONST.} < 0$, $\beta = \sigma = 0$

Similar models to the one that we investigate in this section were investigated by Fjørtoft (1950) and Thrane (1963). These authors, however, obtained only a wave solution of the Rossby type, omitting the inertia wave solutions, whereas we shall consider all the possible solutions.

The differential equation relating the amplitude of the ω wave to the pressure is obtained by setting β (and therefore C_R) equal to zero in (3.13). The latter equation then reduces to

$$(c-U)\left[1-\frac{(c-U)^2}{C_I^2}\right]\frac{d^2\hat{\omega}}{dp_*^2} + 2\frac{dU}{dp_*}\frac{d\hat{\omega}}{dp_*} = 0 . \qquad (3.33)$$

If we now assume that

$$U(p_*) = U_o + U_T(1-p_*) \qquad (3.34)$$

where U_o is the speed of the basic current at $p_* = 1$ and $U_T = -dU/dp_* = \text{constant}$, we can then write (3.33) in the form

$$(p_*+c_*-1)\left[1-\frac{(p_*+c_*-1)^2}{C_{I*}^2}\right]\frac{d^2\hat{\omega}}{dp_*^2}-2\frac{d\hat{\omega}}{dp_*}=0 \tag{3.35}$$

where
$$c_* = \frac{c-U_o}{U_T} \tag{3.36}$$

and
$$C_{I*} = \frac{C_I}{U_T} = \frac{f}{kU_T}. \tag{3.37}$$

We now change the independent variable by means of the transformation

$$\xi = \frac{p_*+c_*-1}{C_{I*}} = \frac{c-U}{C_I} \tag{3.38}$$

so that (3.35) now takes the more convenient form

$$\xi(1-\xi^2)\frac{d^2\hat{\omega}}{d\xi^2}-2\frac{d\hat{\omega}}{d\xi}=0. \tag{3.39}$$

We note that this differential equation has three singular points, namely, $\xi = 0$ and $\xi = \pm 1$. If we use the definitions of ξ, c_*, C_{I*}, and U given above, we find that these singular points correspond to $c = U$ and $c = U\pm f/k$, respectively. We will discuss the effect of these singular points on the ω wave structure after we obtain the solution to (3.39).

To solve (3.39) we first introduce $Q = d\hat{\omega}/d\xi$ so that the equation can be written in the form

$$\frac{dQ}{Q} = -\frac{2}{\xi(\xi^2-1)}\,d\xi.$$

After separating the right-hand side of this equation into a sum of partial fractions we can integrate term by term to obtain

$$\ln Q = 2\ln\xi - \ln(\xi+1) - \ln(\xi-1) + \ln A'$$

$$Q = \frac{d\hat{\omega}}{d\xi} = A'\frac{\xi^2}{\xi^2-1},$$

where A' is a constant. We use the same procedure again, that is, we separate the right-hand side into a sum of partial fractions and integrate. The resulting expression for ω takes the form

$$\hat{\omega} = A[2\xi + \ln Z] + B \tag{3.40}$$

where

$$Z = \frac{\xi - 1}{\xi + 1}$$

$$A = \frac{1}{2}A'$$

and B is a constant. Since Z depends on the phase velocity c, it can in general be complex and hence we can write (3.40) as

$$\hat{\omega} = A[2\xi + \ln|Z| + i\theta] + B \tag{3.41}$$

where θ is the argument of Z, that is,

$$\theta = \tan^{-1}\left(\frac{Z_i}{Z_r}\right) \quad . \tag{3.42}$$

The logarithm of a complex number is multi-valued since θ, given by (3.42), is multi-valued. Here we will consider only the principal branch of the logarithm of Z by specifying the range of θ to be

$$-\pi < \theta < \pi \quad . \tag{3.43}$$

Choosing any other branch, we note, would lead to the same results for c and $\hat{\omega}$ (p). The range of θ given by (3.43) implies that ln Z has a branch cut along the negative real axis as shown in Figure 21.

We note that the inequalities (3.43) leave θ undefined along the negative real axis, so that ln Z is as yet undefined when Z is real and negative. In order to be able to attach a meaning to the logarithm of a real and negative quantity, it seems reasonable to give θ either the value π or $-\pi$ along the branch cut shown in Figure 21. Using arguments similar to Lin's (1955), we take the first choice, that is, we let $\theta = \pi$ along the negative real axis so that, for example,

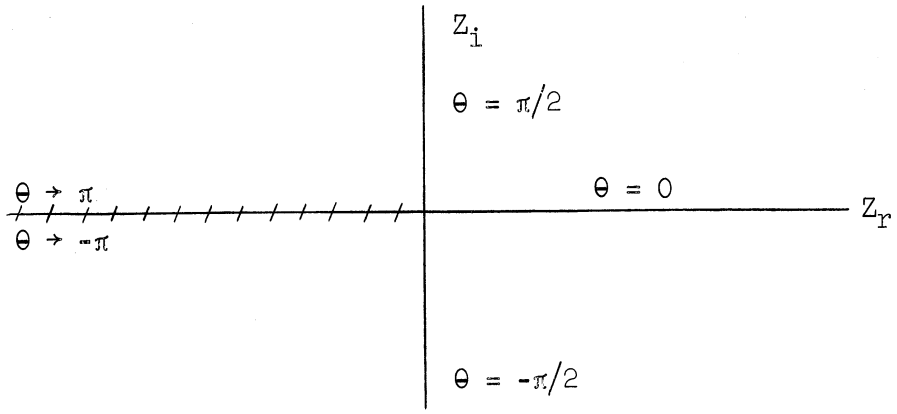

Figure 21. The complex Z plane showing the discontinuity of θ, and hence of ln Z, across the negative real axis (branch cut).

$$\ln -2 = \ln 2 + i\pi$$

but <u>not</u>

$$\ln -2 = \ln 2 - i\pi.$$

The presentation of the arguments which justify this choice is beyond the scope of this report but nevertheless we can point out the implications of our choice. Let us suppose that for the present model all waves with a wavelength L greater than some L_N are unstable while all those with $L \leq L_N$ are stable. In the unstable domain we have, for every wavelength, both an amplified and a damped wave while in the stable domain both waves are stable. Choosing $\theta = \pi$ along the negative real axis implies that both solutions in the stable domain are the analytic continuation of the <u>amplified</u> wave of the unstable domain. Had we made the choice $\theta = -\pi$ along the negative real axis, then both solutions of the stable domain would have been the analytic continuation of the <u>damped</u> wave of the unstable region. For a more detailed discussion of this topic we refer the reader to Lin (loc. cit.).

Now that we have established how our solution (3.40) is to be interpreted when Z (and hence c) can be complex for some wavelengths and real for others, we turn our attention to the problem of determining the possible values of the phase speed c. We do this by using the boundary conditions for $\hat{\omega}$, namely, $\hat{\omega} = 0$ for $p_* = 0$, that is, for $\xi = (c_*-1)/C_{I*}$ and $\hat{\omega} = 0$ for $p_* = 1$, that is, $\xi = c_*/C_{I*}$. Applying our solution (3.40) at the upper boundary we obtain

$$A\left[\frac{2(c_*-1)}{C_{I*}} + \ln\left(\frac{c_*-1-C_{I*}}{c_*-1+C_{I*}}\right)\right] + B = 0 \qquad (3.44)$$

while applying it at the lower boundary yields

$$A\left[\frac{2c_*}{C_{I*}} + \ln\left(\frac{c_*-C_{I*}}{c_*+C_{I*}}\right)\right] + B = 0. \qquad (3.45)$$

Subtracting (3.45) from (3.44) and dividing the resultant equation by A we arrive at the following frequency equation:

$$-\frac{2}{C_{I*}} + \ln\left[\left(\frac{c_*-1-C_{I*}}{c_*-1+C_{I*}}\right)\left(\frac{c_*+C_{I*}}{c_*-C_{I*}}\right)\right] = 0$$

which can then be rewritten in the form

$$\frac{(c_*-1-C_{I*})(c_*+C_{I*})}{(c_*-1+C_{I*})(c_*-C_{I*})} = e^{2/C_{I*}} \quad . \qquad (3.46)$$

This equation is a quadratic in c_* and can be solved in a straightforward manner. The result is

$$c_* = \frac{1}{2} \pm \left[\frac{1}{4} + C_{I*}^2 - C_{I*} \coth\left(\frac{1}{C_{I*}}\right)\right]^{1/2}.$$

To arrive at an explicit expression for c we eliminate c_* between this last equation and (3.36) and obtain

$$c = U\left(\frac{1}{2}\right) \pm U_T\sqrt{\delta} \qquad (3.47)$$

where

$$= \frac{1}{4} + C_{I*}^2 - C_{I*} \coth\left(\frac{1}{C_{I*}}\right) \qquad (3.48)$$

and we have introduced $U(1/2) = U_0 + 1/2\ U_T$.

We see from (3.47) that c is real and the waves stable if $\delta \geq 0$ while c is complex and the waves unstable if $\delta < 0$. The condition separating the stable and the unstable domains is therefore $\delta = 0$, that is,

$$\frac{1}{4} + C_{I*}^2 - C_{I*} \coth\left(\frac{1}{C_{I*}}\right) = 0. \qquad (3.49)$$

Since

$$C_{I*} = \frac{C_I}{U_T}$$

$$C_I = \frac{f}{k} = \frac{10^6 \ell f}{2\pi}$$

and

$$U_T = 20\frac{dU}{dZ},$$

where ℓ is the wavelength in thousands of kilometers and dU/dZ is the vertical wind shear in m $sec^{-1} km^{-1}$, we can write (3.49) in the more convenient form

$$\tanh\left[1.257\left(\frac{dU/dZ}{\ell}\right)\right] = \frac{12.57\left(\frac{dU/dZ}{\ell}\right)}{4\left(\frac{dU/dZ}{\ell}\right)^2 + 10}.$$

By trial and error we find that this equation has the solution

$$\frac{dU/dZ}{\ell} = 1.85 \quad \text{(approximately)}. \tag{3.50}$$

The graph of this equation, which is the neutral stability curve separating the stable and unstable domains, appears in Figure 22 as the thick straight

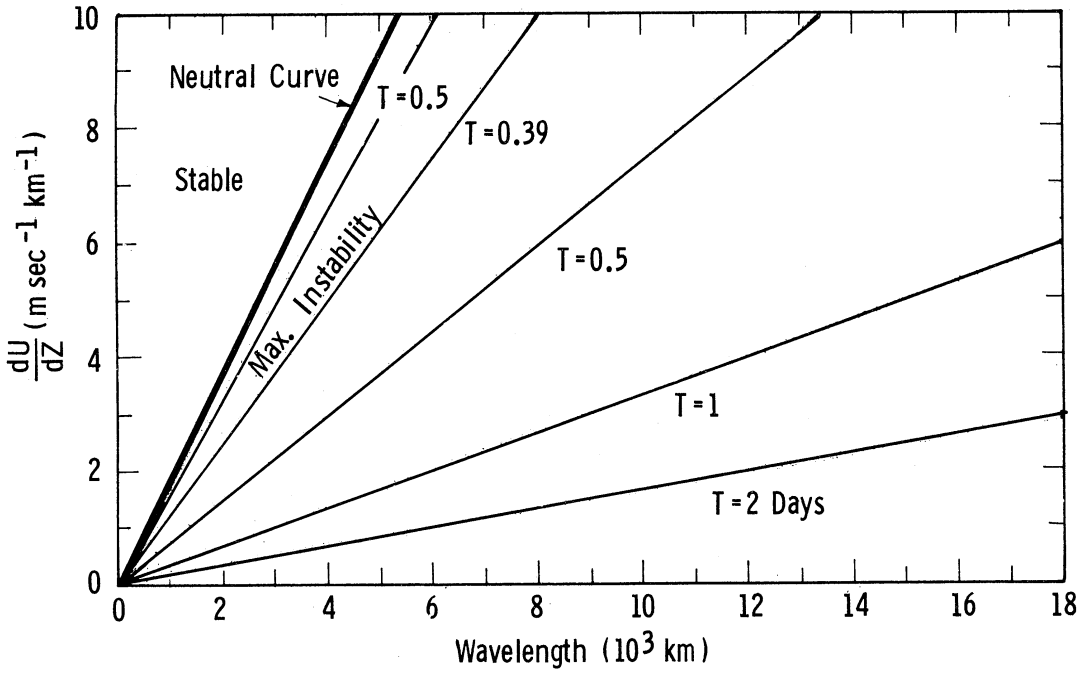

Figure 22. Stability diagram showing the variation of the e-folding time T as a function of the vertical wind shear and the wavelength. Parameters: $\beta = \sigma = 0$.

line. To the left of this curve δ, given by (3.48), is positive so that the waves in that region are stable; to the right of this curve, on the other hand, δ is negative and hence the waves in that region are unstable.

To determine the rate at which the amplitude of the unstable waves changes with time we compute the e-folding time given by

$$T = \frac{1}{kc_i} \quad . \tag{3.51}$$

From (3.47) we find that

$$c_i = U_T\sqrt{-\delta} = [C_I U_T \coth\left(\frac{U_T}{C_I}\right) - \frac{1}{4}U_T^2 - C_I^2]^{1/2}$$

so that

$$kc_i = [kf_o U_T \coth\left(\frac{U_T}{C_I}\right) - \frac{1}{4}k^2 U_T^2 - f_o^2]^{1/2} \quad .$$

If we now substitute this expression for kc_i into (3.51) and make use of the expressions for C_I and U_T following (3.49) we obtain

$$T = \frac{1.1574}{\{125.664\left(\frac{dU/dZ}{\ell}\right)\coth[1.257\left(\frac{dU/dZ}{\ell}\right)] - 40\left(\frac{dU/dZ}{\ell}\right)^2 - 100\}^{1/2}}$$

where f_o has been taken to be 10^{-4}sec^{-1} and T is given in days. We see, therefore, that for each value of $(dU/dZ)/\ell$ there corresponds one value of T; in other words, along any straight line $(dU/dZ)/\ell$ = constant, to the right of the neutral stability curve in Figure 22, T is a constant.

Figure 22 illustrates a few of the infinite number of isopleths of T which can be computed from the last equation above. If we fix our attention on a given wavelength, say 4000km, we see that the e-folding time is large for small wind shears, decreases gradually as the wind shear increases until a value of T = 0.39 days is reached, and then increases rapidly to reach an infinitely large value on the neutral stability curve. By trial and error we find from the above equation for T that 0.39 days is the minimum value (approximately) that T can attain. Since a minimum value in the e-folding time corresponds to a maximum in the instability (i.e. rate of growth or decay) we find, therefore, that the isopleth T = 0.39 days in the figure corresponds to the line of maximum instability.

To see how the non-geostrophic effects introduced in the present chapter affect the stability of the waves under study, we merely have to compare the stability diagram shown in Figure 22 to the one shown in Figure 3, the latter of which was obtained under the assumption of quasi-geostrophic motion. We observe that the main role of the non-geostrophic effects is to stabilize the short waves which in our quasi-geostrophic model were extremely unstable (the so-called "ultraviolet catastrophe"). We note also that in the quasi-geostrophic model the instability increases (the e-folding time decreases) monotonically as the wind shear increases; in the present model, on the other hand, there is a finite value of the wind shear for which the instability is a maximum (the e-folding time is a minimum, namely, 0.39 days). Finally we observe that for values of the wind shear in the range $0 \leq dU/dZ \leq 10\text{m sec}^{-1}\text{km}^{-1}$ the e-folding time of the very long waves is not severely affected by the non-geostrophic effects.

We recall that in the quasi-geostrophic analogue of the present model all waves travel with the speed of the basic current at p = 500 mb. The speed of propagation c_r for the corresponding waves in the present model, as obtained from (3.47), appears as a function of the wavelength in Figure 23. We note that just as in the quasi-geostrophic model all the unstable waves travel with the speed of the basic flow at p = 500 mb. We observe, on the other hand, that the speed of propagation of the short stable waves is double-valued and, moreover, that both values of c_r lie in the range $U(1) \leq c_r \leq U(0)$. As an example, for the case $U(1/2) = 15\text{m sec}^{-1}$ and $dU/dZ = 4\text{m sec}^{-1}\text{km}^{-1}$ in Figure 23, we have $U(1) = -25\text{m sec}^{-1}$, $U(0) = 55\text{m sec}^{-1}$ and we see by inspection of the graph that indeed $-25 \leq c_r \leq 55\text{m sec}^{-1}$ holds true.

Contrary to the procedure that we followed in the study of our quasi-geostrophic model, we will not, here, discuss in detail the structure of the waves. The reason for this is that when we investigate the structure of the short stable waves we find that for every wavelength there is a pressure level at which the amplitude of the wave becomes infinite. This occurs because at some pressure level $|\xi| = 1$ so that as we approach this level Z in (3.40) approaches either 0 or infinity (depending on whether $\xi \to 1$ or -1, respectively) in which case ln Z and $\hat{\omega}$ both approach infinity. In turn this difficulty as $|\xi| \to 1$ is directly related to the fact that (3.39) has singularities at $|\xi| = 1$. We note here that $\xi = 0$ is only an apparent singularity of (3.39) since the solution (3.40) is well-behaved at that point.

It seems likely that the infinite amplitudes in the stable perturbations result from our neglect of friction, a mechanism which, if present, would bably tend to reduce the amplitudes at the pressure levels where $|\xi| = 1$. Unfortunately the inclusion of friction in our model renders the equations so complicated that no closed analytical solution can be found for the entire range of pressure $0 \leq \quad _* \leq 1$. Instead of trying to solve the equations of a viscous atmosphere for the entire range of pressure, we could probably use the method of "cross-substitution" as suggested by Kuo (1949) in connection with the barotropic instability problem. The method consists in solving the equations for a

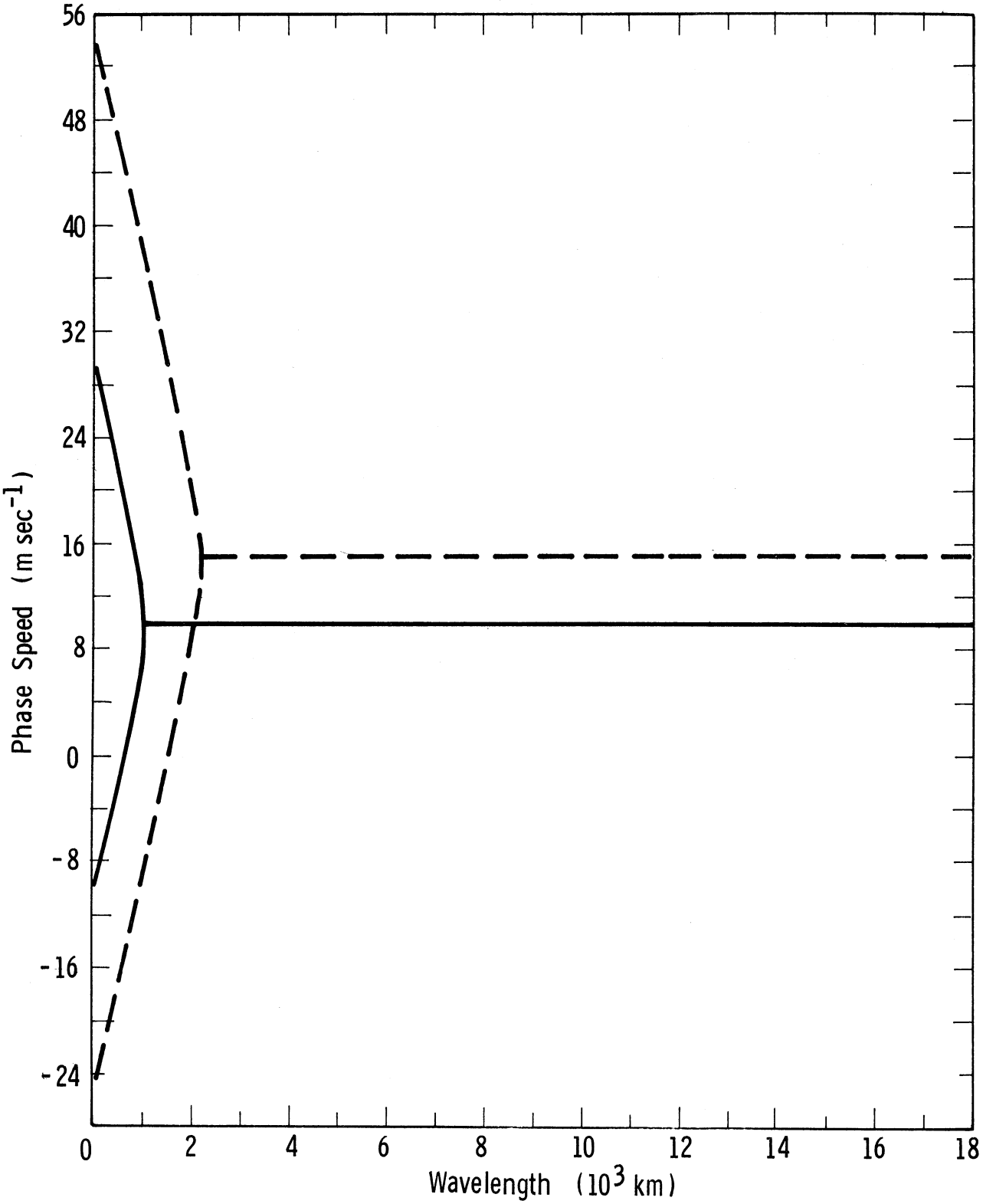

Figure 23. Phase speed of the Rossby type waves as a function of wavelength for the case $\beta = \sigma = 0$. For the solid curve $U(1/2) = 10$ m sec^{-1}, $dU/dZ = 2$ m sec^{-1} km^{-1} whole for the dashed curve $U(1/2) = 15$ m sec^{-1} and $dU/dZ = 4$ m sec^{-1}km^{-1}.

viscous atmosphere in the immediate neighborhood of the points $|\xi| = 1$ while continuing to use the equations for an inviscid atmosphere (as done above) outside this neighborhood. The solution for the complete range of pressure $0 \leq p_* \leq 1$ would then be obtained by matching the solutions for the equations with and without friction at a short distance away from each of the points $|\xi| = 1$.

Thrane (1963) has suggested another approach for finding stable wave solutions which have finite amplitudes at all pressure levels. His method consists in first finding a solution of the form (3.40) and then in integrating it over the wave number (or frequency) regime to obtain a new solution. This new solution is then also integrated over the wave number regime, and so on, each integration relegating the discontinuity in the solution to a higher and higher derivative. As Thrane has pointed out, the solution which is obtained contains an error, but this error can be made arbitrarily small.

Since the detailed treatment of the methods mentioned above is beyond the scope of this report, we shall leave the subject of the wave structure and return to the problem of determining all the possible types of wave motion in our model. So far we have encountered one type of waves which can be stable or unstable depending on their wavelength and travel at a speed c_r lying in the range $U(1) \leq c_r \leq U(0)$. We shall now show that there exists another type of waves, namely, inertia waves modified by the vertical wind shear.

Let us consider our general solution (3.40) for the amplitude of the ω wave as a function of ξ (which, in turn, is a function of p_* and c_*), that is,

$$\omega = A[2\xi + \ln Z] + B$$

where

$$Z = \frac{\xi - 1}{\xi + 1}$$

and A and B are constants. If we now assume that the phase speed is real for all values of the wavelength, then ξ and hence Z will also be real for all wavelengths. It is important to note that, in this case,

$$\omega = A[2\xi + \ln |Z|] + B \qquad (3.52)$$

also satisfies the differential equation (3.39), as can easily be seen by substituting (3.52) into (3.39).

We now proceed to determine the phase speed of the waves whose amplitude is given by (3.52). As before, to do this we apply (3.52) at the upper and lower boundaries, that is, at $\xi = (c_* - 1)/C_{I*}$ and at $\xi = c_*/C_{I*}$, respectively. From the resulting two equations we obtain the frequency equation

$$-\frac{2}{C_{I*}} + \ln\left|\frac{(c_*-1-C_{I*})(c_*+C_{I*})}{(c_*-1+C_{I*})(c_*-C_{I*})}\right| = 0$$

which we can rewrite in the form

$$\frac{(c_*-1-C_{I*})(c_*+C_{I*})}{(c_*-1+C_{I*})(c_*-C_{I*})} = \pm e^{2/C_{I*}} \quad . \tag{3.53}$$

We note that if we choose the plus sign on the right-hand side of (3.53) we obtain the same frequency equation as before, that is, (3.46). We should keep in mind that strictly speaking (3.53) is valid only when c_* is real whereas (3.46) is valid for c_* both real and complex. In any case, since we have already discussed this solution we need to be concerned, here, only with the solution obtained by choosing the negative sign on the right-hand side of (353). With the latter choice of sign, the quadratic (3.53) has the following two roots:

$$c_* = \frac{1}{2} \pm \left[\frac{1}{4} + C_{I*}^2 - C_{I*}\tanh\left(\frac{1}{C_{I*}}\right)\right]^{1/2} . \tag{3.54}$$

To obtain an explicit expression for the phase speed c, we eliminate c_* between (3.54) and (3.36) and find that

$$c = U\left(\frac{1}{2}\right) \pm U_T\sqrt{\Delta} \tag{3.55}$$

where

$$\Delta = \frac{1}{4} + C_{I*}^2 - C_{I*}\tanh\left(\frac{1}{C_{I*}}\right) .$$

For all values of $C_{I*} = f/kU_T$ we have $\Delta \geq 0$ so that c given by (3.55) is always real which, in turn, implies that the waves are stable for all values of the wavelength and wind shear.

To show that (3.55) gives the speed of inertia waves as modified by the wind shear we take the limit of c as U_T goes to zero and find

$$\lim_{U_T \to 0} c = \lim_{U_T \to 0} \{U\left(\frac{1}{2}\right) \pm \sqrt{U_T^2\Delta}\}$$

$$= \lim_{U_T \to 0}\{U\left(\frac{1}{2}\right) \pm \left[\frac{U_T^2}{4} + \frac{f^2}{k^2} - \frac{fU_T}{k}\tanh\left(\frac{U_Tk}{f}\right)\right]^{1/2}\}$$

$$= U \pm \frac{f}{k} .$$

This, we recall, is the expression for the phase speed of inertia waves in a zonal current with speed U when the β term is neglected.

The phase speed of the inertia waves appears in Figure 24 as a function of the wavelength for vertical wind shears of 0, 2 and 4m $sec^{-1}km^{-1}$. The uppermost and lowermost three curves are obtained by choosing the upper and lower signs, respectively, in (3.55). We see that the effect of the wind shear is to increase the speed (in absolute value) of the very short waves and to decrease the speed of the longer waves. The phase speed of the ultra-long waves, we note, is very large and nearly independent of the wind shear.

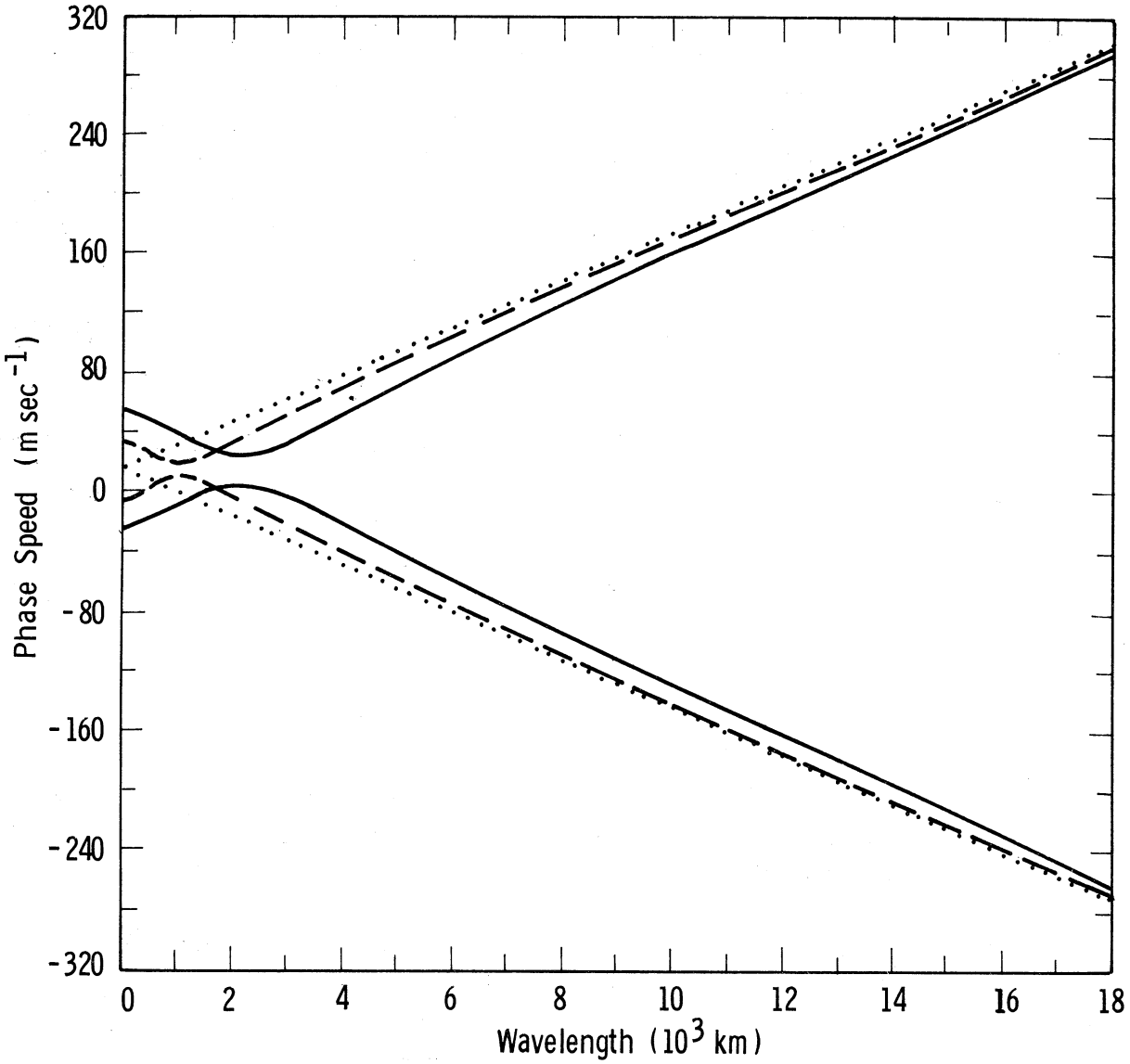

Figure 24. Phase speed of the inertia waves as a function of the wavelength. The dotted, dashed and solid curves refer to the cases where $dU/dZ = 0$, 2 and 4 m $sec^{-1}km^{-1}$, respectively. Parameters: $U(1/2) = 15$ m sec^{-1}, $\sigma = \beta = 0$.

In the next section we shall investigate the wave solutions of a model which differs from the one that we have just discussed only in that it includes the effects of the β term. We shall again assume that $\sigma = 0$ and use the boundary conditions $\omega = 0$ at $p = 0$ and 1000mb, thus filtering out both internal and external gravity waves. We can therefore again expect to find wave solutions of the Rossby and inertia types.

3.5 THE CASE $dU/dp_* = \text{CONST.} < 0$, $\beta = \text{CONST.} > 0$, $\sigma = 0$

The purpose of this section is to investigate the effects of the β term on the behavior of wave disturbances in a baroclinic model based on a system of "primitive equations". Our model is similar to the one used by Holmboe (1959) and yields substantially the same results as far as the stability of Rossby waves is concerned. In addition to the treatment of the Rossby waves, however, we also derive the phase speed of the inertia waves in this model, something which was not included in Holmboe's paper.

The equation relating the amplitude of the ω wave to the pressure for this model, namely,

$$(c-\hat{U})(c-U+C_R)\left[(c-U)(c-U+C_R)-C_I^2\right]\frac{d^2\hat{\omega}}{dp_*^2}$$

$$- C_I^2\left[2(c-U)+C_R\right]\frac{dU}{dp_*}\frac{d\hat{\omega}}{dp_*} = 0, \qquad (3.56)$$

is obtained by setting σ equal to zero in the general equation (3.13). We now assume that the basic zonal wind varies linearly with pressure as in (3.34) so that (3.56) takes the form

$$(p_*-1+c_*)(p_*-1+c_*+C_{R*})\left[(p_*-1+c_*)(p_*-1+c_*+C_{R*})-C_{I*}^2\right]\frac{d^2\hat{\omega}}{dp_*^2} +$$

$$+ C_{I*}^2\left[2(p_*-1+C_*) + C_{R*}\right]\frac{d\hat{\omega}}{dp_*} = 0 \qquad (3.57)$$

$$C_{R*} = \frac{C_R}{U_T} = \frac{\beta}{k^2U_T}$$

$$C_{I*} = \frac{C_I}{U_T} = \frac{f_o}{kU_T}$$

and $$c_* = \frac{c-U_o}{U_T}.$$

If we now introduce the notation

$$\xi = \frac{p_*-1+c_*+C_{R*}}{C_{I*}}$$

and $$\mu = \frac{C_R}{C_I} \qquad (3.58)$$

we find that we can write (3.57) in the more convenient form

$$\xi(\xi-\mu)[\xi(\xi-\mu)-1]\frac{d^2\hat{\omega}}{d\xi^2} + (2\xi-\mu)\frac{d\hat{\omega}}{d\xi} = 0 \qquad (3.59)$$

which, in turn, is equivalent to

$$\xi(\xi-\mu)\frac{d}{d\xi}\{[\xi(\xi-\mu)-1]\frac{d\hat{\omega}}{d\xi}\} - (2\xi-\mu)[\xi(\xi-\mu)-1]\frac{d\hat{\omega}}{d\xi} = 0. \qquad (3.60)$$

Equation (3.59), and hence (3.60), has singularities at $\xi = 0$, $\xi = \mu$ and $\xi(\xi-\mu) = 1$. As we shall see, $\xi = 0$ and $\xi = \mu$ are only apparent singularities since the solution to (3.59) is well behaved at these points. Such is not the case, however, for the singular points occurring at the two roots of $\xi(\xi-\mu) = 1$; at these points the solution to (3.59) becomes infinite just as the solution to (3.39), for the previous case, did at the points $\xi = \pm 1$. Again we could probably use the methods suggested in the previous section to construct finite amplitude solutions but the application of these methods is beyond the scope of this report.

To find the solution to (3.59) we first introduce

$$Q = [\xi(\xi-\mu)-1]\frac{d\hat{\omega}}{d\xi} \qquad (3.61)$$

so that the equation can be written as

$$\frac{dQ}{Q} = \frac{2\xi-\mu}{\xi(\xi-\mu)}\,d\xi \quad .$$

After separating the right-hand side of this equation into a sum of partial

fractions and integrating term by term we obtain

$$\ln Q = \ln \xi + \ln(\xi-\mu) + \ln A'$$

or

$$Q = A'\xi(\xi-\mu). \tag{3.62}$$

If we now substitute for Q from (3.61) and rearrange terms we find that (3.62) can be written as

$$\frac{d\hat{\omega}}{d\xi} = A'\frac{\xi(\xi-\mu)}{\xi(\xi-\mu)-1} .$$

Again we separate the right-hand side of the equation into a sum of partial fractions and integrate term by term to obtain

$$\hat{\omega} = A'[\xi+ \frac{1}{2\lambda} \ln Z] + B$$

or

$$\hat{\omega} = A[2\xi+ \frac{1}{\lambda} \ln Z] + B \tag{3.63}$$

where

$$Z = \frac{\xi-\frac{\mu}{2}-\lambda}{\xi-\frac{\mu}{2}+\lambda}$$

$$A = \frac{1}{2}A'$$

$$\lambda = (1+\frac{\mu^2}{4})^{1/2} \tag{3.64}$$

and B is a constant of integration. By the same argument as in the last section we choose the range of θ, the argument of Z, to be

$$-\pi < \theta \leq \pi.$$

So far we have assumed that c (and hence Z) could be complex but we have not found its possible values. To do this we use the boundary conditions for $\hat{\omega}$, namely,

$\hat{\omega} = 0$ for $p_* = 0$, that is, for $\xi = \xi_1 = \dfrac{c_*-1+C_{R*}}{C_{I*}}$ and

$\hat{\omega} = 0$ for $p_* = 1$, that is, for $\xi = \xi_2 = \dfrac{c_*+C_{R*}}{C_{I*}}$.

We note that if we use the definitions of c_*, C_{R*} and C_{I*} we can, for future convenience, rewrite ξ_1 and ξ_2 as

$$\xi_1 = \mu + \frac{c-U_o}{C_I} - \frac{U_T}{C_I} \tag{3.65}$$

and

$$\xi_2 = \mu + \frac{c-U_o}{C_I} \quad . \tag{3.66}$$

Applying our solution (3.63) at the upper and lower boundaries, that is, at ξ_1 and ξ_2, respectively, we obtain

$$A\left[2\xi_1 + \frac{1}{\lambda}\ln\left(\frac{\xi_1-\mu/2-\lambda}{\xi_1-\mu/2+\lambda}\right)\right] + B = 0$$

and

$$A\left[2\xi_2 + \frac{1}{\lambda}\ln\left(\frac{\xi_2-\mu/2-\lambda}{\xi_2-\mu/2+\lambda}\right)\right] + B = 0.$$

After subtracting this last equation from the previous one and then dividing by A we arrive at the following frequency equation:

$$2(\xi_1-\xi_2) + \frac{1}{\lambda}\ln\left[\frac{(\xi_1-\mu/2-\lambda)(\xi_2-\mu/2+\lambda)}{(\xi_1-\mu/2+\lambda)(\xi_2-\mu/2-\lambda)}\right] = 0 \ . \tag{3.67}$$

If we now note from (3.65) and (3.66) that $\xi_2 = \xi_1 + U_T/C_I$ we can rewrite (3.67) as

$$\frac{(\xi_1-\mu/2-\lambda)\ (\xi_1+U_T/C_I-\mu/2+\lambda)}{(\xi_1-\mu/2+\lambda)(\xi_1+U_T/C_I-\mu/2-\lambda)} = e^{2\lambda U_T/C_I}$$

or, after some manipulation, as

$$\xi_1^2 - (\mu - \frac{U_T}{C_I})\xi_1 - \left[1 + \frac{\mu U_T}{2C_I} - \frac{\lambda U_T}{C_I}\coth(\lambda U_T/C_I)\right] = 0 \ . \tag{3.68}$$

It is convenient at this point to substitute for ξ_1, μ and λ from (3.65), (3.58) and (3.64), respectively, so that (3.68) takes the form

$$X^2 + (C_R-U_T)X - [C_I^2+C_RU_T/2-U_T(C_I^2+C_R^2/4)^{1/2} \coth (\lambda U_T/C_I)] = 0 \tag{3.69}$$

where

$$X = c-U_o.$$

The two solutions to the above quadratic in X can easily be found to be

$$X = \frac{1}{2}(U_T-C_R\pm\sqrt{\delta})$$

from which we obtain

$$c = U(1/2) - C_R/2 \pm \frac{1}{2}\sqrt{\delta} \tag{3.70}$$

where we have introduced $U(1/2) = U_o+U_T/2$ and defined δ by

$$\delta = C_R^2 + U_T^2 + 4C_I^2 - 4U_T(C_I^2 + C_R^2/4)^{1/2}\coth(\lambda U_T/C_I). \tag{3.71}$$

We see from (3.70) that the waves are stable (c real) if $\delta \geq 0$ and unstable (c complex) if $\delta < 0$. The condition separating the stable and unstable domains is therefore $\delta = 0$ and hence setting δ equal to zero in (3.71) gives us the equation for the neutral stability curve. We note that when f and β are given constant values this equation for the neutral stability curve expresses a relationship between U_T and L, the wavelength, but only in an implicit manner. In other words, we are unable, after setting equal to zero in (3.71), to obtain U_T as an explicit function of L as we have done in the previous sections. In view of this, we shall use a somewhat less accurate but still quite satisfactory method to obtain the neutral stability curve. The first step in the procedure is to superimpose a grid on a coordinate system having dU/dZ as ordinate and ℓ (or L) as abscissa. We then use (3.71) to compute δ at each of the grid points, a value of $\delta > 0$ indicating that the point lies in the stable domain and a value of $\delta < 0$ indicating that the point falls in the unstable domain. Having computed the value of δ for each of the grid points, it is then a simple matter to draw, by visual interpolation, the isopleth of $\delta = 0$ which gives us the neutral stability curve. This neutral stability curve appears as the thick line in Figure 25, where a grid spacing of $\Delta L = 500$ km and $\Delta(dU/dZ) = 0.5$m sec^{-1}km^{-1} was used.

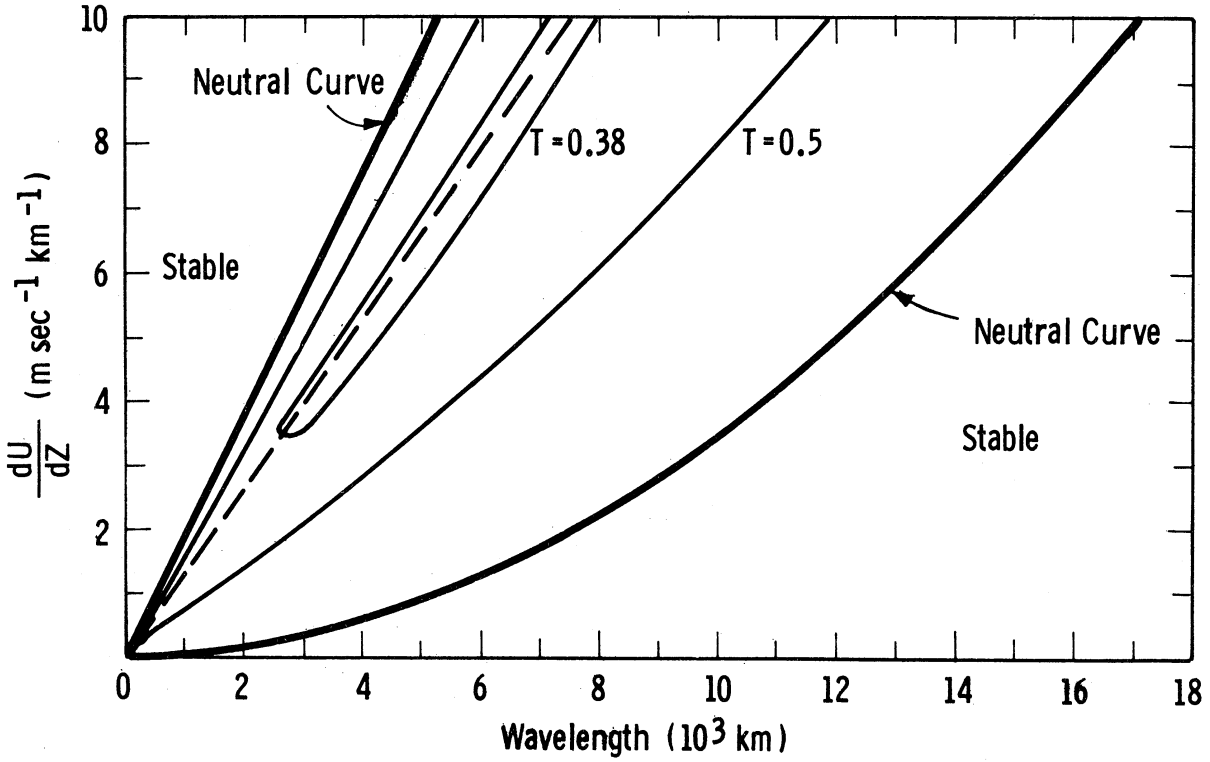

Figure 25. Stability diagram showing the variation of the e-folding time T as a function of the vertical wind shear and the wavelength. Parameters: $\beta = 16 \times 10^{-12}$ m^{-1} sec^{-1}, $\sigma = 0$.

In the region where $\delta < 0$ (unstable region) in Figure 25 we can compute the e-folding time of the waves as a measure of their instability. If we note from (3.70) that the absolute value of c_i is given by

$$c_i = \frac{1}{2}\sqrt{-\delta}$$

we find, then, that the e-folding time $T = 1/kc_i$ can be computed by means of the relation

$$T = \frac{2}{k\sqrt{-\delta}} \tag{3.72}$$

where δ is given by (3.71). Since the values of δ have already been computed in the unstable domain, we merely have to substitute them into (3.72) to obtain the e-folding time at each of the grid points in the unstable region. With this information we can then draw isopleths of the e-folding time as was done in Figure 25 for T = 0.5 days and T = 0.38 days.

We can now observe the effect of the β term on the stability of the waves of the Rossby type by comparing the stability diagram in Figure 25 (obtained with the β term) to the one in Figure 22 (obtained without the β term). We find that, just as in the quasi-geostrophic model, the effect of the β term is to stabilize the long waves. We note also that the inclusion of the β term increases somewhat the slope of the line of maximum instability (dashed line in Figure 25). Finally we note that the position of the left-hand portion of the neutral stability curve in Figure 25 is very nearly in the same position as the one in Figure 22, indicating that the short waves are stable independently of the β term. If we now compare the stability diagram in Figure 25 to the one in Figure 6 for the analogous quasi-geostrophic case, we find that the main difference is the presence of the stable domain in the short wave region of Figure 25 which, as already noted in the previous section, is clearly due to the non-geostrophic effects.

The speed c_r with which the waves under discussion travel can be obtained from (3.70) and appears as a function of the wavelength in Figure 26. We note that c_r is double-valued in the stable domains and single-valued in the unstable domain. The solid curve in Figure 26 applies for the case $U(1/2) = 10\text{m sec}^{-1}$ and $dU/dZ = 2\text{m sec}^{-1}\text{km}^{-1}$ while the dashed curve applies for the case $U(1/2) = 15\text{m sec}^{-1}$ and $dU/dZ = 4\text{m sec}^{-1}\text{km}^{-1}$. If we compare these curves to the ones shown in Figure 23 (obtained without the β term) we notice that the phase speed of the short stable waves is not severely affected by the β term; this is not the case, however, for the longer waves. In fact, we find that these longer waves travel at very nearly the same speed as those in the quasi-geotrophic analogue of the present model (see Figure 7). In other words, the β effect is important and the non geostrophic effects unimportant in determining the speed of propagation of the long Rossby waves while the reverse holds for the very short waves.

For the same reasons as in the previous section, we shall omit the discussion of the wave structure and restrict our attention to the problem of finding all the possible types of wave solutions for the present model. So far we have seen that the model has wave solutions of the Rossby type; we shall now show that it also has wave solutions of the inertia type as modified by both the vertical wind shear and the β effect. To do this we use exactly the same procedure as we did in the preceding section. We start with our general solution (3.63) for the amplitude of the ω wave as a function of ξ (which, in turn, depends on p_* and c_*), namely,

$$\hat{\omega} = A\left[2\xi + \frac{1}{\lambda}\ln Z\right] + B$$

where λ, Z, A and B have been defined after (3.63). If we now assume that there exists a type of waves for which the phase speed c (and hence ξ and Z) is real for all wavelengths, we then find that in this case

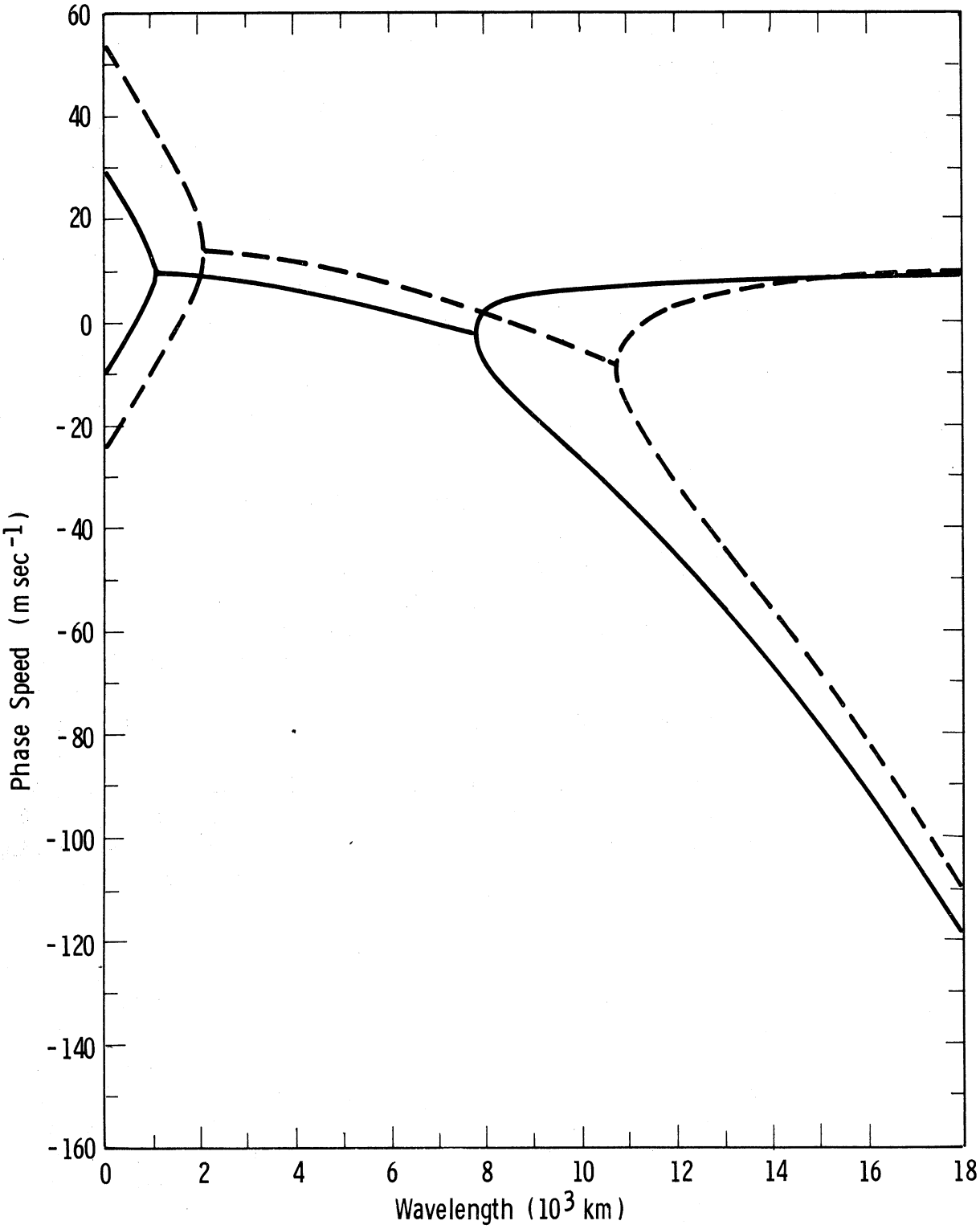

Figure 26. Phase speed of the Rossby type waves as a function of wavelength for the case $\beta = 16 \times 10^{-12}$ m^{-1} sec^{-1} and $\sigma = 0$. For the solid curve U(1/2) = 10 m sec^{-1}, dU/dZ = 2 m sec^{-1}km^{-1} while for the dashed curve U(1/2) = 15 m sec^{-1} and dU/dZ = 4 m sec^{-1}km^{-1}.

$$\omega = A[2\xi + \frac{1}{\lambda} \ln |Z|] + B \tag{3.73}$$

satisfies the differential equation (3 59), as can be verified by direct substitution. Our problem is now to find the phase speed of the wave whose amplitude is given by (3.73) and to verify our assumption that the waves are stable, independently of the wavelength.

To find the phase speed we apply our solution (3.73) at the upper and lower boundaries, namely, at $\xi = \xi_1 = (c_* - 1 + C_{R*})/C_{I*}$ and at $\xi = \xi_2 = (c_* + C_{R*})/C_{I*}$, respectively. From the resulting two equations we arrive at the frequency equation

$$2(\xi_1 - \xi_2) + \frac{1}{\lambda} \ln \left| \frac{(\xi_1 - \mu/2 - \lambda)(\xi_2 - \mu/2 + \lambda)}{(\xi_1 - \mu/2 + \lambda)(\xi_2 - \mu/2 + \lambda)} \right| = 0. \tag{3.74}$$

Noting that $\xi_2 = \xi_1 + U_T/C_I$ we can then rewrite (3.74) as

$$\frac{(\xi_1 - \mu/2 - \lambda)(\xi_1 + U_T/C_I - \mu/2 + \lambda)}{(\xi_1 - \mu/2 + \lambda)(\xi_1 + U_T/C_I - \mu/2 - \lambda)} = \pm e^{2\lambda U_T/C_I} . \tag{3.75}$$

We observe that if we choose the positive sign on the right-hand side of (3.75) we obtain the same frequency equation as before (see the equation preceding (3.68)). Since we have already discussed the solution of this frequency equation, we shall only concern ourselves here with the frequency equation obtained by choosing the negative sign in (3.75). With this choice of sign, we find that (3.75) can be rewritten, after some manipulation, as

$$\xi_1^2 - (\mu - \frac{U_T}{C_I})\xi_1 - [1 + \frac{\mu U_T}{2C_I} - \frac{\lambda U_T}{C_I} \tanh (\lambda U_T/C_I)] = 0. \tag{3.76}$$

We now substitude for ξ , μ and λ from (3.65), (3.58) and (3.64), respectively, so that (3.76) now takes the form

$$X^2 + (C_R - U_T)X - [C_I^2 + C_R U_T/2 - U_T(C_I^2 + C_R^2/4)^{1/2} \tanh(\lambda U_T/C_I)] = 0 \tag{3.77}$$

where $X = c - U_o$.

We can then write the two solutions to this quadratic in X as

$$X = \frac{1}{2}(U_T - C_R \pm \sqrt{\Delta})$$

from which we obtain

$$c = U(1/2) - C_R/2 \pm \frac{1}{2}\sqrt{\Delta} \qquad (3.78)$$

where we have used $U(1/2) = U_O + U_T/2$ and introduced

$$\Delta = C_R^2 + U_T^2 + 4C_I^2 - 4U_T(C_I^2 + C_R^2/4)^{1/2}\tanh(\lambda U_T/C_I) \; . \qquad (3.79)$$

For all values of U_T and L we have $\Delta \geq 0$ so that c given by (3.78) is real which, in turn, implies that the waves are stable for all values of the wind shear and wavelength.

The waves whose phase speed is give by (3.78) are inertia waves modified by the β effect and the vertical wind shear. We can show this by setting both β (and hence C_R) and U_T equal to zero in (3.78) in which case we obtain the classical phase speed of pure inertia waves, namely, $c = U \pm C_I = U \pm f/k$.

The speed of the inertia waves, as given by (3.78), appears as a function of wavelength in Figure 27 for the vertical wind shears of 0, 2 and 4m sec^{-1} km^{-1}. The uppermost and lowermost three curves are obtained by choosing the upper and lower signs, respectively, in (3.78). First we note that increasing the wind shear from 0 to 2 and 4m $sec^{-1}km^{-1}$ has the effect of increasing the speed (in absolute value) of the very short waves and of decreasing that of the longer waves. Just as in the previous section, where the β term was neglected, we find that the speed of the ultra-long waves is nearly independent of the wind shear.

To find the effect of the β term on the speed of these inertia waves, we merely have to compare the curves of Figure 27 to those of Figure 24, the latter having been obtained without the β term. We find that the difference between the two sets of curves becomes more and more noticeable as the wavelength increases. When the β term is included, the westward moving waves (three lowermost curves) travel faster to the west and the eastward moving waves (three uppermost curves) travel more slowly to the east than when the β term is omitted. In other words, the β term gives a westward "push" to both the eastward and westward moving waves.

The case that we have discussed in this section is the last one for which an exact analytical solution has been found. For the other cases, that is, for those where dU/dp is a negative constant, σ is a positive constant and β is either zero or a positive constant, solutions could be found in approximate

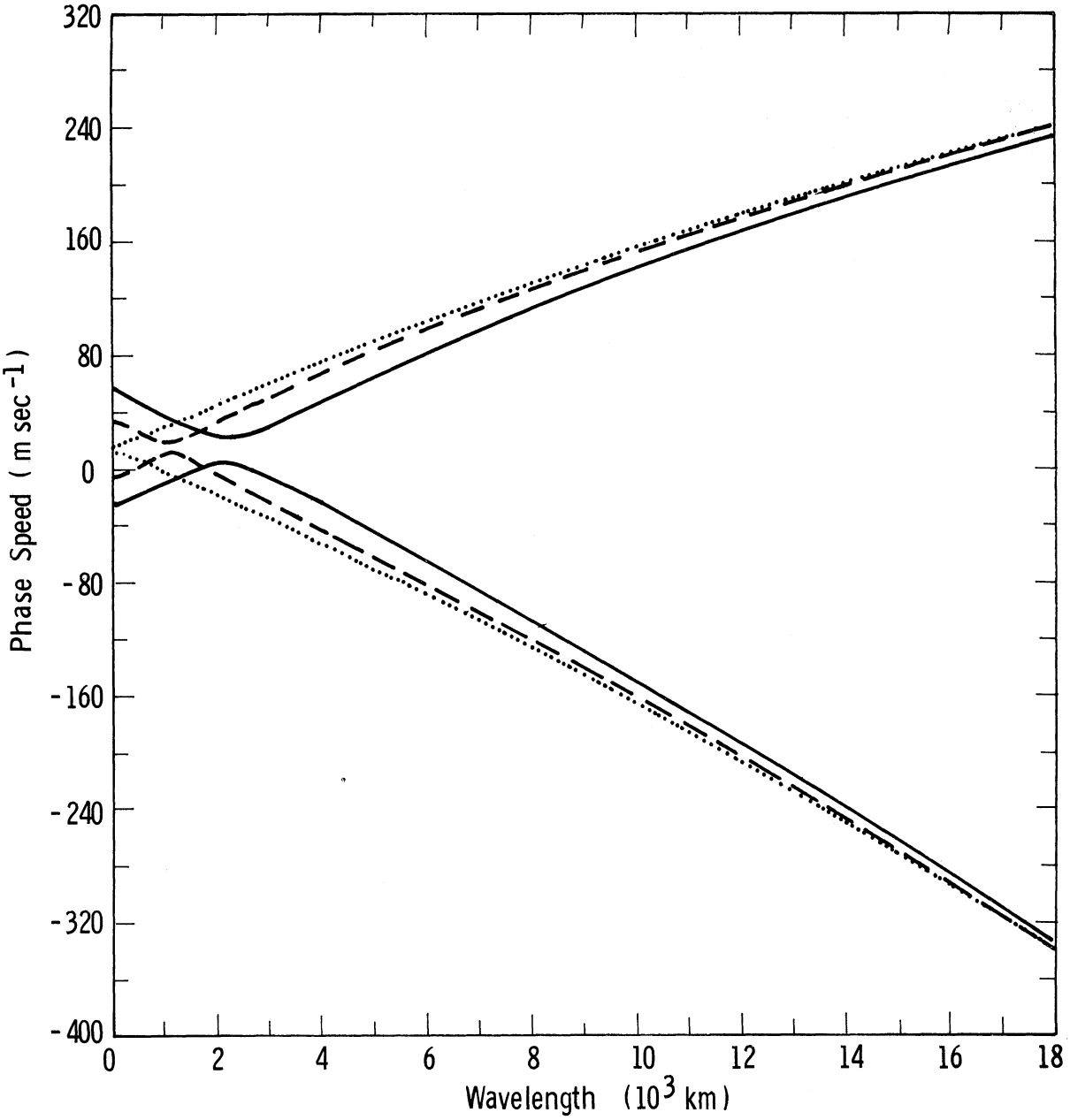

Figure 27. Phase speed of the inertia waves as a function of the wavelength. The dotted, dashed and solid curves refer to the cases where $dU/dZ = 0$, 2 and 4 m sec^{-1}km^{-1}, respectively. Parameters: $U(1/2) = 15$ m sec^{-1}, $\sigma = 0$.

forms such as truncated power series, for example. We shall not investigate these cases here but the reader can find similar ones in a paper by 'Arnason (1963) where the author shows essentially that the effect of the static stability is to broaden the stable domain in the short wave region of Figures 22 and 25.

4. THE ENERGETICS OF BAROCLINIC WAVES

The approach that we have used in the previous chapters enabled us to find the criteria which determine whether a given wave is stable or unstable. It revealed little, however, about the energy transformations taking place in our model atmospheres. It is our purpose now to present a brief discussion of the energy transformations which are necessary for the growth or decay of a wave disturbance.

We can separate the total energy in any of our model atmospheres into two main classes, namely, the energy of the basic state and that of the perturbations. Since the basic state was defined as one which does not vary with time, it follows that the energy associated with it is also time independent. The perturbations, on the other hand, have amplitudes which either vary exponentially with time or remain constant depending on whether the waves are unstable or not. If a certain wave is unstable and amplifying, the kinetic energy associated with it is clearly increasing with time and the interesting problem, here, is to determine the source of this energy as well as the type of motion necessary to accomplish the transfer of energy from the source to the growing perturbation. In the real atmosphere, wave disturbances of different wavelengths can exchange energy among themselves by nonlinear interactions but in our model atmospheres such exchanges have been precluded by our linearization procedure. In our models, therefore, a given wave can undergo an increase or decrease in total energy only if energy is being transfered from or to the basic state, respectively.

To discuss the exchange of energy between the basic state and a perturbation in greater detail, it is useful to subdivide the energy of each into its component forms, namely, the internal, potential and kinetic energies. In a hydrostatic atmosphere the amounts of the first two forms of energy are proportional to each other and hence we can refer to their sum as the "potential energy". Moreover, only a part of this potential energy, called the available potential energy, can be converted to the other form of energy, that is, to kinetic energy (Lorenz (1955)).

The total available potential energy of the perturbations between $y = y_1$ and $y = y_2$ is defined as

$$A = \frac{1}{2g}\int_0^{p_0}\int_S \frac{\alpha^2}{\sigma}\, dS\, dp \qquad (4.1)$$

where S is the area between the latitudes $y = y_1$ and $y = y_2$ ($dS = dxdy$), α is the perturbation specific volume and σ is the average value of the static stability parameter over the area S and hence is the same as the static stability

parameter of the basic flow. From (4.1) it follows that the time rate of change of the perturbation available potential energy A is given by

$$\frac{dA}{dt} = \frac{1}{g}\int_0^{p_o}\int_S \frac{\alpha}{\sigma}\frac{\partial\alpha}{\partial t}\,dS\,dp. \qquad (4.2)$$

Similarly we can write the expression for the perturbation kinetic energy between $y = y_1$ and $y = y_2$ as

$$K = \int_0^{\infty}\int_S \rho\left(\frac{u^2+v^2}{2}\right) dS\,dz$$

or

$$K = \frac{1}{2g}\int_0^{p_o}\int_S (u^2+v^2)\,dS\,dp \qquad (4.3)$$

and its time rate of change as

$$\frac{dK}{dt} = \frac{1}{2g}\int_0^{p_o}\int_S \frac{\partial}{\partial t}(u^2+v^2)\,dS\,dp\ . \qquad (4.4)$$

We note from (4.1) that the available potential energy of the perturbations is undefined when $\sigma = 0$. In this case the surfaces of constant potential temperature in the basic state are vertical since $\sigma = 0$ implies that $\partial\theta/\partial p = 0$. Since we make use of (4.1) in our treatment of the energy transfers, we shall then have to restrict our attention to the energetics of a model in which $\sigma > 0$. Moreover, since a discussion of the energetics of stable waves would be trivial, we shall further restrict our attention to the energetics of a model which has unstable wave solutions. Only one of the seven special cases treated in this report satisfies both requirements, that is, in having $\sigma > 0$ and yielding unstable wave solutions for certain wavelengths. This is the case presented in section 2.5 in which we have: (a) quasi-geostrophic motion, (b) $dU/dp =$ constant < 0, (c) $\sigma =$ constant > 0 and (d) $\beta = 0$. We shall now investigate the mechanisms which can change the energy (kinetic and available potential) of an unstable perturbation in this model.

We recall that in our quasi-geostrophic model the perturbation horizontal wind speeds, omitting the primes on the perturbation quantitities, are given by

$$u = -\frac{\partial\psi}{\partial y} = 0$$

and

$$v = \frac{\partial \psi}{\partial x}$$

so that (4.4) takes the form

$$\frac{dK}{dt} = \frac{1}{2g} \int_0^{p_o} \int_S \frac{\partial}{\partial t}\left(\frac{\partial \psi}{\partial x}\right)^2 dS\, dp$$

$$= \frac{1}{g} \int_0^{p_o} \int_S \frac{\partial \psi}{\partial x} \frac{\partial}{\partial t}\left(\frac{\partial \psi}{\partial x}\right) dS\, dp$$

$$= \frac{1}{g} \int_0^{p_o} \int_S \frac{\partial}{\partial x}\left[\psi \frac{\partial}{\partial t}\left(\frac{\partial \psi}{\partial x}\right)\right] dS\, dp$$

$$- \frac{1}{g} \int_0^{p_o} \int_S \psi \frac{\partial}{\partial t}\left(\frac{\partial^2 \psi}{\partial x^2}\right) dS\, dp.$$

Since the first integral on the right-hand side is identically zero we then have

$$\frac{dK}{dt} = - \frac{1}{g} \int_0^{p_o} \int_S \psi \frac{\partial}{\partial t}\left(\frac{\partial^2 \psi}{\partial x^2}\right) dS\, dp, \qquad (4.5)$$

in which the integrand is simply the stream function multiplied by the local time rate of change of vorticity. The latter, as obtained from the vorticity equation (2.6), is given by

$$\frac{\partial}{\partial t}\left(\frac{\partial^2 \psi}{\partial x^2}\right) = -U \frac{\partial}{\partial x} \frac{\partial^2 \psi}{\partial x^2} - \beta \frac{\partial \psi}{\partial x} + f_o \frac{\partial \omega}{\partial p} \quad . \qquad (4.6)$$

Strictly speaking, β should be set equal to zero in (4.6) since we are investigating the energetics of a model in which $\beta = 0$. Retaining the β term, however, does not alter the subsequent results because the Coriolis force, acting perpendicular to the velocity vector, has no effect on the time rate of change of the kinetic energy. In other words, the energy equations which we are deriving apply not only for the case where $\beta = 0$ but also for the more general one where β = constant > 0.

If we now substitute (4.6) into (4.5) we find that the time rate of change of the perturbation kinetic energy is given by

$$\frac{dK}{dt} = -\frac{f_o}{g} \int_0^{p_o} \int_S \psi \frac{\partial \omega}{\partial p} \, dS \, dp$$

or

$$\frac{dK}{dt} = -\frac{f_o}{g} \int_0^{p_o} \int_S \left[\frac{\partial \omega \psi}{\partial p} - \omega \frac{\partial \psi}{\partial p} \right] dS \, dp \quad , \tag{4.7}$$

since the integral involving each of the first two terms on the right-hand side of (4.6) is zero. Using the boundary conditions $\omega = 0$ for $p = 0$ and $p = p_o$ and the fact that ψ is bounded at the top and bottom of the atmosphere we find that (4.7) reduces to

$$\frac{dK}{dt} = \frac{f_o}{g} \int_0^{p_o} \int_S \omega \frac{\partial \psi}{\partial p} \, dS \, dp. \tag{4.8}$$

We recall that in our quasi-geostrophic model $\psi = \phi/f_o$ so that

$$\frac{\partial \psi}{\partial p} = \frac{1}{f_o} \frac{\partial \phi}{\partial p}$$

or, by the hydrostatic equation,

$$\frac{\partial \psi}{\partial p} = -\frac{\alpha}{f_o} . \tag{4.9}$$

Substituting (4.9) into (4.8) we arrive at the following expression for the time rate of change of the perturbation kinetic energy:

$$\frac{dK}{dt} = -\frac{1}{g} \int_0^{p_o} \int_S \omega\alpha \, dS \, dp \quad . \tag{4.10}$$

Equation (4.10) tells us that the total perturbation kinetic energy in the volume in question will increase with time if the perturbation ω and α fields are positioned in such a way that on the average warm air (α large) is rising ($\omega < 0$) and cold air (α small) is sinking ($\omega > 0$). Conversely the perturbation kinetic energy will decrease with time if, on the average, warm air is sinking and cold air is rising.

When the perturbation kinetic energy changes through the process just described, the available potential energy of the perturbations is also affected. To show this we shall derive the equation for the time rate of change of the perturbation available potential energy. We start by writing the adiabatic thermodynamic equation (2.7) in the form

$$\frac{\partial}{\partial t}\left(\frac{\partial \psi}{\partial p}\right) = - U \frac{\partial}{\partial x}\left(\frac{\partial \psi}{\partial p}\right) + \frac{dU}{dp}\frac{\partial \psi}{\partial x} - \frac{\sigma}{f_o}\omega$$

which, with the help of (4.9), becomes

$$\frac{\partial \alpha}{\partial t} = - U\frac{\partial \alpha}{\partial x} - f_o \frac{dU}{dp}\frac{\partial \psi}{\partial x} + \sigma\omega \ . \qquad (4.11)$$

If we now substitute (4.11) into (4.2) we find that the time rate of change of the perturbation available potential energy is given by

$$\frac{dA}{dt} = \frac{1}{g}\int_0^{p_o}\int_S \frac{\alpha}{\sigma}\left[- f_o \frac{dU}{dp}\frac{\partial \psi}{\partial x} + \sigma\omega\right] dS\ dp \qquad (4.12)$$

since the first term on the right hand side of (4.11) gives no contribution to the integral. Noting that f_o, dU/dp and σ are constants and that $\partial\psi/\partial x = v$ we can write (4.12) in the form

$$\frac{dA}{dt} = \underbrace{- \frac{f_o}{g\sigma}\frac{dU}{dp}\int_0^{p_o}\int_S v\alpha\ dS\ dp}_{(a)} + \underbrace{\frac{1}{g}\int_0^{p_o}\int_S \omega\alpha\ dS\ dp}_{(b)} \qquad (4.13)$$

The perturbation available potential energy can therefore change with time through the action of two mechanisms described by terms (a) and (b) in (4.13). If dU/dp is negative, as is the case in our model, term (a) is positive and the perturbation available potential energy tends to increase with time whenever, on the average over the volume, the perturbations transport warm air (α large) northward ($v > 0$) and cold air (α small) southward ($v < 0$). Conversely, the perturbation available potential energy tends to decrease with time whenever, on the average over the volume, the perturbations transport warm air southward and cold air northward. It is important to note that term (a) contains both perturbation and basic state quantities and hence represents an interaction between these two modes of flow. More precisely, it represents the rate at which available potential energy is being exchanged between the basic state and the perturbations.

As for term (b) in (4.13), we note that it also appears in (4.10), the equation for dK/dt, but with the opposite sign. This means that term (b) expresses the rate at which the perturbation kinetic energy is being converted into perturbation available potential energy or vice versa depending on whether term (b) is positive or negative, respectively.

Let us consider, as an example, the direction in which the energy conversions (a) and (b) are going in the case where an <u>amplifying</u> disturbance is superimposed on the basic state. It should be clear that when a perturbation is amplifying its kinetic energy increases with time. In other words, dK/dt in

(4.10) is positive and hence term (b) in (4.13) is negative. The amplifying perturbation is therefore increasing its kinetic energy at the expense of its own available potential energy. Now the perturbation available potential energy, defined by (4.1), is itself growing with time since the amplitude of the α wave is increasing exponentially with time. This means that dA/dt in (4.13) is positive and since term (b) has been shown to be negative we can then conclude that term (a) is positive and greater in absolute value than term (b). The direction of the energy conversions is shown schematically in Figure 28.

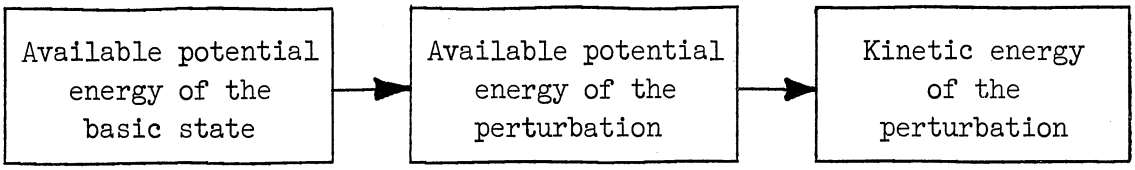

Figure 28. Schematic representation of the energy conversions taking place in the case of an amplifying disturbance superimposed on a basic flow. The direction of the arrows is reversed for the case of a damping disturbance.

We should note that in our models we have forced the available potential energy of the basic state to be constant by specifying that all basic state quantities be independent of time. This implies that the perturbations can extract available potential energy from the basic state without ever changing the basic state. We emphasize, however, that our perturbation analysis is valid only as long as the perturbations have small amplitudes and hence as long as the energy conversions between the boxes in Figure 28 are small. We can therefore look upon the first box on the left-hand side of Figure 28 as being a large reservoir whose energy level is not appreciably affected by the small exchanges with the perturbations. In the real atmosphere, on the other hand, the amplifying disturbances can have large amplitudes and hence can transport a considerable amount of heat northward as described by term (a) of (4.13). By doing so they tend to warm the northern latitudes and cool the southern ones thus destroying the existing meridional temperature gradient. If we now note that

$$\frac{dU}{dp} = \frac{R}{f_o p}\frac{\partial T}{\partial y} \qquad \text{(thermal wind equation)}$$

in which the quantities U, p and T refer to the basic state, we see that the northward heat transport by the perturbations tends to destroy the meridional temperature gradient and the vertical wind shear simultaneously. After a certain time, therefore, the vertical wind shear becomes so small that the perturbations are no longer unstable and hence they stop growing.

5. SUMMARY OF THE RESULTS

We have investigated the stability properties of wave disturbances superimposed on a time-independent basic flow. Since we wanted to restrict our attention to the problem of baroclinic instability, we removed the possibility of barotropic instability by specifying that the basic zonal wind speed be independent of the latitude.

In Chapter 2 we have used a quasi-geostrophic model and investigated four special cases of it to isolate the effects of (a) the vertical wind shear in the basic flow, (b) the variation of the Coriolis parameter with latitude or β effect and (c) the static stability parameter σ on the behavior of the perturbations. The results that we have obtained concerning the stability of the waves are summarized in Table I. We find, by comparing the results of cases 1 and 2, that the vertical wind shear tends to make all waves unstable when the β and σ terms are neglected. A comparison of cases 3 and 4 with case 2 reveals, on the other hand, that the β term tends to stabilize the long waves and that the static stability parameter σ tends to stabilize the very short waves.

For each of the cases listed in Table I we have investigated the structure of the waves and shown that the stable waves have vertical ridge (and trough) lines whereas the amplified and damped waves have ridge (and trough) lines which slope to the west and east, respectively, with height.

In Chapter 3 we have investigated the stability properties of a model in which the quasi-geostrophic assumption is not used. Just as in the previous chapter, no solution could be found for the general model so that we had to consider special cases of it. In all cases we found solutions corresponding to the slowly moving Rossby-type waves and others corresponding to the fast moving gravity-inertia waves (or simply "inertia" waves in the cases where $\sigma = 0$). The fast moving waves were found to be stable for all values of the wavelength but this, however, was not the case for the Rossby-type waves. The results obtained from the stability analysis of the latter are summarized in Table II. We see from the table that in our "primitive equations" model the very short waves are stable independently of the presence or absence of wind shear. By comparing the results of cases 1 and 2 we observe that the vertical wind shear tends to make the medium and long waves unstable if β and σ are both set equal to zero. Finally, a comparison of the results of cases 2 and 3 reveals that the β term has the effect of stabilizing the long waves, a result which was also obtained with our quasi-geostrophic model.

Our analysis of cases 2 and 3 in Table II is somewhat unsatisfactory since some of the wave solutions have infinite amplitudes for some pressure levels. Two methods have been mentioned in Chapter 3 for constructing solutions with finite amplitudes at all levels but these methods still remain to be applied.

TABLE I

RESULTS OF THE STABILITY ANALYSES WITH THE QUASI-GEOSTROPHIC MODELS

Case	Section	Assumptions	Results
1	2.2	$U = \text{const.} > 0$ $\beta = \text{const.} > 0$ $\sigma = \text{const.} > 0$	All waves are stable.
2	2.3	$dU/dp = \text{const.} < 0$ $\beta = 0$ $\sigma = 0$	All waves are unstable. The rate of growth (or decay) increases without bounds as the wind shear increases and/or the wavelength decreases. Figure 3.
3	2.4	$dU/dp = \text{const.} < 0$ $\beta = \text{const.} > 0$ $\sigma = 0$	The long waves are stable and the shorter one are unstable. The latter have a rate of growth (or decay) which increases without bounds as the wind shear increases and/or the wavelength decreases. Figure 6.
4	2.5	$dU/dp = \text{const.} < 0$ $\beta = 0$ $\sigma = \text{const.} > 0$	The very short waves are stable and the longer ones are unstable. The latter have a rate of growth (or decay) which increases without bounds as the wind shear increases. Figure 14.

TABLE II

RESULTS OF THE STABILITY ANALYSIS WITH THE "PRIMITIVE-EQUATIONS" MODELS
(Waves of the Rossby Type)

Case	Section	Assumptions	Results
1	3.3	U = const. > 0 β = const. > 0 σ = const. > 0	All waves are stable.
2	3.4	dU/dp = const. < 0 $\beta = 0$ $\sigma = 0$	For a given wind shear the very short waves are stable and the longer ones are unstable; the range of wavelengths which are stable increases as the wind shear increases. Figure 22.
3	3.5	dU/dp = const. < 0 β = const. > 0 $\sigma = 0$	The short and long waves are stable whereas the intermediate waves are unstable. Figure 25.

In Chapter 4 we have presented a brief description of the energy exchange taking place during the growth or decay of a disturbance. We have shown that during the growth of a baroclinic disturbance in our quasi-geostrophic model there is a conversion of energy from the available potential energy of the basic flow to that of the disturbance and also a conversion from the latter form of energy to the kinetic energy of the disturbance.

BIBLIOGRAPHY

'Arnason, G. "A Study of the Dynamics of a Stratified Fluid in Relation to Atmospheric Motions and Physical Weather Prediction," Tellus, 13, No. 2, 156-170 (1961).

'Arnason, G. "The Stability of Nongeostrophic Perturbations in a Baroclinic Zonal Flow," Tellus, 15, No. 3, 205-229 (1963).

Barcilon, V. "Role of the Ekman Layers in the Stability of the Symmetric Regime Obtained in a Rotating Annulus," Journal of the Atmospheric Sciences, 21, No. 3, 291-299 (1964).

Bretherton, F. P. "Critical Layer Instability in Baroclinic Flows," Quarterly Journal of the Royal Meteorological Society, 92, No. 393, 325-334 (1966a).

Bretherton, F. P. "Baroclinic Instability and the Short Wavelength Cut-Off in Terms of Potential Vorticity," Quarterly Journal of the Royal Meteorological Society, 92, No. 393, 335-345 (1966b).

Burger, A. P. "On the Non-Existence of Critical Wavelengths in a Continuous Baroclinic Stability Problem," Journal of the Atmospheric Sciences, 19, No. 1, 31-38 (1962).

Charney, J. G. "The Dynamics of Long Waves in a Baroclinic Westerly Current," Journal of Meteorology, 4, No. 5, 135-162 (1947).

Eady, E. T. "Long Waves and Cyclone Waves," Tellus, 1, No. 3, 33-52 (1949).

Fjørtoft, R. "Application of Integral Theorems in Deriving Criteria of Stability for Laminar Flows and for the Baroclinic Circular Vortex," Geofysiske Publikasjoner, 17, No. 5, 1-52 (1950).

Fleagle, R. G. "A Note on the Barotropic Rossby Wave," Journal of the Atmospheric Sciences, 22, No. 3, 329-331 (1965).

Hollmann, G. "Über Prinzipielle Mängel der Geostrophischen Approximation und die Einführung Ageostrophischer Windkomponenten," Meteorologishe Rundschau, 9, 73-78 (1956).

Holmboe, J. "On the Behavior of Baroclinic Waves," The Atmosphere and the Sea in Motion, Rockefeller Institute Press, New York, 333-349 (1959).

Huppert, H. E., and J. W. Miles. "A Note on Baroclinic Instability of the Zonal Wind to Short Waves," Journal of the Atmospheric Sciences, 23, No. 1, 125-126 (1966).

Kamke, E. Differentialgleichungen: Lösungsmethoden und Lösungen, Vol. 1, Akademische Verlagsgesellschaft, Leipzig, 1943, 642.

Kuo, H. L. "Dynamic Instability of Two-Dimensional Nondivergent Flow in a Barotropic Atmosphere," Journal of Meteorology, 6, No. 2, 105-122 (1949).

Kuo, H. L. "Three-Dimensional Disturbances in a Baroclinic Zonal Current," Journal of Meteorology, 9, No. 4, 260-278 (1952).

Kuo, H. L. "The Stability Properties and Structure of Disturbances in a Baroclinic Atmosphere," Journal of Meteorology, 10, No. 4, 235-243 (1953).

Lin, C. C. The Theory of Hydrodynamic Stability, Cambridge University Press, New York (1955).

Lorenz, E. N. "Available Potential Energy and the Maintenance of the General Circulation," Tellus, 7, No. 2, 157-167 (1955).

Miles, J. W. "Baroclinic Instability of the Zonal Wind," Reviews of Geophysics, 2, No. 1, 155-176 (1964a).

Miles, J. W. "Baroclinic Instability of the Zonal Wind: Part II," Journal of the Atmospheric Sciences, 21, No. 5, 500-506 (1964b).

Miles, J. W. "Baroclinic Instability of the Zonal Wind: Part III," Journal of the Atmospheric Sciences, 21, No. 6, 603-609 (1964c).

Pedlosky, J. "On the Stability of Baroclinic Flows as a Functional of the Velocity Profile," Journal of the Atmospheric Sciences, 22, No. 2, 137-145 (1965).

Phillips, N. A. "Geostrophic Errors in Predicting the Appalachian Storm of November 1950," Geophysica, 6, 389-404 (1958).

Phillips, N. A. "An Overlooked Aspect of the Baroclinic Stability Problem," Tellus, 16, No. 2, 268-270 (1964).

Thrane, P. "Perturbations in a Baroclinic Model Atmosphere," Geofysiske Publikasjoner, 25, No. 2, 1-13 (1963).

Wiin-Nielsen, A. "On Certain Integral Constraints for the Time-Integration of Baroclinic Models," Tellus, 11, No. 1, 45-59 (1959).

Wiin-Nielsen, A. "On Truncation Errors Due to Vertical Differences in Various Numerical Prediction Models," Tellus, 14, No. 3, 261-280 (1962).